University of Naples Federico II

Polytechnic and Basic Sciences School

Ph.D. in Chemical Sciences

XXXVIII Cycle

Bacterial and algal polysaccharides from marine sources: potential bioactive compounds

Ph.D. candidate:

Silvia Fanina

Supervisor:

Prof. Maria Michela Corsaro

Examiner:

Prof. Antonio Molinaro

Coordinator: Prof. Alessandra Napolitano

Index

Abbreviations

AA	Alditol Acetate
AC	Autotrophic Conditions
AE	Acidic Extraction
AEP	Acidic Extraction Precipitate
AlgNa	Sodium Alginate
AlgNa-S-AEP	Sodium Alginate Submerged Acidic Precipitate Extract film
AlgNa-S-P	Sodium Alginate Submerged Powder film
AMG	Acetylated Methyl Glycoside
AOG	Acetylated Octyl Glycosides
BSUD	Bold Sea Urchin Disease
C/N	Carbon/Nitrogen ratio
CCAP	Culture Collection of Algae and Protozoa
COSY	Double Quantum-Filtered Correlation Spectroscopy
CPS	Capsular Polysaccharides
CWPS	Cell-Wall Polysaccharide
DEPT-HSQC	Distortionless Enhancement by Polarization Transfer Heteronuclear Single Quantum Coherence
Dha	3-deoxy-L-*threo*-heptulosaric Acid
DMSO	Dimethyl Sulfoxide
DOC-PAGE	Sodium Deoxycholate PolyAcrylamide Gel Electrophoresis
DPPH	α,α-2,2-diphenyl-1-picrylhydrazyl
DSC	Differential Scanning Calorimetry
E.	Exposed
EDTA	Ethylenediaminetetraacetic Acid
EMBRC	European Marine Biological Resource Center
EMVs	Extracellulare embrane vesicules
EPA	Eicosapentaenoic Acid
EPM	Extracellular Polymeric material
EPS	Exopolysaccharides
EX_{PCP}	Phenol/Chloroform/Petroleum ether Extract
EX_{Wat}	Water Extract
EX_{WP}	Water/Phenol Extract
FAMEs	Fatty Acids Methyl Esters
FT-IR	Fourier-Transform Infrared Spectroscopy
Fuc	Fucose
FucN	2-amino-2-deoxy-L-fucosamine
GAGs	Glycosaminoglycans
Gal	Galactose
GalN	2-Amino-2-deoxy-galactose
GC-MS	Gas chromatography-Mass spectrometry
Glc	Glucose
GlcA	Glucuronic Acid
GlcN	2-amino-2-deoxy-glucose
GRAS	Generally Referred As Safe
GulNA	Gulosaminuronic Acid
HC	Heterotrophic Conditions
Hep	Heptose
HF	Hydrofluoric acid
HMBC	Heteronuclear Multiple Bond Correlation
HPLC	High Performance Liquid Chromatography
HSQC	Heteronuclear Single Quantum Correlation

IOM	Insoluble Organic Matter
Kdo	3-deoxy-D-manno-oct-2-ulosonic Acid
L:D	Light:Dark circle
LOS	Lipooligosaccharide
LPS	Lipopolysaccharide
Man	Mannose
MixC	Mixotrophic Conditions
NMR	Nuclear Magnetic Resonance
NOE	Nuclear Overhauser Effect
NOESY	Nuclear Overhauser Enhancement Spectroscopy
OD	Optical Density
OM	Outer Membrane
OW	Outer wall
P.	Powder
PCP	Phenol/Chloroform/Petroleum ether
PCW	Primary Cell Wall
PMAA	Partially Methylated Alditol Acetate
PTR	Pre-treatment
PTRE	Pre-treatment Extract
R.	Re-submerged
Rha	Rhamnose
Rib	Ribose
RID	Refractive Index Detector
S.	Submerged
SCW	Secondary Cell Wall
SDS	Sodium Dodecyl Sulfate
SNFG	Symbol Nomenclature For Glycans
SOM	Soluble Organic Matter
TFA	Trifluoroacetic Acid
TOCSY	Total correlation Spectroscopy
WE	Water Extraction
WED	Water Extract Dialysed
WEP	Water Extract Precipitate
Xyl	Xylose

Abstract

Marine environments represent a vast and largely untapped reservoir of unique glycoconjugates and extracellular polysaccharides (EPSs) with remarkable physicochemical and biological properties. These compounds hold promising potential for pharmaceutical, cosmetic, and biotechnological applications. The present study aimed to explore the structural diversity, chemical features, and potential bioactivities of polysaccharides from multiple marine organisms, including bacteria, red macroalgae, and microalgae.

In second chapter, the surface polysaccharides of *Shewanella vesiculosa* HM13 *nfnB*, including capsular polysaccharides (CPS) associated with extracellular membrane vesicles, were investigated. Extraction and purification revealed a previously unreported disaccharide repeating unit consisting of a 4-substituted glucose alternated with a 3-substituted *N*-acetylglucosamine. This unique CPS structure expands the known chemical diversity of marine bacterial polysaccharides and provides insights into the functional roles of surface glycoconjugates and their impact on vesicle cargo loading.

The thrid chapter focused on the CPS of *Vibrio crassostreae*, a marine gram-negative bacterium potentially associated with Bald Sea Urchin disease. Detailed structural characterization demonstrated that the CPS is composed primarily of L-fucose, D-acetylated 2-amino-2-deoxy-L-fucosamine, and D-mannose arranged in a trisaccharide repeating unit. Preliminary analysis of the LPS fraction revealed phosphorylated Kdo residues. These findings provide a molecular framework for understanding the role of surface polysaccharides in pathogenicity and host interactions, laying the groundwork for future functional studies.

In the fourth chapter, the EPS produced by *Alteromonas macleodii* Mo169 was isolated and characterized. Chemical and NMR analyses revealed a linear disaccharide repeating unit composed of glucosamine and gulaminuronic acid, with an *O*-acetyl substitution at position 3 of the gulaminuronic acid residue. The study provides a coherent structural description of this marine bacterial EPS, highlighting the occurrence of uronic acids and acetyl groups within Alteromonas polysaccharides and expanding knowledge of their structural diversity.

The fifth chapter explored the polysaccharides of the red macroalga *Ellisolandia elongata* under three environmental conditions: submerged, exposed, and re-submerged. Aqueous and acidic extraction methods were compared, with the acidic procedure providing higher yield and purity. Structural analyses revealed the coexistence of α-1,4-glucan (Floridean starch) and a sulfated xylogalactan. Environmental stress influenced both polysaccharide yield and sulfation patterns. Functional assays demonstrated significant antioxidant and antibiofilm activities, supporting the potential of *E. elongata* extracts for biomedical and biotechnological applications. Furthermore, preliminary thermal analyses (DSC) and incorporation into sodium alginate films indicated that purified extracts exhibit defined thermal transitions and good

compatibility with polymeric matrices, highlighting their potential for material and functional applications.

Finally, the sixth chapter focused on EPSs from three *Tetraselmis* strains, cultivated under autotrophic, heterotrophic, and mixotrophic conditions. Results highlighted strain- and trophic mode-dependent variability in biomass accumulation and EPS production. *Tetraselmis chuii* produced the highest EPS yield in mixotrophic conditions, with a galactan polysaccharide consisting of a linear 1,3-β-D-galactan backbone and sparsely distributed 3,6-linked branch points. Structural features were influenced by cultivation conditions, demonstrating the interplay between metabolism and polysaccharide biosynthesis, and supporting potential biotechnological applications.

This work provides a comprehensive investigation of marine polysaccharides from diverse organisms, elucidating their chemical structures, environmental influences, and preliminary bioactivities. The findings contribute to expanding the understanding of marine glycobiology, offering new perspectives for sustainable biotechnological exploitation of marine biodiversity. The study was supported by the European Marine Biological Resource Centre (EMBRC), which promotes the discovery of novel marine resources while minimizing environmental impact.

Acknowledgment

The author of the present PhD thesis acknowledges: Prof. Corsaro M. M., Prof. Casillo A., Dr. D'Amico R., Prof. Parrilli E, Dr. Olimpo D., Prof. Freitas F., Dr. Concordio-Reis P., Prof. Saggese O., and Dr. Gomez D'ayala G. for the scientific support.

All graphical layouts and schematic illustrations included in this thesis were originally made by the author using Canva® and BioRender.com®.

Papers included in this thesis

Casillo A., **Fanina S.**, Kamasaka K., Kawamoto J., Kurihara T., Lanzetta R., Corsaro M. M. (2024) Structural study of a polysaccharide component of *nfnB* mutant of *Shewanella vesiculosa* HM13. Carbohydr Res. Jul;541:109148. doi: 10.1016/j.carres.2024.109148. Epub 2024 May 20.

Fanina S., Concòrdio Reis P., Moppert X., Freitas F., Casillo A., Corsaro M. M. Characterization of a new glycosaminoglycan produced by the marine bacterium

Alteromonas macleodii Mo169**.** Carbohydr. Res. Volume 562, 2026, 109847, ISSN 0008-6215. https://doi.org/10.1016/j.carres.2026.109847

Fanina, S., Casillo, A., & Corsaro, M. M. (2026). Mediterranean Seaweed Polysaccharides: Insight into Chemical Structures, Applications, and Structure/Application Correlations. *Marine Drugs*, *24*(1), 11. https://doi.org/10.3390/md24010011.

Chapter 1

Introduction

1.1Marine polysaccharides

The marine environment is the largest ecosystem on Earth, covering 70% of its surface and hosting 50% of the whole globe's biodiversity in a wide range of habitats and environmental conditions. A huge part of this ecosystem is still unexplored (Atanasov et al., 2021; Harris et al., 2007). Moreover, it is an exceptional reservoir of bioactive molecules due to its vast biodiversity and the unique conditions in which marine organisms thrive. It poses unique challenges, such as high salinity, fluctuating temperature, pressure, and nutrient availability, that have driven the evolution of biomolecules with specific adaptive features (Mayer et al., 2011). Marine biomolecules show diverse molecular structures, many of which have a specific role in providing defence against predators, competitors, or pathogens (Mayer et al., 2011). These unique compounds are uncommon in terrestrial organisms and are proven to be superior in terms of chemical originality (Kong et al., 2010).

Marine polysaccharides represent one of the major classes of organic macromolecules produced by both macro- and micro-organisms (Fig.1), and they constitute a substantial fraction of the organic carbon and structural biomass (Arnosti et al., 2021; Z.-Z. Sun et al., 2021). Commonly, polysaccharides are high-molecular-weight carbohydrates formed by the polymerization of monosaccharide units linked by glycosidic linkages. The structural composition of these polysaccharides varies markedly between organisms: branching degree, monosaccharide composition, presence of sulfate or uronic acid groups, and molecular weight.

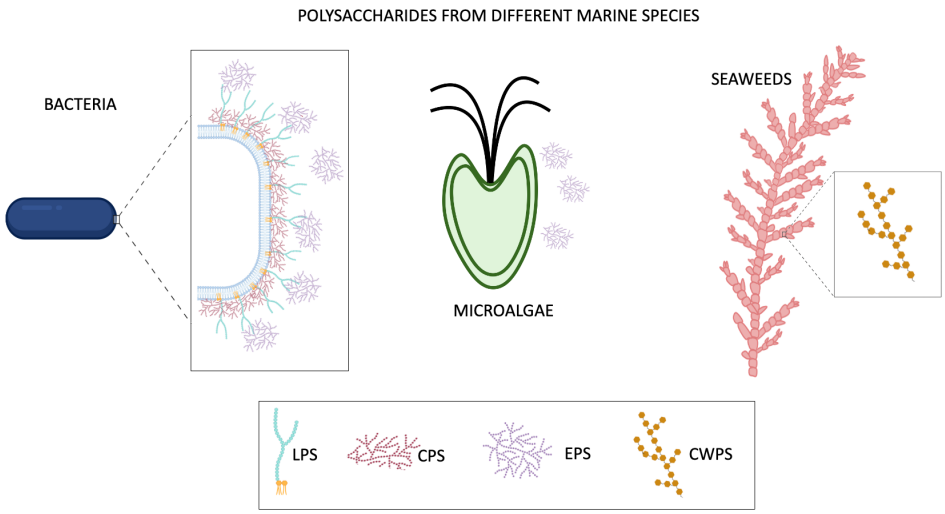

Figure 1. Overview of marine polysaccharides from bacteria, microalgae and seaweeds.

Marine bacteria produce cell-associated polysaccharides such as capsular polysaccharides (CPS) and lipopolysaccharides (LPS) (Stevenson et al., 1996), as well as exopolysaccharides (EPS) as a defence mechanism (Al-Hussaniy et al., 2025). Extracellular polysaccharides can contribute to the formation of biofilms that provide survival in marine habitats (Flemming & Wingender, 2010). Seaweeds synthesize abundant structural polysaccharides (CWPS) in their

cell walls that give them structural support and flexibility (Hentati, Tounsi, et al., 2020; Shao & Duan, 2022). These polysaccharides differ among phyla: red algae (Rhodophyta) produce sulfated galactans such as agar and carrageenan; brown algae (*Phaeophyceae*) contain alginate and fucoidan; while green algae (Chlorophyta) possess ulvans and glucans (Alexander & Dalgleish, 2007; Popper et al., 2011). Marine microalgae produce polysaccharides both as structural components of the cell wall (CWPS), often forming scales, thecae, or mucilage, and as EPS released into the surrounding environment (Mariani et al., 1985). This comparative framework highlights how the marine biosphere offers a remarkable repertoire of structurally and functionally distinct polysaccharides, whose biological origin determines their chemical complexity and ecological role. Given their abundance, structural complexity, and functional versatility, marine polysaccharides are increasingly investigated for biotechnological applications (Sacramento et al., 2022; Y. Sun et al., 2021) and are considered as one of the promising marine-derived bioresources in the context of sustainability and marine biorefinery concepts (Y. Sun et al., 2021).

1.2 Marine bacteria

Bacteria are unicellular, prokaryotic microorganisms that constitute one of the most abundant and ecologically significant groups of life on Earth. The marine environment is teeming with bacterial life, with estimates ranging from 10^6 to 10^8 bacteria per millilitre of seawater, depending on the specific location and environmental conditions, both Gram-negative and Gram-positive thrive (Fuhrman et al., 2008). Gram-negative bacteria inhabit every environment, including extreme marine habitats such as deep-sea (Maruyama et al., 2000), hydrothermal vents (Cambon-Bonavita et al., 2002; Raguenes et al., 1997), hypersaline lagoons (Di Donato et al., 2018), and polar oceans (Bowman et al., 1997; D'Amico et al., 2006), demonstrating remarkable adaptability. In the marine environment, bacteria are key drivers of biogeochemical cycles, indispensable for maintaining the health and functionality of marine ecosystems. Firstly, marine bacteria are critical mediators of nutrient cycling. They facilitate the decomposition of organic matter, thus recycling essential nutrients such as nitrogen and phosphorus back into the food web, not only supporting the microbial loop, a crucial process of marine food webs, but also enhancing the availability of nutrients to phytoplankton, which are primary producers in the ocean (Robertson et al., 2024; Urvoy et al., 2022). Secondly, bacteria play a pivotal role in carbon cycling, influencing the ocean's role as a carbon sink (Pinhassi et al., 2022). The interaction of bacteria with other marine organisms enhances their ecological significance. They can form mutualistic relationships with phytoplankton that support productivity and community structure (Urvoy et al., 2022; Yang et al., 2024). Lastly, among marine Gram-negative bacteria, members of the genus *Vibrio* are particularly widespread and ecologically relevant, embracing both free-living (Raguenes et al., 1997) and host-associated species (Bruto et al., 2017).

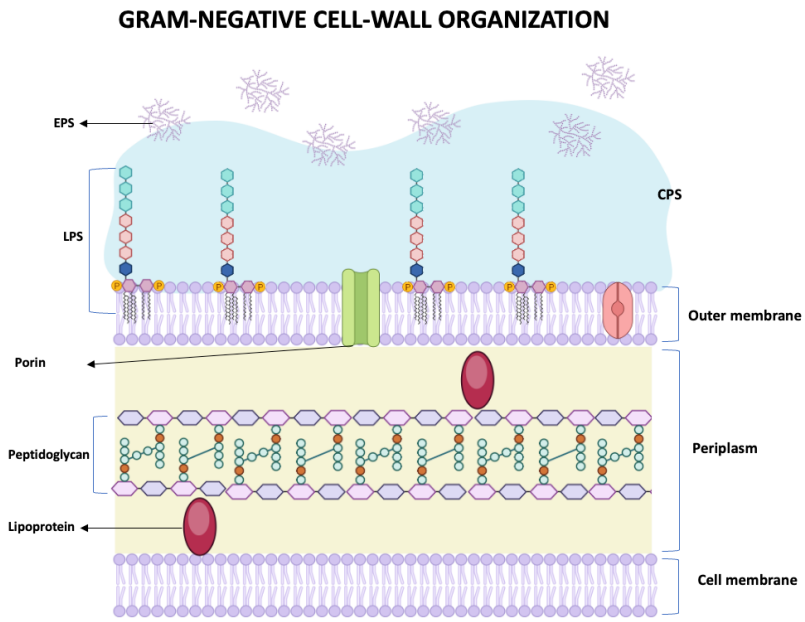

Figure 2. Gram-negative cell-wall structure.

From a structural perspective, the Gram-negative bacterial cell envelope builds up a characteristic architecture (Fig.2): an inner cytoplasmic membrane; an aqueous space called periplasm which contains a thin and rigid peptidoglycan layer, consisting in a network of alternating chains of N-acetylglucosamine and N-acetylmuramic acid that are cross-linked by penta-peptide chains; and the most external layer of the Gram-negative bacteria, the Outer Membrane (OM). The last consists of an asymmetrical lipid bilayer connected to the peptidoglycan by lipoproteins (Sankaran & Wu, 1994). The OM is composed of glycerophospholipids in the inner leaflet and LPSs on the outer leaflet, which act as a virulent factor and contribute to the OM integrity and permeability (Kamio & Nikaido, 1976). Finally, a wide range of bacterial species produce polysaccharides either as part of their cell envelope CPS or as secreted polymers EPS, that mediate interactions with their surroundings (Delbarre-Ladrat et al., 2014).

1.2.1 Gram-negative cell-wall polysaccharides

The capsule is a layer of polysaccharide that is either covalently or non-covalently attached to the bacterial surface, so it can be found weakly attached to the surface or tightly bonded to it (Fresno et al., 2006; Whitfield, 1988). While lipopolysaccharides (LPS) are essential structural components of the outer membrane and participate in host recognition and membrane stability, CPSs often constitute the most structurally diverse and functionally exposed polysaccharide fraction at the bacterial surface. CPSs are high-molecular-weight polymers composed of

monosaccharide residues linked to each other by glycosidic bonds. CPS is highly variable and may include neutral, acidic, or sulfated sugars such as glucose, galactose, fucose, and uronic acids (Corbett & Roberts, 2008). Classified as homo- or heteropolymers, respectively constituted of one type or different types of monosaccharide, CPSs can be linear or branched and display different types of substituents. The CPS layer can extend for 100-400 nm from the cellular surface, and its glycan chains can have up to 200 sugars. A single species can produce structurally diverse CPSs, up to 80 found in *Escherichia coli* (Whitfield, 2006) and up to 90 serotypes in *Streptococcus pneumoniae* (Van Selm et al., 2003). The genetic foundations of this diversity lie in the CPS synthesis locus, with numerous genetic variants contributing to differences in capsular thickness, composition, and virulence factors (Kolkman et al., 1997; Llull et al., 2001). The roles of the CPS are multifold: i) it can act as a protective barrier that enhances resistance to environmental stress, desiccation; ii) it can host immune defences; iii) it promotes biofilm formation; iv) it mediates its interaction with the environment (Corbett & Roberts, 2008; Whitfield, 2006). Moreover, CPSs are among the bacterial virulence factors; in fact, they enhance the ability of bacteria to cause disease, avoiding phagocytosis and improving cell adhesion to host tissues (Costerton et al., 1987). This is particularly evident in members of the genus *Vibrio*, which include numerous species associated with marine organisms, ranging from commensals to opportunistic and pathogenic bacteria (Hewson, 2025; Hira & Stensvåg, 2022).

Psychrophilic marine bacteria, which thrive at temperatures typically below 5 °C, exhibit unique biochemical adaptations that enable survival and metabolic activity in these extreme environments (Methé et al., 2005). The composition of CPS in cold-adapted bacteria typically includes a variety of monosaccharides that can vary significantly across different species. For instance, the psychrophilic bacterium *Colwellia psychrerythraea* synthesizes a CPS characterized by a tetrasaccharide repeating unit composed of two amino sugar residues and two galacturonic acid units, one of which is further functionalized by an amide-linked threonine. This distinctive CPS architecture closely mimics structural features of antifreeze glycoproteins (Carillo et al., 2015). Cold-adapted bacterial CPSs provide significant protection against environmental stressors common in cold marine settings by enhancing cell integrity and stability (Methé et al., 2005). These polysaccharides form a protective barrier that shields bacterial cells from harmful agents, such as antimicrobial compounds and desiccation, thereby promoting survival under extreme conditions (Casillo et al., 2018). Moreover, these polysaccharides facilitate biofilm formation, a critical process that enables bacteria to adhere to surfaces such as ice, sediments, and marine debris; thus, the ability to form biofilms through CPSs supports colonization and nutrient acquisition in a competitive environment (Helmke & Weyland, 1995; Marx et al., 2009). The exploration of CPS from psychrophilic bacteria not only enhances our understanding of microbial life but also paves the way for novel biotechnological innovations.

1.2.2 Gram-negative exopolysaccharides

Exopolysaccharides (EPS) are polysaccharides secreted into the extracellular environment, where they either form loose slime layers or contribute to the structured matrix biofilm (Casillo et al., 2018). Marine bacteria produce EPS in a variety of habitats: seawater sediments (Matsuyama et al., 2006), sea-ice (Nichols et al., 2005), hydrothermal vents (Delbarre-Ladrat et al., 2017), hypersaline ponds (Llamas et al., 2012), and as animal hosts (Concórdio-Reis et al., 2021). These niches impose stress conditions such as low temperature, high pressure, high salinity, metal toxicity, and low nutrients, which often are the main trigger for the abundant EPS production (Casillo et al., 2018; Delbarre-Ladrat et al., 2014). EPS production is therefore useful to the gram-negative bacteria to help maintain hydration, protect from ice crystal damage, bind and sequester metal ions, and act as a barrier to predators or viruses (Casillo et al., 2018; De Carvalho, 2018; Poli et al., 2010). Moreover, EPSs enable bacteria to attach to surfaces and initiate biofilm formation (Lipsman et al., 2024). EPS produced by bacteria also represents a crucial component of microbial life. In fact, these molecules contribute to influencing carbon fluxes by taking part in the marine snow formation and microbial aggregates, and they serve as substrates for other microbes (Decho & Gutierrez, 2017).

EPS are high molecular weight heteropolysaccharides mostly composed of two or more different monosaccharides arranged within repeating units of often 5-12 residues. Marine EPS exhibit exceptional structural diversity and often contain uronic acids, sulfate groups, and monosaccharides such as rhamnose or fucose (Alharbi et al., 2023; Zhang et al., 2015). The structural features of EPS strongly influence their function: higher molecular weight and branching may increase viscosity and structural stability of biofilms, or uronic acid and sulfate groups increase polyanionic charge and metal-binding capacity, enhancing protection and gel formation, and rare sugars and substituents may confer unique rheological properties desirable for biotechnological applications (Concórdio-Reis et al., 2022; Ibrahim et al., 2022; Zhang et al., 2015). The structural variability of EPS often leads to functional similarities with glycosaminoglycans (GAGs), such as hyaluronic acid, chondroitin sulfate, and heparan sulfate (Pomin & Mourao, 2008). These "GAG-like" EPS share structural motifs such as alternating uronic acid and hexosamine residues, sulfation patterns, and polyanionic nature, which confer biological activities including cell signalling, antioxidant, anticoagulant, and immunomodulatory effects (Delbarre-Ladrat et al., 2014; Casillo et al., 2018). Among the various types of marine bacterial EPS, those derived from the *Alteromonas* genus, particularly *Alteromonas infernus*, have garnered attention (Raguénès et al., 1997). These polysaccharides display structural features similar to naturally occurring GAGs. Moreover, the EPS known as diabolican produced by *Vibrio diabolicus* has been demonstrated to possess the capacity to mimic GAGs, offering advantages over traditional GAG sources derived from animals in reducing immunogenicity and ethical concerns associated with animal farming (Chong et al., 2005; Liu et al., 2011; Restaino et al., 2017).

1.3 Seaweeds

Seaweeds, also known as marine macroalgae, are multicellular, photosynthetic organisms found primarily in coastal marine environments. Seaweeds are classified into three major groups: Brown algae (*Phaeophyceae*), Red algae (*Rhodophyceae*), and Green algae (*Chlorophyceae*) (Belghit et al., 2017; Mohamed et al., 2012; Wan et al., 2019). This classification is based on photosynthetic pigments, with brown algae containing fucoxanthin, green algae containing chlorophylls a and b, and red algae containing a specific combination of pigments, such as chlorophylls *a* and *d*, carotenoids, and phycobiliproteins (Cian et al., 2015; Gurgel & Lopez-Bautista, 2007). They play a fundamental ecological role as primary producers, oxygen generators, and habitat formers, sustaining coastal food webs and providing shelter for a wide range of marine organisms (De Clerck et al., 2013; Popper et al., 2011)

The roles of polysaccharides derived from macroalgae fulfil critical functions within marine ecosystems, contributing significantly to ecological balance and ecosystem services. They are a fundamental component of the marine food web, supplying essential polysaccharide-derived carbon sources for herbivores. Additionally, they play a pivotal role in nutrient cycling through the utilisation of anionic polysaccharides, which function as biological filters by binding dissolved nutrients such as nitrogen and phosphorus, thereby enhancing water quality in coastal ecosystems (Xie et al., 2024).

Polysaccharides present in seaweeds serve as storage polysaccharides and are renowned for their high content of CWPS. The functions of seaweed CWPS are diverse, including providing mechanical shear resistance, facilitating cell-cell adhesion (Shao & Duan, 2022), and enhancing flexibility (Hentati, Tounsi, et al., 2020). Additionally, they are utilized by the cell for photosynthetic storage or function as osmoprotectants (Iwamoto & Shiraiwa, 2005). The quantity and composition of these polysaccharides differ among various genera and are influenced by several factors, such as seasonal changes (Jothisaraswathi et al., 2006) and the growth stage of the algae (Falshaw & Furneaux, 1995). Furthermore, variations in polysaccharides may also result from abiotic factors like salinity and temperature, as well as biotic factors such as pathogens. These polysaccharides act as a barrier against these factors, providing a protective layer that helps prevent infections and mitigate stress conditions (Mokrosnop & Zolotariova, 2020). CWPS are one of the main cell wall components, reaching 75% of the dry weight. They form microfibrillar scaffolds embedded in amorphous matrices of heterogeneous polysaccharides and glycoproteins. The compositional and structural diversity of CWPS is considerable: for example, brown algae are enriched in anionic polymers such as alginates and fucoidans (Beuder & Braybrook, 2023); red algae contain abundant sulfated galactans, including agar and carrageenan (Usov, 2011); and green algae synthesise ulvans and other sulfated rhamnose-rich polysaccharides (Rioux et al., 2017). These polymers differ not only in monosaccharide composition and linkage types, but also in degrees of sulfation, branching, molecular weight, and association with metals or mineral phases (Zhong et al., 2020).

1.3.1 Coralline cell-wall polysaccharides

Red algae are the largest group of seaweeds, with an amount of 6,000 different species. They thrive in a wide range of marine environments, from intertidal zones to depths up to 200 m, aided by accessory pigments and specialized cell-wall matrices (Carpena et al., 2023). The polysaccharides comprising a major portion of their cell walls are sulfated galactans, notably agar and carrageenan, which may account for 40-50 % of dry matter in some species (Alfinaikh et al., 2025). Carrageenans are composed of linear, sulfated D-galactans consisting of a disaccharide repeating unit of 3-linked β-D-galactopyranose called G-units and 4-linked α-D-galactopyranose called D-units, or 3,6-anhydro-α-D-galactopyranose called DA-units (Perez Recalde et al., 2016). The major commercial types are κ-, ι-, and λ-carrageenan (Campo et al., 2009). Agar is composed of a disaccharide of alternating (1,3)-linked *β*-D-galactose and (1,4)-linked 3,6-anhydro-*α*-L-galactose. Agar can be constituted by agarose and agaropectin. Agarose is a linear and neutral polysaccharide composed of β-D-galactose and 4-linked 3,6-anhydro-α-L-galactose (Araki et al., 1967). Instead, agaropectin is an acid polysaccharide since agarobiose can be linked to sulfate groups, pyruvic acid, and D-glucuronic acid. The composition and yield of these polysaccharides are influenced by seasonal changes, species, harvest time, and extraction method (Abou Zeid et al., 2014; Ismail & Kanaan, 2022)

Coralline red algae are a specialised clade within Rhodophyta characterised by deposition of calcium carbonate within their cell walls, thereby contributing to reef structure and substrate consolidation (Venuleo & Giordano, 2019). In fact, they act as ecosystem engineers in shallow marine habitats, forming biogenic crusts that stabilize sediments, create microhabitats for invertebrates, and contribute significantly to global carbonate budgets (Foster, 2001; Kamenos et al., 2013)

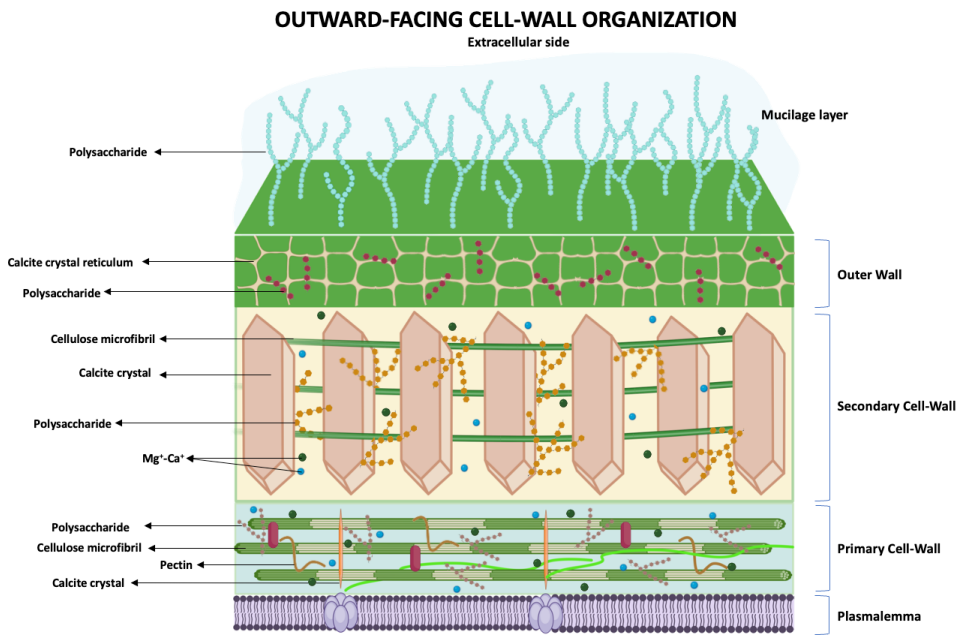

Figure 3. Coralline seaweeds outward-facing cell-wall structure.

The cell wall of coralline red algae is typically stratified into multiple layers (Fig.3). These zones are organized from the inner to the outer surface as follows: the plasma membrane, a thin primary cell wall (PCW), and a thick secondary cell wall (SCW) (Bracchi et al., 2021; Nash et al., 2019), and the most external layer is the Outer Wall (OW), for those cells facing the extracellular environment, while an interfilamentous space is present between adjacent cells (Liyanage et al., 2023; Yermak et al., 2022). The PCW can be non-calcified or slightly mineralized, and it consists mainly of hydrated, amorphous polysaccharides and cross-linked fibrils that provide elasticity and permeability. This region serves as the primary site for crystal nucleation. The SCW is dominated by Insoluble Organic Matter (IOM), forming the fibrillar scaffolds rich in cellulose-like microfibrils, β-glucans, and acidic polysaccharides, due to the presence of uronic acids, which bind the Ca^{+} and Mg^{+} and allow the calcifications. In fact, Mg-calcite crystals are also present and are embedded within or attached to the fibrillar matrix (Bergstrom et al., 2023; McCoy & Kamenos, 2015; Rahman & Halfar, 2014), providing both rigidity and flexibility to withstand hydrodynamic stress (Kamenos et al., 2013; Nash et al., 2019). The OW is densely packed with calcite crystals embedded in a dense polysaccharidic matrix with highly sulfated galactans. The OW can be covered in a mucilage layer with soluble polysaccharides, which helps with cell adhesion and acts as a defence against environmental stress (Liyanage et al., 2023; Yermak et al., 2022). On the other hand, the interfilamentous space between cells is filled with Soluble Organic Matrix (SOM) rich in sulfated galactans and glycoproteins. In corallines, the CWPS thus contribute to dual functionality: they provide an organic scaffold for calcification and mechanical resilience. They differ from flashy red algae both in composition and structure (Venuleo & Giordano, 2019). In fact, they possess some specific cells highly specialized to the deposition of high-Mg calcite within an organic polysaccharide and protein matrix (Nash et al., 2019). Nonetheless, recent analyses have shown that the monosaccharide composition of CWPS among Coralline taxa varies considerably, probably due to environmental stress (Venuleo & Giordano, 2019). In terms of polysaccharides, the main differences with fleshy red algae are the presence of sulfated xylogalactan, which has high quantities of xylose (Malagoli et al., 2014), and 3,6-anhydrogalactose, which is absent in Coralline (Bilan & Usov, 2001). Nonetheless, the main polysaccharides found in Coralline algae, besides cellulose, hemicellulose, and pectin in the form of fibrils, are alginic acid, which bonds with calcium thanks to its high cation affinity for the calcification process, and xylo-galanctans (Malagoli et al., 2014; Okazaki et al., 1982).

1.4 Marine microalgae

Microalgae are a diverse group of autotrophic microorganisms that play crucial functions in aquatic ecosystems. In the marine environment, they constitute the phytoplankton, a group of photosynthetic unicellular organisms that play an essential role as primary producers in the marine trophic chains. Although the term ‘microalgae’ lacks strict taxonomic meaning, it typically denotes organisms with a cell size between 0,2 to 200 µm in aquatic environments

(Gualtieri & Barsanti, 2022; Sieburth et al., 1978). Many microalgae are found in freshwater or marine systems and belong to various taxonomic groups, each with distinct cellular morphologies and adaptations (Liber et al., 2020). Morphologically, microalgae can exhibit various shapes, including spherical, rod-like, filamentous, and plate-like structures, which can influence their buoyancy and ability to capture light (Coêlho et al., 2019; Raven & Girard-Bascou, 2001). Microalgae are categorized into planktonic forms, which drift freely in the water column, and benthonic forms, which grow on submerged surfaces (Dolganyuk et al., 2020). Many of them, such as Clamydomonas and Tetraselmis, possess flagella, which aid in their motility and enable them to navigate through different water layers in pursuit of light and nutrients (Blanchard, 1990; Dolganyuk et al., 2020)

Microalgae's ecological roles are foundational. Besides being responsible for a large fraction of global primary production, they also contribute significantly to CO_2 fixation (Falkowski et al., 1998; Field et al., 1998), colonize benthic or biofilm niches, influencing habitat structure and nutrient flows (Azam et al., 1983; Juranek et al., 2020). Through the production of extracellular substances, including EPSs, they influence particle aggregation, marine snow formation, sediment stability, and therefore biogeochemical transport of carbon and nutrients (Alldredge & Silver, 1988; Decho & Gutierrez, 2017).

Microalgae EPSs are synthesized via biosynthetic pathways that involve various metabolic processes, ultimately exuding these polysaccharides into the surrounding medium, and partially, they remain bonded to the external side of the cell wall (Cunha et al., 2019). The ratio of released to cell-associated vs EPS can vary significantly with the growth phase, salinity, and nutrient status (Boonchai et al., 2015; Guzmán-Murillo et al., 2007). Microalgae produce and secrete EPS for several reasons: utilize EPS to shield themselves against biotic stressors, such as predation by microzooplankton (Zhu et al., 2024), defence against pathogens and viruses (Pointcheval et al., 2025), and abiotic stresses such as desiccation and osmotic pressure (Li et al., 2023, 2022). Moreover, these polysaccharides can serve as a barrier to toxic substances, assisting in the detoxification of harmful compounds present in their environment (Freyria et al., 2024; Gongi et al., 2023). By forming a matrix through which nutrients and pollutants can be trapped, the EPS facilitates their absorption, thus enhancing nutrient retention and uptake (Agoun & Avci, 2025; Kronusová et al., 2022; Vergnes et al., 2019). Lastly, EPSs influence the stickiness of algal colonies. Thanks to these mucous aggregates, microalgae create a cohesive matrix that binds individual cells together to remain in the photic zone, maximizing light exposure and enhancing photosynthesis (Lee et al., 2023; Ye et al., 2024). EPSs not only change based on the species, but microalgae can modulate their production by nutrient limitations such as nitrogen or phosphorus deprivation, changes in light intensity, or other stresses (Moreira et al., 2022; Pierre et al., 2019). In fact, microalgae proved a high metabolic plasticity since they can grow in different culture conditions, such as autotrophic, mixotrophic, and heterotrophic, thanks to their capacity to modulate carbon allocation under stress or nutrient limitation (Brennan & Owende, 2010; Vásquez - Piñeros et al., 2012). Specifically, it was proven that in heterotrophic conditions, they produce highly valuable metabolites, including

EPSs (Choix et al., 2012; Gladue & Maxey, 1994; Parra-Riofrío et al., 2020). Microalgae EPS are typically heteropolysaccharides, and their composition can vary widely among taxa and growth conditions. Some EPS are more complex and contain sulfated polysaccharides, while others are simpler in structure, composed mainly of neutral carbohydrates (Borjas Esqueda et al., 2022). Monosaccharides commonly found in microalgal EPS include glucose, galactose, rhamnose, and mannose, contributing to distinctive polysaccharide profiles (Costa et al., 2021).

1.4.1 Tetraselmis Exopolysaccharides

The genus Tetraselmis belongs to the class *Chlorodendrophyceae*, in the phylum Chlorophyta, with around 20 species identified to date. Phylogenetic analyses using nuclear ribosomal data indicate that Tetraselmis represents an early branching clade among green algae (Sun et al., 2016). Molecular studies have provided insights into the chloroplast genome of Tetraselmis, which has been found to lack several genes necessary for chlorophyll synthesis that are typically present in other core chlorophytes, contributing to the understanding of its evolutionary adaptations (Turmel et al., 2016). The Tetraselmis genus includes unicellular green microalgae species (10-20 μm) characterized by an ellipsoid or ovoid shape, four flagella in the apical depression of the cell (called pit), and a solid cell wall called theca made of different-shaped "scales" that fuse in the extracellular environment (Baudelet et al., 2017; Mata et al., 2023). In the Tetraselmis genus, the cell wall organization and components of single layers vary strongly among species, making the identification extremely difficult. For instance, two different types of thecae were identified. The Type I is a simple bilayer theca; the Type II is a multilayered theca composed of up to 5 layers (Domozych et al., 1981; Hori et al., 1982). Briefly, a type II, three-layer theca layers are described as follow (Fig.4): a thick electron-dense inner layer is located just outside the plasma membrane; a thin, electron-dense middle layer with a fibrous or reticulate texture constituted by two sublayers, is a connection between the inner and outer parts; and then a thick, slightly electron-dense outer layer is composed of fused scales and rich in fibrils. Lastly, there is a really thin granular coat made of hairs and granules that form the cell's characteristic spiny, alveolar, smooth, or ornamented surface (Becker et al., 1998; Domozych et al., 1981). In terms of polysaccharides, the theca scales are mainly made of acidic polysaccharides, including 3-deoxy-D-*manno*-octulosonic acid (Kdo) as the main theca component reaching up to 60% (Becker et al., 1995), 3-deoxy-L-*threo*-heptulosaric acid (Dha), deoxy-5-*O*-methyl-*manno*-2-octulosonic acid (5OmeKdo), GalA, and natural ones like gulose, galactose, and arabinose (Amna Kashif et al., 2018; Becker et al., 1998; Mclachlan & Parke, 1967).

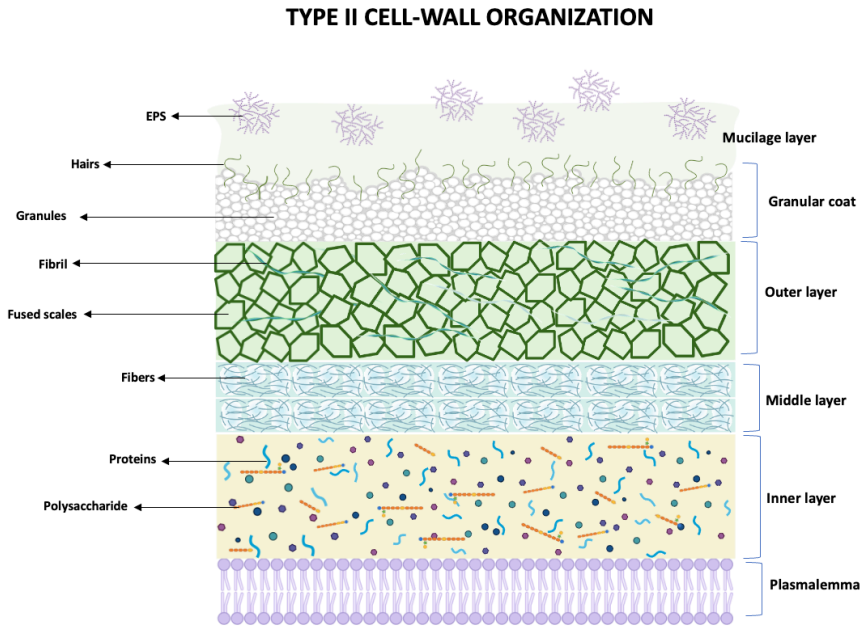

Figure 4. Tetraselmis type II cell-wall structure.

In *Tetraselmis* spp., the extracellular space is often surrounded by a thin mucilaginous envelope, resulting from the secretion of EPS through vesicular transport or shedding of cell wall layers during growth and environmental stress (Domozych & LoRicco, 2023). EPS secretion can occur passively through diffusion or sloughing of the cell wall surface or actively, via exocytosis of vesicles containing polysaccharide precursors synthesized in the Golgi apparatus (Domozych et al., 1993; Domozych & LoRicco, 2023)

When it comes to structural analysis and characterization of *Tetraselmis* EPS, little is still known. Reported EPS from *Tetraselmis* species show variable monosaccharide composition, including glucose, galactose, mannose, rhamnose, xylose, arabinose, and uronic acids (Gaignard et al., 2019), with the relative abundance of these sugars differing between species and strains.

1.5 Polysaccharides biological activities and applications

Many marine biomolecules, including polysaccharides, are classified as GRAS (Generally Recognized As Safe) and are thus biodegradable and biocompatible. Polysaccharides, thanks to their chemical diversity, have attracted growing biotechnological interest and potential applications in pharmaceuticals, cosmetics, aquaculture, and biotechnology (Fig. 5). Consequently, understanding the structural variability of marine polysaccharides is essential not only for understanding marine biology but also for sustainable biotechnology development.

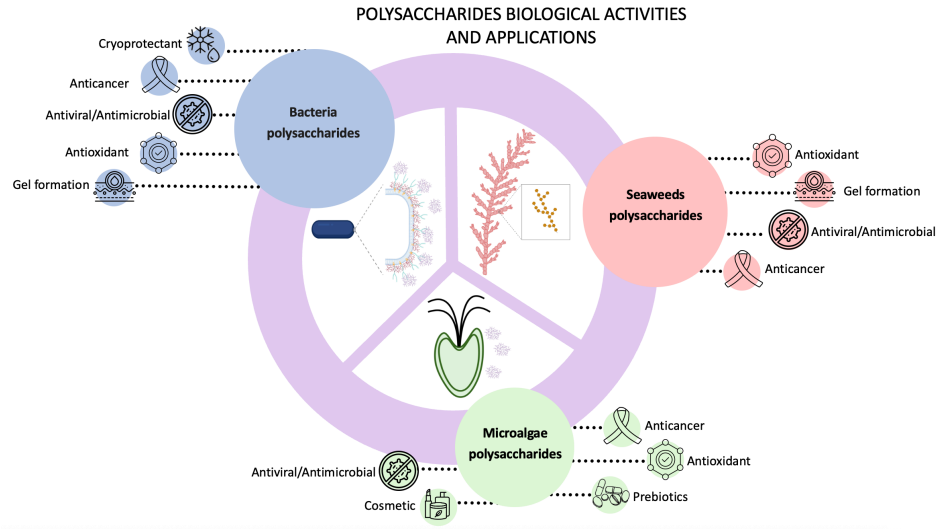

Figure 5. Overview of polysaccharides' biological activities and applications.

1.5.1 Antioxidant activities

A large body of literature shows that marine polysaccharides, including algal sulfated polysaccharides and microbial EPSs, have antioxidant activity. The antioxidant activity of polysaccharides is significantly influenced by factors such as their solubility, monosaccharide compositions, molecular weight, the presence of positively or negatively charged groups, the presence of proteins, and phenolic compounds that are covalently linked (Fernandes & Coimbra, 2023).

Bacterial EPSs isolated from extreme marine environments, such as deep sea and hypersaline waters, showed strong antioxidant activity (Arun et al., 2017; Squillaci et al., 2016; Sun et al., 2014). The applications of antioxidant marine microbial EPSs are found in cosmetic, food, and medicine fields, showing not only antioxidant activity per se but also low toxicity, biocompatibility, and potential anticancer (El-Newary et al., 2017; Manivasagan et al., 2013; Ramamoorthy et al., 2018; Wang et al., 2018)

Various studies have evaluated the antioxidant activities of EPS derived from different microalgae species, revealing that these microalgae can produce EPS with substantial antioxidant capabilities, often in correlation with other compounds (Azaman et al., 2017; Mousavian et al., 2022). Microalgae EPS high diversity has been attributed to the versatile regulation of polysaccharide biosynthesis to adapt to different environmental conditions, uncovering new antioxidant EPSs (Fimbres-Olivarria et al., 2018; Xie et al., 2024), suitable for cosmetic and nutraceutical applications. In the former, EPSs are utilized in cosmetic formulations to provide protection against environmental stressors and enhance skin health,

developing antioxidant therapies against degenerative diseases and oxidative stress (Burg & Oshrat, 2015; Gargouch et al., 2021), whereas in the latter, they promote health and prevent lifestyle-related diseases (Sun et al., 2009).

A plethora of studies indicates that the antioxidant properties of seaweed polysaccharides can be attributed to their ability to scavenge free radicals, which is essential in fighting oxidative stress, an underlying factor in numerous chronic diseases (Wang et al., 2008; Yang et al., 2012). The structure, molecular weight, type of monomer residues, degree of sulfation, and the sulfate position within these polysaccharides significantly affect their antioxidant activity (Arunkumar et al., 2021). The extraction of these bioactive compounds can influence their antioxidant performance. Enzyme-assisted extraction has proven effective in isolating polysaccharides that maintain or even enhance antioxidant activities compared to traditional extraction methods (Wei et al., 2024). Polysaccharides from *Laminaria japonica, Gracilaria* spp., and *Fucus vesiculosus* exhibit strong antioxidant activities (Rupérez et al., 2002; Wang et al., 2008; Yangthong et al., 2009). Specifically, the ones extracted from brown algae generally possess superior properties (Bhuyar et al., 2021). Their ability to protect cells from oxidative damage has been documented in several models, including zebrafish, emphasizing their applicability in both healthcare and food preservation (Wei et al., 2024; Yang et al., 2012).

1.5.2 Antimicrobial and antiviral activities

Both bacterial CPS, EPS, and algal polysaccharides display antimicrobial and antiviral activities. Gram-negative bacterial surface polysaccharides can interfere with colonisation and biofilm formation by competitors or pathogens, while certain algal and microalgal EPS directly inhibit virus adsorption or replication (Wang et al., 2023). Specifically, bacterial EPSs have been found to inhibit the growth of drug-resistant pathogens such as *Pseudomonas aeruginosa* and *Candida albicans* (Abinaya et al., 2018; Wu et al., 2016). Isolated CPS from marine strains have been associated with antibiofilm and antimicrobial effects, modulation of host immunity in host-associated bacteria (Casillo et al., 2019; D'Amico et al., 2025).

Microalgae exopolysaccharides exhibit significant antimicrobial and antiviral activities, providing a promising avenue for developing new therapeutic agents. EPSs from *Tetraselmis suecica* and *Porphyridium cruentum* showed activity against fish viruses (Parra-Riofrio et al., 2023), while other *Tetraselmis* strains have exhibited antibacterial activity, specifically against antibiotic-resistant bacteria (Hussein et al., 2020). EPS derived from *Chlamydomonas reinhardtii* and *Porphyridium marinum* demonstrate potent antibacterial activities against a variety of pathogens, including both gram-negative and gram-positive bacteria, by disrupting bacterial membranes or interfering with their metabolic processes, pointing to their potential use as natural antibiotics (Gargouch et al., 2021; Vishwakarma & Vavilala, 2019). Microalgae EPS composition and structure are influenced by growth conditions, which can affect their bioactivity and efficacy as antimicrobial or antiviral agents (Jung et al., 2022; Pointcheval et

al., 2025). Microalgae can produce these bioactive compounds cost-effectively, while also utilizing waste materials and carbon dioxide for their cultivation, representing an environmentally sustainable approach as already explored with bacteria (Concórdio-Reis et al., 2023; Costa et al., 2021).

Polysaccharides like laminarin and ulvan, derived from different brown and green seaweeds, have shown promising antimicrobial activities that inhibit the growth and biofilm formation of pathogenic bacteria, further supporting their use as natural preservatives in food systems (Corino et al., 2021; Jun et al., 2018). Fucoidan, a sulfated polysaccharide predominantly found in brown algae, has been well-documented for its antimicrobial effects. For instance, fucoidan extracted from *Sargassum wightii* exhibits inhibitory activities against a range of human bacterial pathogens, including *Staphylococcus aureus* and *Escherichia coli,* thanks to the interaction of fucoidan with bacterial cell walls and membranes, which can lead to inhibition of growth and cell death (Marudhupandi & Kumar, 2013). Moreover, the combination of fucoidan with antibiotics has shown a synergistic effect in enhancing antibacterial efficacy against drug-resistant strains of *Staphylococcus aureus* (Choi et al., 2015; Poveda-Castillo et al., 2018). Polysaccharides from marine algae have shown promising antiviral effects, making them candidates for infection preventative measures (Saranya et al., 2023). Relevantly, polysaccharides such as λ carrageenan can inhibit the replication of influenza viruses and SARS-CoV-2, which can happen since sulfated polysaccharides disrupt viral life cycles by blocking viral entry into host cells, thus preventing infection (Conesa et al., 2023; Jang et al., 2021).

1.5.3 Anticancer and immunomodulatory activities

Marine bacterial exopolysaccharides hold substantial promise as anticancer agents and immunomodulators. A pivotal study by Cao et al (Cao et al., 2018) highlighted the anticancer effects of a marine bacterial polysaccharide, which was shown to inhibit growth in lung cancer cells by blocking cell adhesion and stimulating “anoikis”, a form of programmed cell death that occurs in detached cells. Another research study demonstrated the anti-metastatic properties of a different marine EPS derivative designed to mimic glycosaminoglycans GAG (Heymann et al., 2016). In addition to their direct cytotoxic effects, marine bacterial EPS have been identified for their immunomodulatory functions, which can further boost their anticancer potential. For instance, polysaccharides derived from *Bacillus* species have shown significant activity against human breast cancer cells, promoting apoptosis through the activation of pro-apoptotic factors (Vidhyalakshmi, 2013). This emphasizes how marine bacterial EPS can target critical cellular pathways to induce cell death in cancer cells. The specific molecular composition and structure of these polysaccharides can influence their biological activities. Uronic acids and neutral sugars in the structure of EPS contribute to their bioactive properties, facilitating interactions with cancer cells and immune components (Delbarre-Ladrat et al., 2022). The sulfation of EPS has been linked to enhanced biological activity, as sulfated polysaccharides have been observed

to exhibit stronger cytotoxic effects against various cancer cell lines compared to their non-sulfated counterparts (Heymann et al., 2016).

The exploration of microalgae-derived EPS has revealed significant anticancer and immunomodulatory activities. Research indicates that EPS from *Porphyridium marinum* demonstrates notable anticancer potential (Gargouch et al., 2021; Park et al., 2017; Xiao et al., 2018). In the *Tetraselmis* genus, *T. suecica* has shown promise for its anticancer and immunomodulatory properties (Hussein et al., 2022). The structural characteristics of EPS play a pivotal role in their bioactivity. The molecular weight, branching degree, and specific structural features of EPS significantly influence their immunomodulatory and anticancer capabilities (Angelis et al., 2012). As an example, sulfated polysaccharides derived from the diatom *Gyrodinium impudicum* demonstrated that modifications in structure could enhance their immunostimulatory activity, impacting macrophage responses against tumour cells (Yim et al., 2005). Additionally, high-molecular-weight polysaccharides have been noted to better modulate immune functions and hold enhanced anticancer properties due to their interactions with immune cells and pathways (Pointcheval et al., 2025). Microalgae's multifaceted roles in direct tumour inhibition and enhancing immune responses signify their potential as bioactive agents in modern therapeutic applications.

The therapeutic benefits of seaweed-derived polysaccharides embrace both anticancer and immunomodulatory effects. Their capability to induce apoptosis, inhibit metastasis, and activate immune responses affirms their significance in cancer treatment strategies, both as standalone agents and as complementary therapies to enhance the effectiveness of conventional cancer treatments. It was reported that fucoidan exhibits substantial anticancer properties against various cancer cell lines, including human colon cancer cells (Hwang et al., 2017; Xue et al., 2012), and in addition to other chemotherapeutic agents, a synergistic effect was highlighted (Chen et al., 2022). Moreover, alginates, carrageenans, and laminarans showed anticancer properties as well, marking how seaweeds' polysaccharides can be a remarkable reservoir of activities for human biotechnological and medical applications (Ko et al., 2012). Lastly, also ulvan polysaccharides from the green algae *Ulva Lactuca* showed antitumour activities (Maray et al., 2023).

1.5.4 Other applications

Beyond their biological and pharmacological activities, marine bacterial polysaccharides (both CPS and EPS) exhibit a wide range of physicochemical properties that make them valuable in biotechnological and industrial applications. Polysaccharides from psychrophilic bacteria modify the structure of ice, creating an organic network that enriches and retains microorganisms within ice matrices (Casillo, Parrilli, et al., 2017). These polysaccharides exhibit high flexibility, increased molecular weight, and a predominance of polar monomers, which enhances their ability to function effectively as cryoprotectants in low-temperature

environments (Casillo, Parrilli, et al., 2017). Such properties are crucial, as they facilitate EPS's role in forming hydrated films that protect against desiccation and freezing damage, which is a key concern in both natural and industrial freezing processes. Moreover, researching the rheological properties of EPS from cold-adapted bacteria has shown promising applications in the food industry, suggesting that manipulating EPS can yield stable thickening agents for food products, which are necessary for maintaining texture during freezing and melting cycles (Radchenkova & Yaşar Yıldız, 2025). The ability of these EPS to form gels and stabilize mixtures enhances their utility in product preservation, especially in cold-chain food logistics. Recent studies have highlighted the potential of marine bacterial polysaccharides as biomaterials in drug delivery systems (Cha et al., 2025), primarily due to their structural similarities to mammalian GAGs. Recent advances have also focused on optimizing polysaccharide formulations to enhance their drug delivery efficiency by combining polysaccharides with other materials, such as biocompatible polymers, to the development of composite systems with improved drug release characteristics (Popa & Atanase, 2021). Furthermore, methods such as encapsulating drugs within polysaccharide nanoparticles or forming hydrogels can further enhance the stability and bioavailability and improve the controlled release of therapeutic agents (Daus & Heinze, 2010). Lastly, capsular polysaccharides derived from non-pathogenic cold-adapted marine species may offer novel antigenic structures with improved stability profiles, which could lead to safer vaccine development (Nakhamchik et al., 2010).

The applications of microalgal exopolysaccharides span across various industries, from food to cosmetics. In the food industry, they serve as additives for texture and stability while also exhibiting health-promoting bioactivities. These polysaccharides are known to enhance food preservation due to their emulsifying properties and are recognized as functional ingredients believed to have prebiotic effects (Qian et al., 2021). In the cosmetics industry, the moisturizing and film-forming capabilities of microalgal EPS make them invaluable components in skincare products. Their ability to create protective barriers against environmental stressors, improve hydration and elasticity, and provide photoprotective effects supports anti-aging formulations (Puchkova et al., 2020).

Seaweed-derived polysaccharides offer a promising array of applications in the form of hydrogels, bioinks for 3D bioprinting, and advanced wound dressings. Their unique properties enable the development of innovative materials that support tissue engineering and regenerative medicine. Alginate hydrogels are widely explored. They can be easily crosslinked using divalent cations like calcium ions, resulting in highly hydrated structures to support cell adhesion and proliferation, making them suitable for applications in tissue engineering (Axpe & Oyen, 2016). Hydrogels based on red algae polysaccharides exhibit unique structural and functional characteristics that are beneficial for wound dressing applications. The ability to form gels in response to temperature changes allows for easy application and removal of dressings, while its gelation properties contribute to efficient moisture retention, which is essential for maintaining a suitable wound healing environment (Deng et al., 2018). Moreover,

these hydrogels have been shown to support the sustained release of bioactive compounds (Jiang et al., 2021), and the antimicrobial properties of certain red algae polysaccharides contribute to their effectiveness as wound dressings, making them suitable candidates for developing antimicrobial wound care products (Cunha & Grenha, 2016; Deng et al., 2018). Recent studies highlight the potential for alginate-based bioinks in creating 3D vascularized tissues and organoids, opening new avenues in regenerative medicine (Jovic et al., 2019; Liu et al., 2022).

1.6 Aim of this work

Marine environments represent an exceptional source of unique glycoconjugates with remarkable physicochemical and biological properties, offering promising applications in the pharmaceutical, cosmetic, and biotechnological fields. Thanks to its vastness, a lot of organic compounds are still unexplored. With this study, we explored:

- The CPS produced by a mutated psychrophilic Gram-negative bacterium *Shewanella vesicula nfnB*, was investigated as a representative model of Gram-negative surface glycoconjugates adapted to extreme marine environments. The study of its altered capsular structure provides valuable insight into the plasticity of bacterial surface polysaccharides, their role in cold adaptation, and their potential for generating novel glycan architectures with biotechnological interest.
- A marine Gram-negative bacterium *Vibrio Crassostreae* associated with Bald Sea Urchins Disease in *Paracentrotus lividus*, was investigated to provide a molecular framework for understanding the role of surface polysaccharides in host-pathogen interactions in marine environments. The structural characterization of the CPS, together with the preliminary analysis of the LPS, offers insight into the chemical diversity of *Vibrio* surface glycoconjugates and represents a crucial step toward elucidating their involvement in pathogenicity and host colonization processes.
- A Gram-negative bacterium, *Alteromonas macleodii* EPS, which possesses glycosaminoglycan (GAG)-like properties, was structurally characterized. Driven by the necessity for a biotechnological alternative to GAGs sourced from animals or pathogens, as their extraction presents significant biosafety and ethical challenges.
- CWPSs extracted from a red Coralline alga, *Ellisolandia elongata,* were studied as an underexplored class of marine glycans with unique sulfation patterns and mineral-associated matrices that revealed novel bio functionalities.
- The EPS secreted by *Tetraselmis* species, were investigated since microalgae are an emerging and largely unexplored source of bioactive polymers, given their ecological significance and their promising antioxidant, antimicrobial, and immunomodulatory properties.

This study focuses on the isolation, extraction, and purification of polysaccharides from three main marine biological sources. Particular attention has been given to optimizing extraction and purification protocols to preserve the native structure of the molecules. The isolated polysaccharides were then characterized through chemical and analytical techniques such as mass spectrometry, ^{1}H, and 2D Nuclear Magnetic Resonance (NMR) spectroscopy, to elucidate their primary structure. Moreover, the present work aims to investigate the potential biological activities of these new marine polysaccharides in order to identify novel bioactive compounds with possible biotechnological relevance. Overall, this study contributes to the understanding of the relationship between the structure and potential bioactivity of marine polysaccharides, to expanding the current knowledge on marine glycobiology, and to valorising marine biodiversity as a sustainable source of bioactive compounds.

This work was founded by the European Biological Resource Center (EMBRC), which actively contributes to the advancement of marine biology and ecology knowledge through academic and research institutions. It intends to discover novel marine resources while significantly mitigating environmental risks, a primary objective of the blue economy.

Chapter 2

Shewanella vesiculosa HM13 *nfnB capsular polysaccharides*

2.1 Shewanella vesiculosa HM13 nfnB

Bacteria produce extracellular membrane vesicles (EMVs) that play important roles in intercellular communication, nutrient acquisition, self-defence, and other functions (Bomberger et al., 2009; Chattopadhyay & Jaganandham, 2015; Schwechheimer & Kuehn, 2015). From an application point of view, EMVs are expected to be useful as a platform for the secretory production of proteins, including membrane proteins. Two different mechanisms for generating EMVs by Gram-negative bacteria have been identified up to now. One has been identified as a blebbing from the outer membrane, whereas the other has been characterized by explosive cell lysis (Roier et al., 2016; Saggese et al., 2022; Schwechheimer & Kuehn, 2015; Turnbull et al., 2016).

Shewanella vesiculosa HM13 is a psychrotrophic Gram-negative bacterium isolated from the intestine of a horse mackerel (*Trachurus japonicus*) and able to produce many EMVs containing a single major cargo protein, named P49 (Chen et al., 2020). It was previously reported that *S. vesiculosa* HM13 produces EMVs via blebbing and pinching off the outer membrane (Chen et al., 2020), carrying a single major cargo protein named P49. In vitro transport assay suggested that P49 is associated with the surface of EMVs. Accordingly, it is essential to reveal the structure of the surface components of EMVs to understand how P49 interacts with EMVs and to develop a recombinant protein production system in which foreign proteins are secreted as cargoes of EMVs. It was demonstrated that the gene coding for P49 is in a gene cluster. This gene cluster contained genes encoding a non-canonical type II secretion system (T2SS), homologs of surface polysaccharide-chain synthesis proteins, including a homolog of a flippase involved in bacterial extracellular polysaccharide synthesis, Wzx, and genes involved in the biosynthesis of surface glycans. The deletion of one of these genes determined the non-association of P49 onto the EMVs. These results suggested that these genes are essential for the synthesis of surface components of EMVs required for P49 loading onto EMVs

To investigate the role of surface polysaccharides in the P49 association, the surface glycoconjugates from the cells and EMVs have been isolated and characterized, starting from *S. vesiculosa* HM13 wild type (Di Guida, Casillo, Yokoyama, et al., 2020; Kamasaka et al., 2020). The cells and the EMVs from *S. vesiculosa* HM13 have been demonstrated to be wrapped by a CPS forming a “corona” layer, the structure of which has been recently characterised (Casillo et al., 2022). Surface polysaccharides may be involved in the adhesion of both cells and EMVs to biotic or abiotic surfaces (Ignatovich, 1975). Since a previous study suggested that the affinity between surface polysaccharides and P49 is reduced in the mutant that lacks *nfnB*, which codes for a nitro-reductase homolog and is in the close vicinity of the P49 gene (Kamasaka et al., 2020), the aim of this work is to characterize surface glycans from this mutant. Here, the isolation, the purification, and the detailed structural determination of a CPS from the cells of the *nfnB* mutant strain of *S. vesiculosa* HM13 are reported. The structure has been determined by using both chemical analysis and NMR spectroscopy.

2.2 Results and discussion

The cells of the *nfnB*-mutant of *S. vesiculosa* HM13 were subjected to extraction by the PCP method, followed by the phenol/water extraction on the cell debris. The precipitation by water from the Ex_{PCP} allowed the pure LPS fraction (yield 1.4%) (Fig. 6).

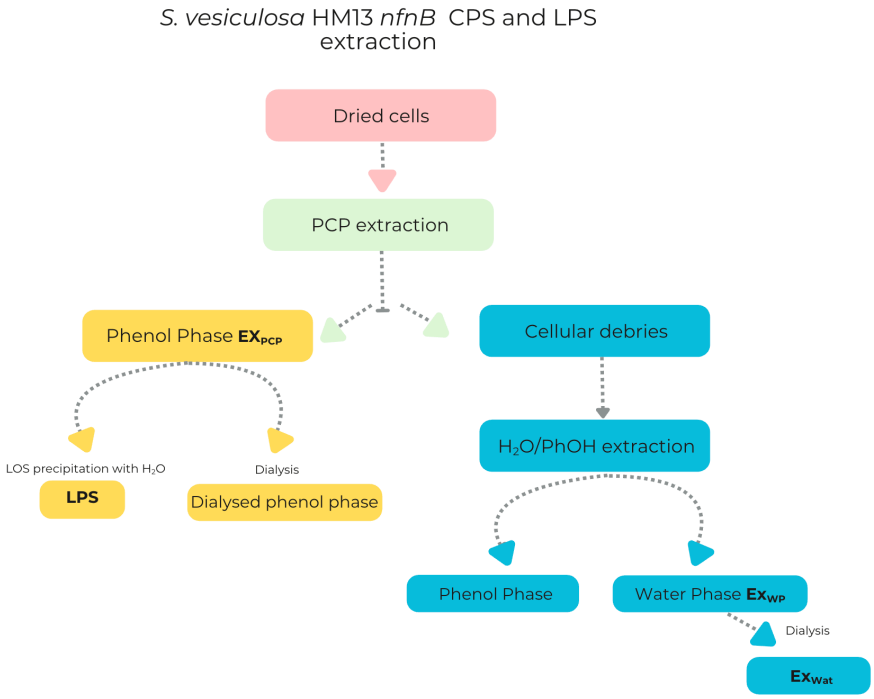

Figure 6. Schematic representation of S. vesiculosa HM13 nfnB CPS extraction.

The glycosyl analysis was identical to the LPS isolated and characterized from *S. vesiculosa* wild-type cells (Di Guida, Casillo, Yokoyama, et al., 2020)(Fig.7).

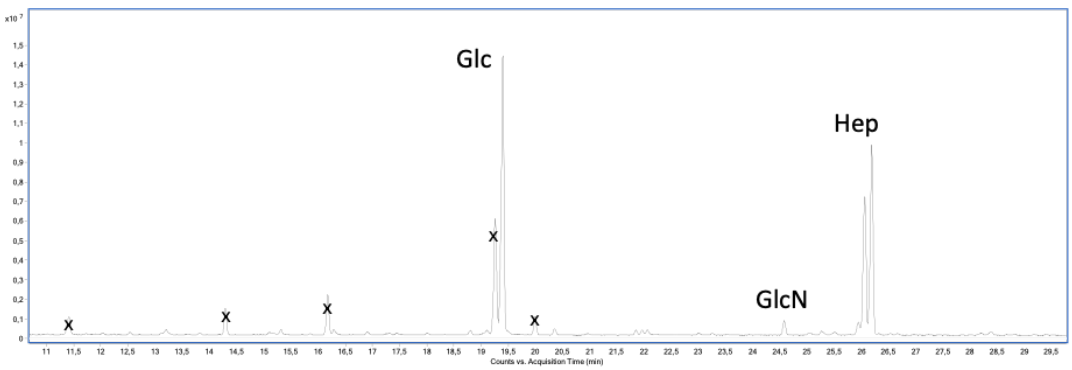

Figure 7. AMG of S. vesiculosa HM13 nfnB LPS. Peaks identified as impurities are marked with an X.

Furthermore, the Ex_{PCP} phenol phase was dialysed and analyzed by GC-MS. The chromatogram revealed the presence of monosaccharides of LPS and the presence of rhamnose (Rha), suggesting the presence of the CPS already isolated from the wild type (Fig. 8).

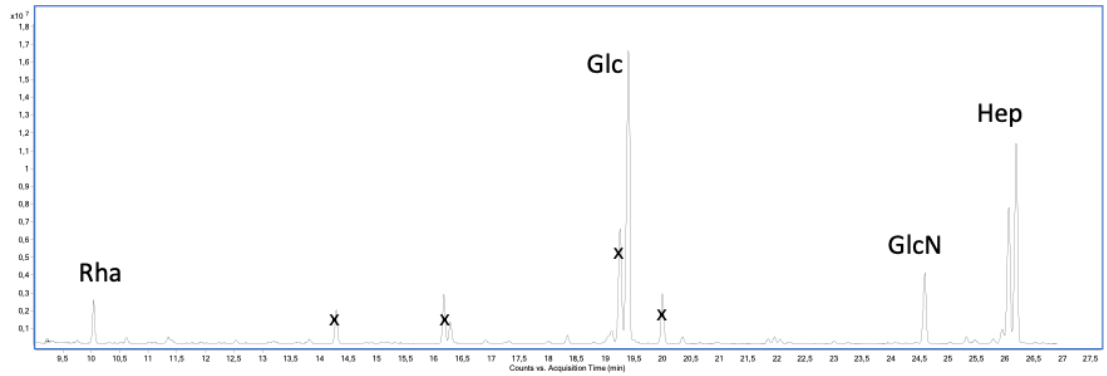

Figure 8. AMG of S. vesiculosa HM13 nfnb Ex_{PCP} phenol phase. Peaks identified as impurities are marked with an X.

Finally, the GC-MS chromatogram of Ex_{WP} water phase extract from the phenol/water extraction revealed the presence of ribose (Rib), usually attributed to the contamination of nucleic acids, glucose (Glc), and traces of 2-amino-2-deoxy-D-glucose (GlcN) and heptose (Hep) (Fig. 9).

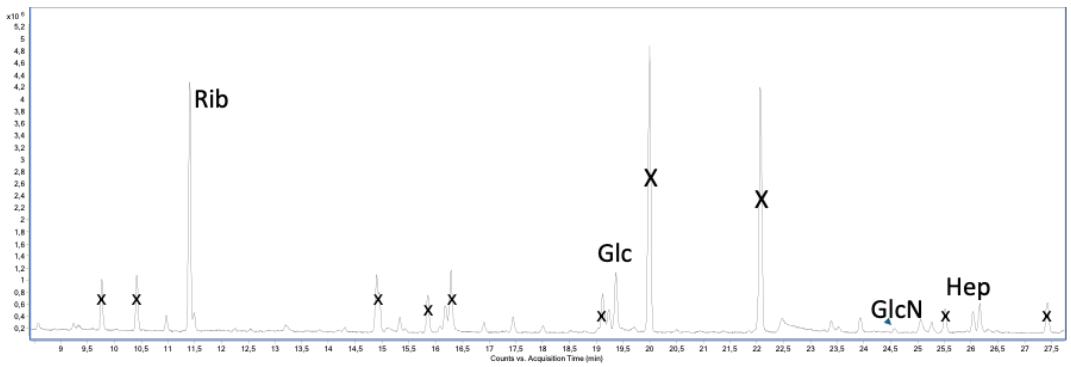

Figure 9. AMG of S. vesiculosa HM13 nfnB Ex_{WP} extract. Peaks identified as impurities are marked with an X.

The dialysed phenol phase was subjected to mild acetic acid hydrolysis and gel filtration chromatography. The fractions were collected and analysed by ^{1}H NMR. The NMR spectrum revealed the presence of the previously characterized CPS (Figure 10a) (Casillo et al., 2022).

Finally, the dialysed water extract Ex_{Wat} was subjected to enzymatic hydrolysis with Dnase, Rnase, and proteinase to remove nucleic acids and proteins. Thereafter, the obtained fraction was subjected to mild acid hydrolysis to remove the remaining LPS, followed by size exclusion gel chromatography. The purified fraction was analysed using chemical analyses and NMR spectroscopy. Overlapped ^{1}H NMR spectra of the CPS corona isolated from the $Ex_{PCP,}$ and the polysaccharide material purified from Ex_{Wat} revealed that the *nfnB*-mutant of *S. vesiculosa* HM13 produces a new polymer (Figure 10b).

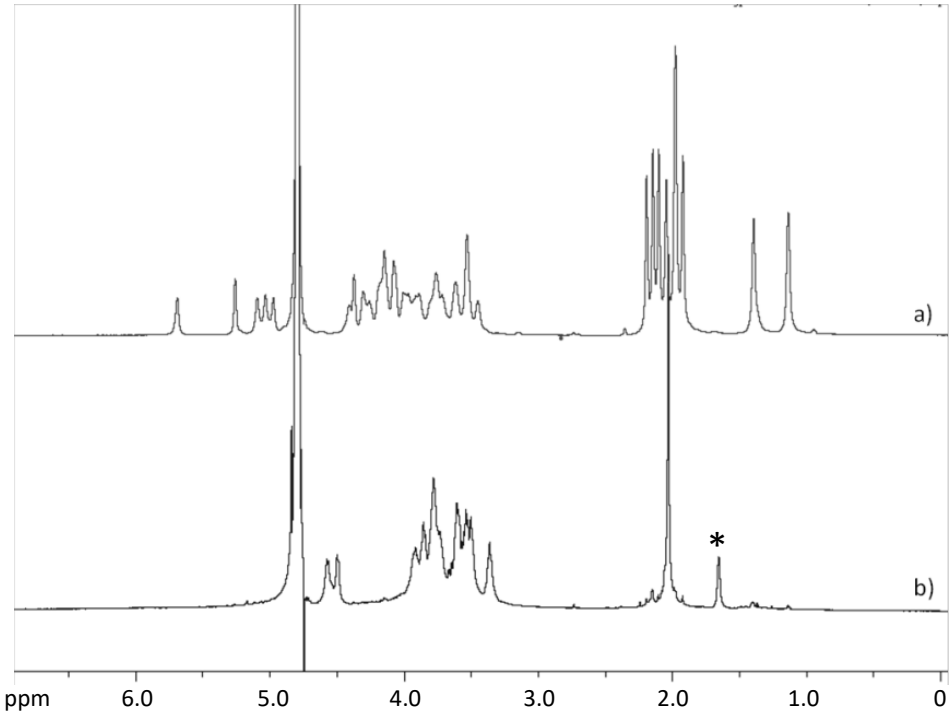

Figure 10. Overlapped [1]H NMR spectra of the polysaccharide material produced by the nfnB-mutant of S. vesiculosa HM13. A) CPS "corona" purified from Ex_{PCP} and b) CPS isolated from Ex_{Wat} of the nfnB-mutant strain of S. vesiculosa HM13. The signal marked with an asterisk refers to a contaminant.

Monosaccharide compositional analysis after derivatisation to obtain acetylated methyl glycoside (AMG) and acetylated 2-octyl glycosides (AOG) disclosed the presence of D-glucose (Glc) and 2-amino-2-deoxy-D-glucose (GlcN). Preliminary inspection of ^{1}H detected β-configured residues, along with a signal at δ 2.02 ppm consistent with the glucosamine N-acetyl group (Figure 10b), confirmed by ^{13}C NMR spectrum (Figure 11).

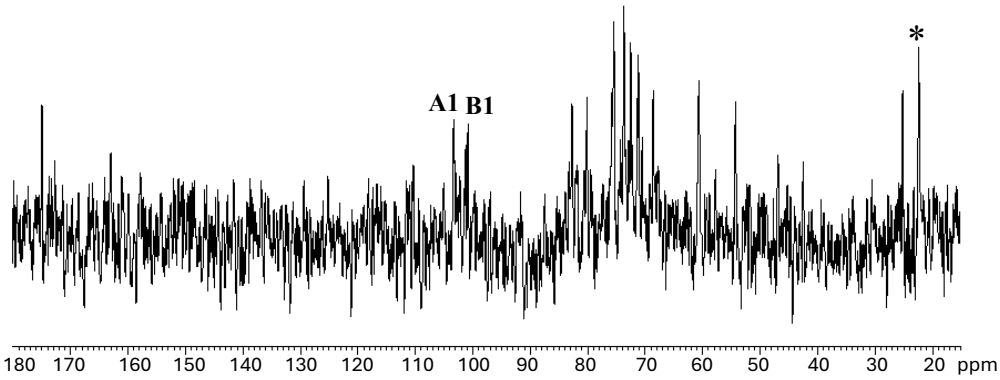

Figure 11. ^{13}C NMR spectrum of the polysaccharide material produced by the nfnB-mutant of S. vesiculosa HM13.

The precise structure was obtained by 2D NMR spectroscopy, and assignments were performed with homo- and heteronuclear 2D NMR spectra (Fig. 12) and are summarized in Table 1. The β anomeric configurations of residues **A** and **B** were deduced from the $^{1}J_{C,H}$ coupling constant values measured in a 2D F*2*-coupled HSQC spectrum (166 Hz and 168 Hz, respectively). Finally, the *gluco*-configuration of both residues was established through the diagnostic correlations in COSY and TOCSY spectra.

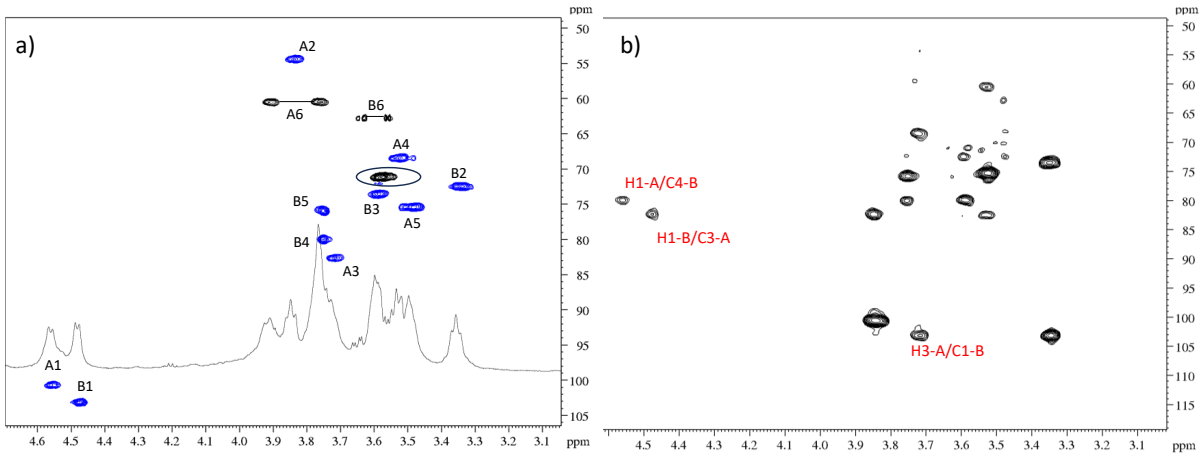

Figure 12. Expanded region of a) ^{1}H-^{13}C DEPT-HSQC and b)^{1}H-^{13}C HMBC spectra of CPS isolated from the nfnB-mutant strain of S. vesiculosa HM13. Spectra were acquired at 298 K by using a 600 MHz in D_2O. The cross-peak signed with a circle is a contaminant.

Residue **A** was identified as β-3-GlcNAc with the anomeric proton chemical shift of 4.56 ppm. The full spin system has been assigned by COSY and TOCSY spectra. The H-2 signal at δ 3.85 ppm, correlating in the HSQC spectrum with a nitrogen-bearing carbon at δ 54.4 ppm (Figure 12a), confirmed the hypothesis. Moreover, the linkage position of this residue was suggested by the glycosylation shift of its C-3 at δ 82.5 ppm with respect to the value of 75.2 ppm of the C-3 of the unsubstituted residue (Bock & Pedersen, 1974). Residue **B** with an

anomeric ^{1}H chemical shift at δ 4.48 ppm was identified as a 4-substituted Glc since its C-4 carbon signal was downfield shifted at δ 79.9 ppm (Bock & Pedersen, 1974).

Table 1. ^{1}H and ^{13}C NMR chemical shifts of polysaccharide isolated from the nfnB-mutant strain of S. vesiculosa HM13 were determined at 298 K by using a 600 MHz instrument. $^{1}J_{C1,H1}$ values are given in Hertz in square brackets. Acetyl group, (CH3) 2.02/22.4 ppm, (CO) 175.0 ppm.

Residue	H1 C1	H2 C2	H3 C3	H4 C4	H5 C5	H6a, 6b C6
β-D-3-Glc*p*NAc **A**	4.56 100.5 [166]	3.85 54.4	3.72 82.5	3.52 68.4	3.49 75.0	3.77 3.92 60.5
β-D-4-Glc*p* **B**	4.48 103.0 [168]	3.35 72.4	3.59 73.4	3.75 79.9	3.75 75.8	3.56 3.62 62.7

Besides the effect of glycosylation on the ^{13}C chemical shift values, glycosidic bonds were also identified based on NOE contacts in a NOESY spectrum and long-range connectivity in an HMBC experiment. Residue **A** was found linked to residue **B** based on a long-range correlation between the H-1 of **A** at δ 4.56 ppm and the C-4 of residue **B** at δ 79.9 ppm (Fig. 12b) and between H-1 of **B** at δ 4.48 ppm and C-3 of **A** at δ 82.5 ppm.

Based on the above-described data, the repeating unit structure of the capsular polymer isolated from the *nfnB* mutant strain of *S. vesiculosa* HM13 is reported in Fig.13.

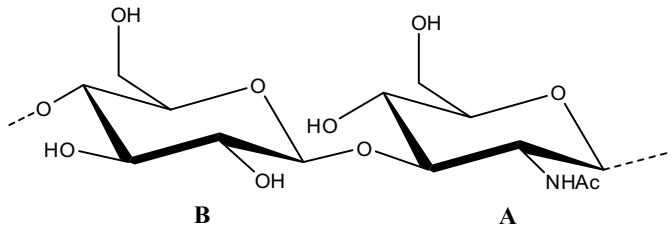

Figure 13. Repeating unit structure of the capsular polymer isolated from the nfnB mutant strain of S. vesiculosa HM13 reported to be →4)-β-D-Glc-(1→3)-β-D-GlcNAc-(1→.

2.3 Conclusion

The surface envelopes of *S. vesiculosa* HM13, from both cells and EMVs, are enriched by a CPS "corona" the structure of which was recently elucidated. In this work, the cells of the *nfnB* mutant of *S. vesiculosa* HM13 have been analysed. Together with the polysaccharide corona already found in its parental strain, HM13-Rif^{r}, the extraction and purification procedures allowed the recovery of an additional CPS. The repeating unit consists of a

disaccharide where a 4-substituted glucose is alternated with a 3-substituted *N*-acetylglucosamine. The same structure has never been reported for other bacterial CPS, although the disaccharide →3)-β-D-GlcNAc-(1→4)-β-D-4-Glc-(1→ occurs as a sub-structure in the pentasaccharide repeating unit of *Shewanella oneidensis* MR4 CPS, leaving the chance to speculate the close similarity of the species *S. vesiculosa* with *S. oneidensis* (Vinogradov et al., 2005). Future studies will be devoted to the comprehension of the role of this polymer on the cell surface and how the mutation of the *nfnB* gene impacts the loading of cargo onto the vesicles.

Chapter 3

Vibrio crassostreae capsular polysaccharides

3.1 Vibrio crassostreae

Vibrio crassostreae is a marine Gram-negative bacterium belonging to the family *Vibrionaceae*, a group that includes several species associated with marine invertebrates (Romalde et al., 2014) and, in some cases, with pathogenic interactions (Bruto et al., 2017). Members of the genus *Vibrio* are well known for their ability to establish close relationships with echinoderms (Hewson, 2025; Hira & Stensvåg, 2022), often mediated by surface-associated macromolecules such as CPS and LPS, which play key roles in host recognition, immune evasion, and virulence.

Bacterial diseases affecting sea urchin populations have gained increasing attention in recent years due to their ecological relevance and potential impact on coastal ecosystems and aquaculture facilities. Among these, Bald Sea Urchins Disease (BSUD) represents a pathological condition characterized by spine loss, epidermal erosion, and progressive tissue damage, ulcer formation (Fig. 14), and has been documented in natural populations of the purple sea urchin *Paracentrotus lividus* in the Mediterranean Sea (Carella et al., 2025). Within this context, *V. crassostreae***,** along with two other Vibrio species, was isolated from *P. lividus* individuals collected in the Bay of Naples (Point Schiavone: 40°45′52″N, 14°02′13″E). Bacterial isolates were obtained from spines and internal tissues of symptomatic individuals and identified by 16S rRNA gene sequencing (Carella et al., 2025). Among the recovered taxa, members of the *Vibrio splendidus* clade, including *Vibrio crassostreae*, were frequently associated with advanced stages of the disease.

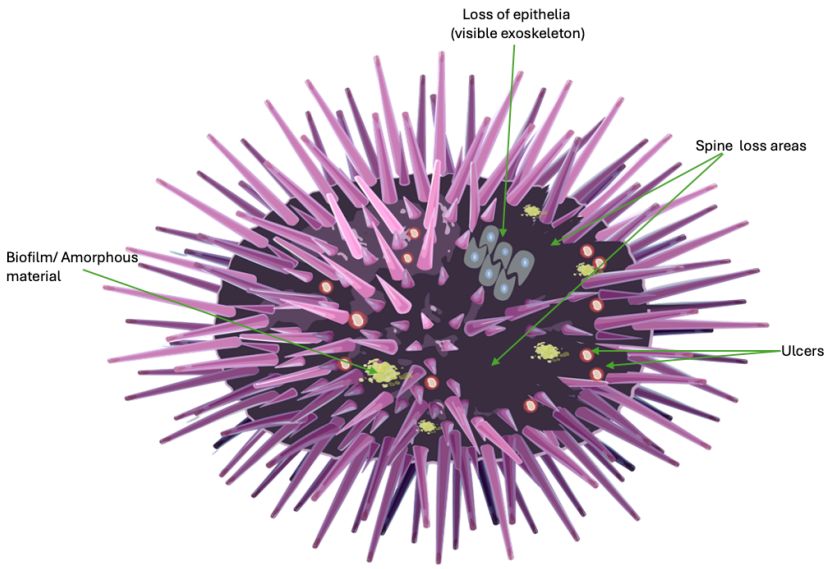

Figure 14. Graphical representation of a sea urchin with BSUD typical symptoms.

CPSs are known to contribute to bacterial persistence in the host environment by protecting host defence mechanisms and by modulating host immune responses (Maue et al., 2013). Similarly, LPS constitute a fundamental component of the outer membrane of Gram-negative

bacteria and act as a potent immunomodulatory molecule, with its lipid A and carbohydrate domains playing distinct biological roles (Zhang et al., 2013). Variations in fatty acid composition and glycosylation patterns of LPS can significantly influence host-pathogen interactions and inflammatory responses (Matsuura, 2013). Given the established role of CPS and LPS, the structural investigation of these macromolecules represents a crucial step toward understanding their possible involvement in host colonization, immune stimulation, and pathogenicity.

In this chapter, the CPS of *V. crassostreae* isolated from *P. lividus* was isolated and structurally characterized in detail. In parallel, LPS was extracted and subjected to preliminary chemical analyses, providing initial insights into its compositional features. Lastly, the LPS sample isolated in this study is under investigation for in vivo experiments on sea urchins to evaluate its potential role in eliciting host responses and contributing to the disease symptoms.

Together, the results presented in this chapter provide a molecular insight for interpreting the biological activity of *V. crassostreae* virulent factors and their possible involvement in Bald Disease affecting *P. lividus*.

3.2 Results and discussion

V. crassostreae cells were treated with PCP solution (Ex_{PCP}) to precipitate the LPS, followed by water/phenol extraction to recover the aqueous phase (Ex_{WP}) containing the capsular polysaccharides (Fig. 15). The WP was subjected to an enzymatic digestion using RNase, DNase, and protease to remove residual nucleic acids and protein.

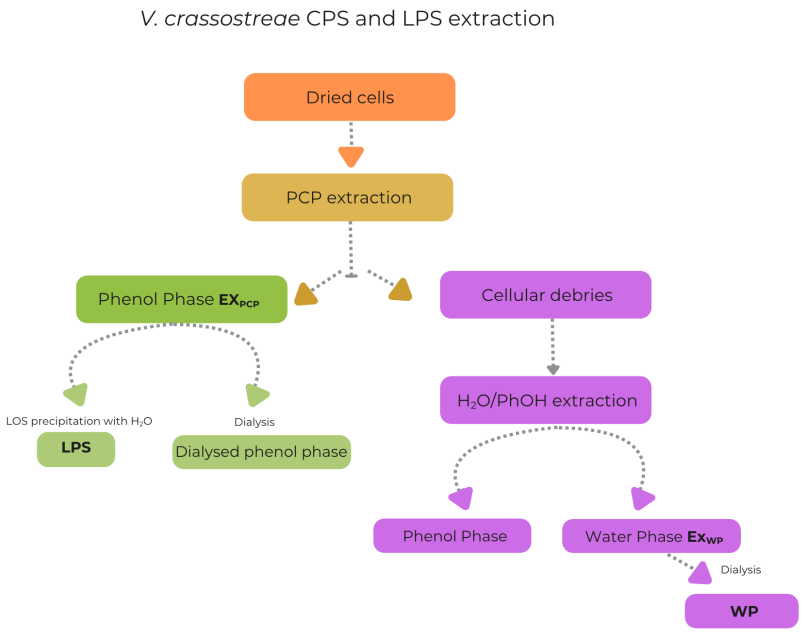

Figure 15. Schematic representation of V. crassostreae LPS and CPS extraction.

The purified extract was visualised after 14% DOC PAGE analysis, stained with Alcian blue and silver nitrate (Fig. 16).

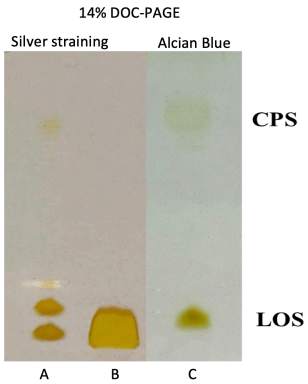

Figure 16. 14% DOC PAGE analysis. (A) Escherichia coli O55:B5 LPS used as standard; (B) V. crassostreae LPS; (C) V. crassostreae WP extract.

DOC-PAGE analysis revealed low-molecular-weight bands related to *V. crassostreae* rough-LPS (LOS) in PCP extract (lane B). Furthermore, the WP extract, dyed with alcian blue, showed high-molecular-weight bands associated with CPS (lane C), allowing for the identification of CPS in addition to LOS.

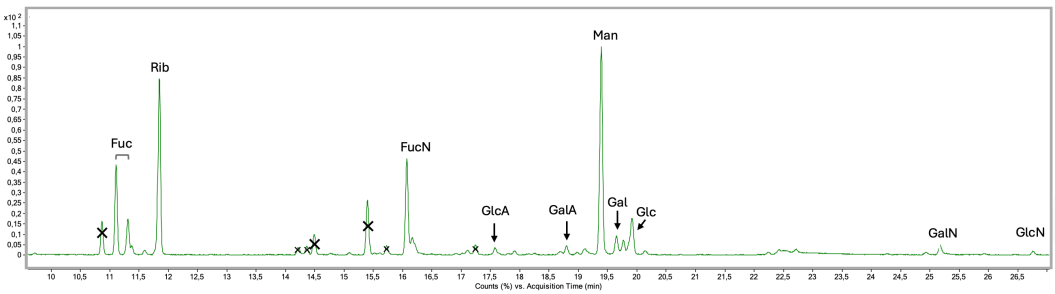

Figure 17. AMG of V. crassostreae WP extract. Peaks identified as impurities are marked with an X.

Monosaccharide composition analysis by acetylated methyl glycoside (AMG) revealed the presence of mainly fucose (Fuc), ribose (Rib), 2-amino-2-deoxy-L-fucosamine (FucN), and mannose (Man), with minor amounts of uronic acids and amino sugars (Fig.17).

3.2.1 CPS isolation and structural characterization

To selectively remove residual LPS and obtain a purified CPS fraction, the water phase was subjected to mild acid hydrolysis (1% AcOH), followed by gel filtration chromatography.

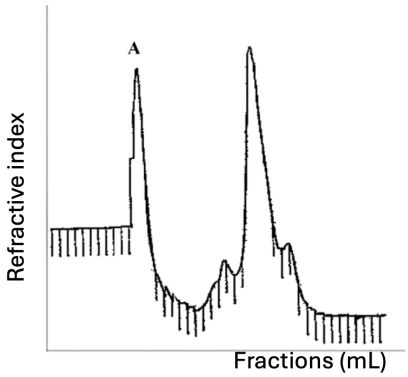

Figure 18. S-400 gel filtration chromatogram of the WP after enzymatic digestion and mild acid hydrolysis. Fraction A is identified as the CPS; the second peak indicates the saccharide portion of LPS.

The chromatographic profile (Fig. 18) showed two fractions, which were collected and analysed by ^{1}H NMR spectroscopy. The fraction A eluted at lower retention times was assigned to the CPS, and the second peak at higher retention times was attributed to the saccharide portion of LPS.

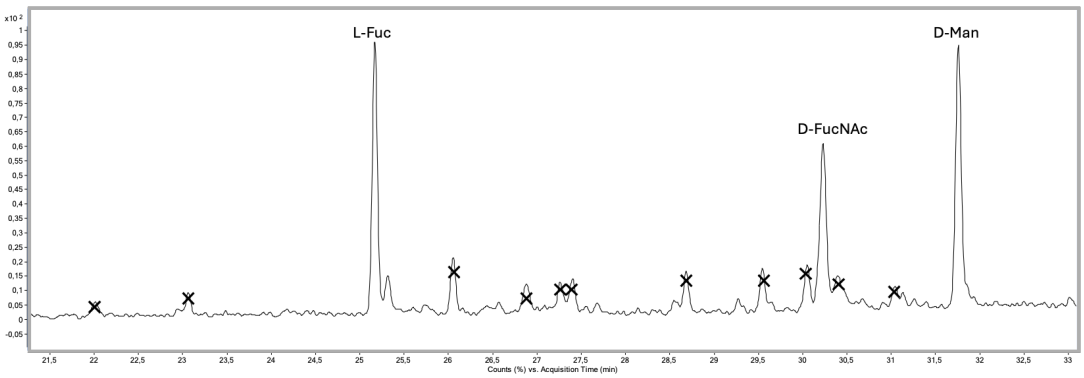

Figure 19. AOG chromatogram analysed at GC-MS of V.crassostreae purified CPS. Peaks identified as impurities are marked with an X.

Further AMG and acetylated 2-octyl glycosides (AOG) analyses were performed to determine the absolute configuration. The monosaccharides belonging to *V. crassostreae* purified CPS were confirmed to be L-fucose, 2-amino-2-deoxy-L-fucosamine, and D-mannose (Fig. 19).

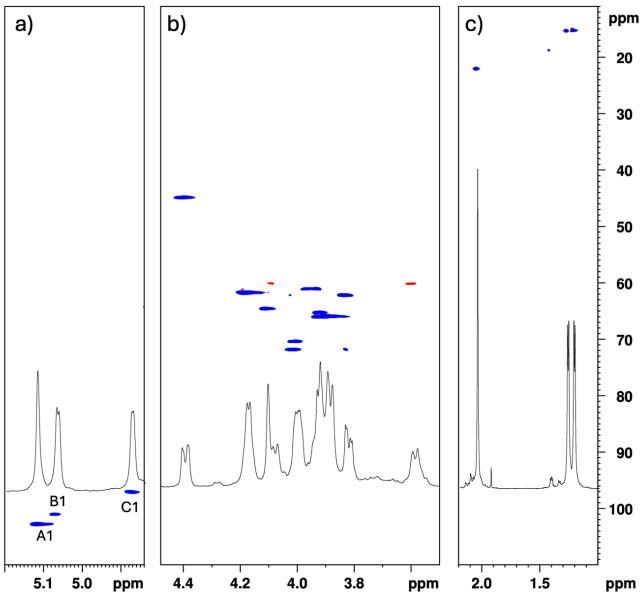

Figure 20. ^{1}H Selected region of ^{1}H, ^{13}C DEPT-HSQC spectrum of V. crassostreae CPS. Panel shows a) anomeric region, b) carbinolic region, and c) methyl region. The spectrum was recorded at 298 K, in D_2O.

The chemical shifts of the ^{1}H and ^{13}C NMR resonances of the sugar residues were assigned by 2D NMR experiments (Fig. 20). The $^{1}J_{C1,\,H1}$ coupling constant values were measured with the 2D F*2*-coupled HSQC of the CPS and indicated that all the residues (**A**-**C**) were α-configured (Bock & Pedersen, 1985).

Residue **A** was assigned to a *manno*-configured residue based on the presence of the correlations in the TOCSY spectrum from H-1 to H-2. In detail, residue **A** with H-1/C-1 signals at δ 5.12/102.7 ppm was assigned to a 6-substituted α-mannose. The remaining proton signals were sequentially assigned based on through-bond scalar correlations observed in the ^{1}H-^{1}H COSY experiment. The downfield chemical shift displacement of the C-6 resonance at δ 65.1 ppm identified its substitution position (Bock and Pedersen, 1983; Casillo et al., 2021). The spin systems **B** and **C** were recognized as *galacto*-configured residues, due to the presence of cross-peaks in the TOCSY spectrum from H-1 to H-4. Residue **B**, with H-1/C-1 signals at δ 5.07/100.9, was identified as a 3-substituted α-fucose residue. COSY and TOCSY spectra suggested a correlation between the H-5 proton at δ 4.18 ppm and a methyl signal at δ 1.21 ppm. The downfield shift of the C-3 carbon resonance at δ 77.9 ppm compared with an unsubstituted residue indicated glycosylation at this position (Bock and Pedersen, 1983).

The residue **C** with H-1/C-1 signals at δ 4.87/96.9 ppm was identified as a 3-substituted α-N-acetyl-2-amino-2-deoxy-L-fucosamine due to the correlation in the DEPT-HSQC experiment of its H-2 proton at δ 4.40 ppm with a nitrogen-bearing carbon at δ 48.3 ppm. Furthermore, both COSY and TOCSY spectra suggested a correlation between the H-5 proton at δ 4.18 ppm and a methyl signal at δ 1.27 ppm. In the HMBC spectrum, the H-2 proton correlated with a CO signal at δ 175.1 ppm. The downfield shift of the C-3 carbon resonance at δ 76.3 ppm compared with an unsubstituted residue indicated glycosylation at this position (Bock & Pedersen, 1983). The complete set of ^{1}H and ^{13}C chemical shift assignments is reported in Table 2.

Table 2. ^{1}H and ^{13}C NMR chemical shifts (ppm) of CPS from V. crassostreae. Spectra were recorded in D_2O solution at 298 K (600 MHz).

Residue	H-1/C-1 $^{1}J_{CH}$	H-2 C-2	H-3 C-3	H-4 C-4	H-5 C-5	H-6 a,b C-6	-NAc
A 6-α-D-Man	5.12 102.7 (170 Hz)	4.11 69.9	3.93 70.7	3.92 66.1	3.84 71.5	4.08, 3.60 65.1	-
B 3-α-L-Fuc	5.07 100.9 (166 Hz)	3.83 67.4	4.01 77.9	3.91 71.5	4.18 66.8	1.21 15.3	-
C 3-α-D-FucNAc	4.87 96.9 (187 Hz)	4.40 48.3	4.00 76.3	3.88 71.4	4.18 66.9	1.27 15.3	2.05 175.1

The sequence of the sugar residues within the CPS repeating unit was established based on ^{1}H-^{1}H NOESY and ^{1}H-^{13}C HMBC experiments.

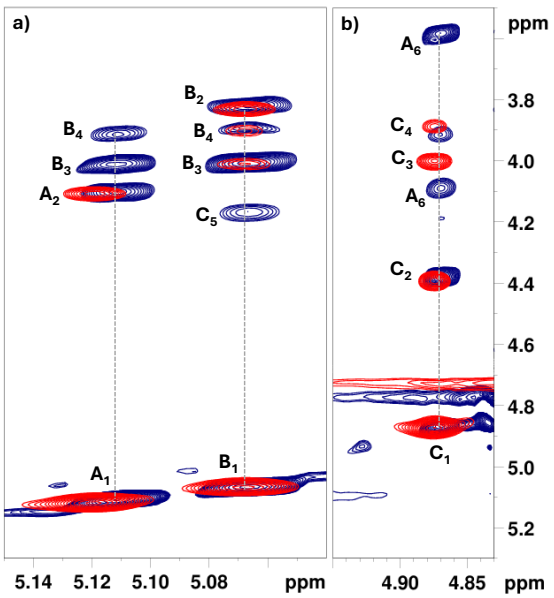

Figure 21. Overlay of ^{1}H–^{1}H TOCSY (red) and ^{1}H–^{1}H NOESY (blue) spectra of the CPS repeating unit from V. crassostreae. Panel a) shows the anomeric regions and correlations for residues A and B, while panel b) displays the corresponding correlations for residue C.

In the NOESY spectrum, the anomeric proton of residue **A** showed a clear correlation with H-3 (δ 4.01 ppm) and H-4 (δ 3.91 ppm) of residue **B**. Furthermore, the anomeric proton H-1 of residue **B** exhibited a NOE correlation with H-5 (δ 4.18 ppm) of residue **C**. In addition, the anomeric proton H-1 (δ 4.87 ppm) of residue **C** showed correlations with H-6a and H-6b (δ 4.08 ppm and 3.60 ppm, respectively) of residue **A** (Fig. 21).

Further evidence was provided by the HMBC experiment, which revealed a *long-range* correlation between C-1 of residue **A** and C-3 of residue **B**, as well as a correlation between C-

1 of residue **B** and C-3 of residue **C** (δ 76.4 ppm). Based on these data, the CPS repeating unit from *V. crassostreae* was shown to consist of a trisaccharide arranged in the sequence α-D-Man*p*-(1→3)-α-L-Fuc*p*-(1→3)-α-D-FucNAc*p*, with the FucN residue further linked at C-6 to the Man unit of the adjacent repeating unit (Fig. 22).

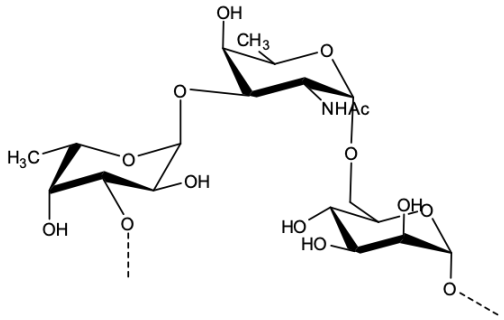

→6)-α-D-Man*p*-(1→3)-α-L-Fuc*p*-(1→3)-α-D-FucNAc*p*-(1→

Figure 22. Repeating trisaccharide unit of the CPS from Vibrio crassostreae.

3.2.2 LOS preliminary characterization

The saccharide composition of *V. crassostreae* LOS was investigated by GC-MS after derivatization of the sugars as acetylated methyl glycosides (AMGs). Following the initial analysis, 3-deoxy-D-manno-oct-2-ulosonic Acid (Kdo), a characteristic sugar of bacterial LPS, was not detected. This observation led to the hypothesis that Kdo might be phosphorylated. For this reason, the LOS was subjected to hydrofluoric acid (HF) hydrolysis. The treated sample was subsequently derivatised as acetylated methyl glycosides and analysed again by GC-MS. Acetylated methyl glycoside (AMG) analysis of the HF-treated sample was then performed by GC-MS (Fig. 23).

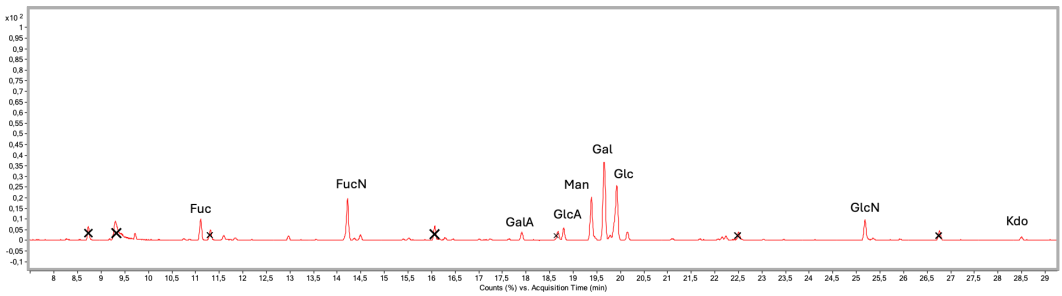

Figure 23. AMG of V. crassostreae LOS. Peaks identified as impurities are marked with an X.

The chromatographic profile revealed characteristic monosaccharide peaks consistent with the presence of Kdo, confirming the occurrence of a phosphorylated Kdo moiety in the LOS inner-core region.

The total fatty acid composition was determined by GC-MS analysis of LPS after derivatization into methyl ester derivatives (FAMEs) (Fig. 24).

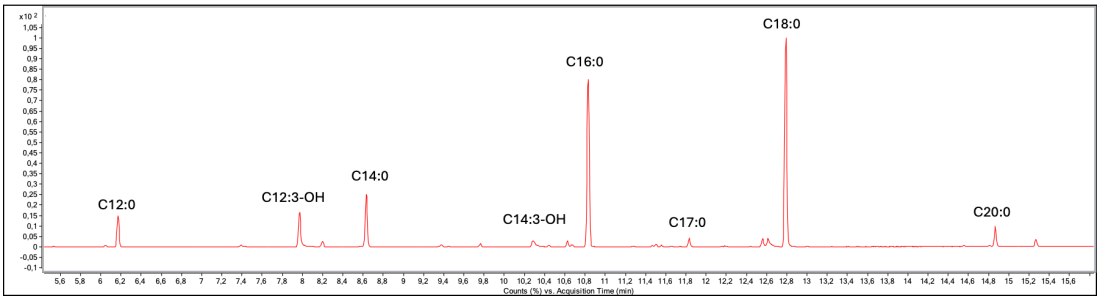

Figure 24. Fatty acid composition of LOS after derivatization into methyl ester derivatives (FAMEs).

Fatty acid analysis mainly indicated 3-hydroxydodecanoic acid [C12:0(3-OH)] and 3-hydroxytetradecanoic acid [C14:0(3-OH)] as the predominant hydroxylated species. The analysis also revealed the presence of dodecanoic acid (C12:0), tetradecanoic acid (C14:0), and hexadecanoic acid (C16:0). Long-chain fatty acids such as heptadecanoic acid (C17:0), octadecanoic acid (C18:0), and eicosanoic acid (C20:0), most likely associated with phospholipids, were also detected (Phillips et al., 2011).

3.3 Conclusions

In this chapter, *V. crassostreae* CPS was successfully isolated and characterized. The CPS was shown to be composed primarily of L-fucose, 2-acetamido-2-deoxy-D-fucose, and D-mannose**,** arranged in a trisaccharide repeating unit with the sequence 6)-α-D-Man*p*-(1→3)-α-L-Fuc*p*-(1→3)-α-D-FucNAc*p*-(1. NMR spectroscopy confirmed the α-configuration of all residues and defined the linkage positions, providing the first detailed structural description of the CPS of *V. crassostreae.* The bacterium displays a lipooligosaccharide on its surface, and a preliminary characterization of this molecule revealed the presence of phosphorylated Kdo residues. Although the LOS characterization is not yet complete, these preliminary data represent an important step for future structural and functional studies.

The results presented here provide a comprehensive molecular framework for understanding the surface polysaccharides of *V. crassostreae*, laying the foundation for further functional in vivo assays to assess the contribution of CPS and LPS to the pathogenicity of Bald Sea Urchins Disease. The structural characterization of these macromolecules represents a critical step toward elucidating the mechanisms of host colonization and immune interaction in marine *Vibrio* species.

Chapter 4

Alteromonas macleodii Mo169 exopolysaccharide

4.1 Alteromonas macleodii Mo169

Alteromonas macleodii is a marine Gram-negative bacterium belonging to the class Gammaproteobacteria (López-Pérez et al., 2012), widely distributed in marine environments and frequently associated with marine organisms (Varasteh et al., 2025). Members of the genus *Alteromonas* are recognized for their metabolic versatility and their ability to produce exopolysaccharides (EPSs), which play important roles in surface adhesion, environmental adaptation, and interactions with biotic and abiotic components of the marine ecosystem. These EPSs are often characterized by high molecular weight and complex chemical compositions, making them of particular interest from both a structural and biotechnological perspective.

As already described in section 1.2.2, marine bacterial EPSs have attracted increasing attention due to their structural resemblance to glycosaminoglycans (GAGs), thanks to their chemical features, including their monosaccharide composition, molecular weight, and functional substitutions, which are directly linked to their biological activity. Since the production of GAGs from animal tissues or pathogenic microorganisms raises ethical and safety concerns, marine bacteria represent a promising and still underexplored reservoir of structurally diverse sources of GAG-like polymers. Several EPSs produced by *Alteromonas* species, including those isolated from deep-sea environments, have been reported to exhibit GAG-like structural motifs and biological properties (Zhang et al., 2017), particularly in applications related to tissue engineering (Delbarre-Ladrat et al., 2014b). These findings highlight the relevance of *Alteromonas* spp. as producers of functional polysaccharides with potential biomedical value.

The *Alteromonas macleodii* strain investigated in this chapter was isolated from a marine giant clam collected in French Polynesia (Concórdio-Reis et al., 2021). The strain was cultivated by Prof. Filomena Freitas (Department of Chemistry, NOVA School of Science and Technology, Caparica, Portugal). The EPS produced by this strain is currently protected by a patent; therefore, specific applications cannot be disclosed at this stage. In this chapter, the EPS produced by *A. macleodii* was isolated and chemically characterized in order to provide structural insights into this GAG-like marine bacterial polysaccharide and to expand current knowledge on EPS diversity within the genus *Alteromonas***.**

4.2 Result and discussion

The crude EPS was obtained by ultrafiltration of the culture media and was then analysed by 14% DOC-PAGE electrophoresis and stained with Alcian blue (Fig. 25).

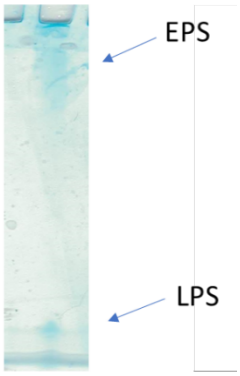

Figure 25. 14% DOC-PAGE of A. macleodii Mo169 EPS crude extract stained with alcian blue.

The analysis showed the presence of high molecular bands attributable to the EPS and a fast-migrating band that can probably be due to residual rough-lipopolysaccharide (LOS).

GC-MS chromatogram of acetylated methyl glycosides (AMG) disclosed the presence of rhamnose (Rha), mannose (Man), glucose (Glc), galactose (Gal), 2-amino-2-deoxy-guluronic acid (GulNA), 2-amino-2-deoxy-glucose (GlcN), and 3-deoxy-*manno*-oct-2-ulosonic acid (Kdo), thus confirming the presence of residual LOS in the sample (Fig. 26).

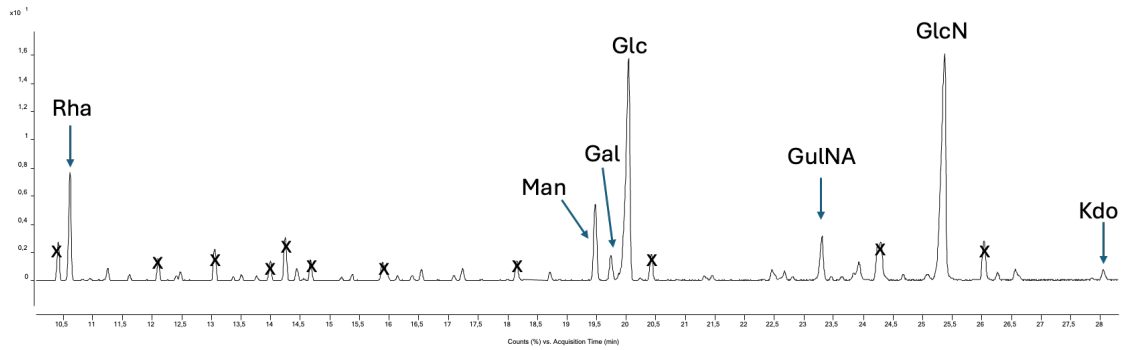

Figure 26. AMG analysis of A. macleodii Mo169 crude EPS

To remove the residual LOS, a mild acid hydrolysis was performed, and the sample was then purified through gel filtration chromatography. The purified EPS was subjected to glycosyl analysis again, and the GC-MS results indicated that only 2-amino-2-deoxy-glucose (GlcN) and 2-amino-2-deoxy-guluronic acid (GulNA) were present.

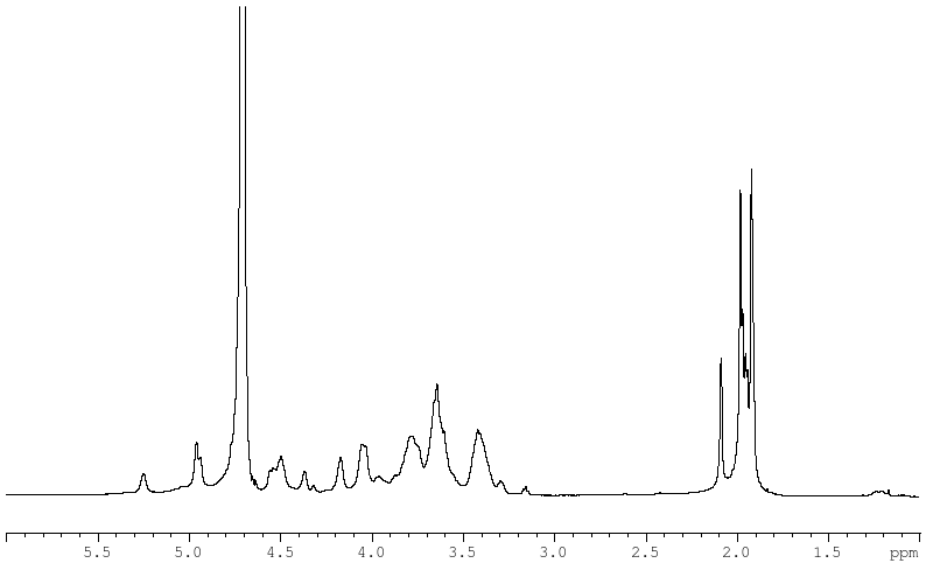

Figure 27. ^{1}H NMR spectrum of the EPS from A. macleodii Mo169 purified EPS. The spectrum was recorded at 298 K, in D_2O.

A ^{1}H NMR spectrum of the purified EPS was also recorded (Fig.27). Acetylated 2-octyl glycosides (OGA) GC-MS analysis of the sample revealed that the GlcN was D-configured, while the GulNA resulted in being L-configured.

4.2.1 EPS structural characterization

In order to better study and identify the punctual structure of *A. macleodii* Mo169, 2D NMR spectra were collected on the purified extract and after the performing a de-*O*-acetylation by an alkaline treatment with aqueous NH_3. The combination of 1D and 2D NMR spectra analysis of both samples was necessary to obtain the final structure.

The ^{1}H,^{13}C DEPT-HSQC NMR experiment of purified EPS showed three correlations in the anomeric region, of which only two were attributable to anomeric signals (at δ 4.95/97.7 and 4.45/101.8 ppm) (Table 4). The third correlation at δ 5.25/69.3 ppm suggested the presence of an *O*-acetyl group. Furthermore, the up-field region of the ^{1}H spectrum showed signals attributable to *N*- and *O*-acetyl groups in the range 1.8-2.2 ppm (Table 3).

Table 3. ^{1}H,^{13}C-NMR assignments of the EPS obtained from A. macleodii Mo169. All the chemical shifts are referred to those of the acetone, used as the internal standard (^{1}H = 2.225 ppm, ^{13}C = 31.45 ppm). The spectra were recorded at 298 K. Acetyl groups, O-acetyl (CH_3) 2.08/ 20.5 ppm, (CO) 173.2 ppm; N-Acetyl, (CH_3) 1.98/ 22.0 ppm, (CO) 173.4, (CH_3) 1.90/ 21.9 ppm, (CO) 173.5.

	Residue	H-1 C-1	H-2 C-2	H-3 C-3	H-4 C-4	H-5 C-5	H-6a,b C-6
A	α-L-GulNAc3OAcA	4.93	4.36	5.25	4.06	4.72	-
		96.8	44.5	69.3	76.2	66.1	175.4
B	3-β-D-GlcNAc	4.49	3.63	3.66	3.42	3.39	3.78
		101.8	55.2	78.7	68.5	75.7	60.8

At this stage, the EPS was de-*O*-acetylated by an alkaline treatment with aqueous NH_3, purified through S400 gel filtration chromatography, and analysed by ^1H NMR to verify the occurrence of the reaction (Fig.28).

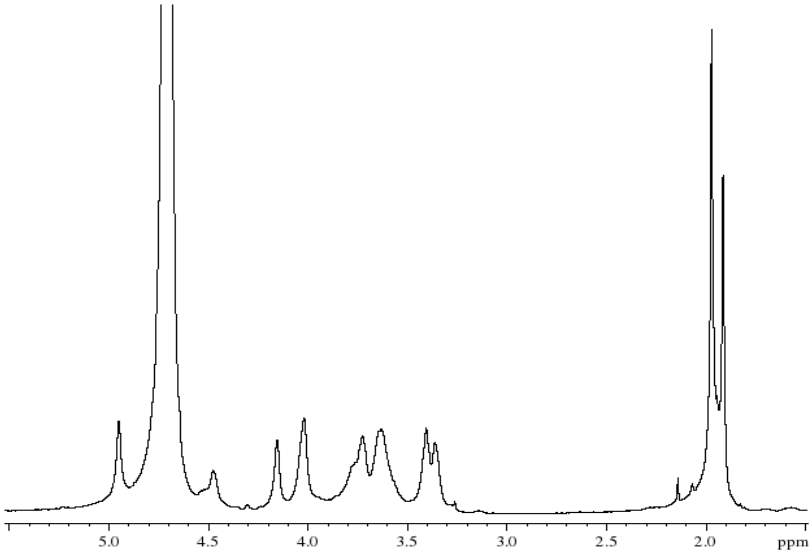

Figure 28. ^1H NMR spectrum of the O-deacetylated A. macleodii Mo169 EPS. Spectrum was recorded at 298 K, in D_2O.

The spectrum revealed only a few signals compared to the previous one, thus proving the occurrence of the reaction. Finally, the purified EPS was subjected to 1D and 2D homo- and heteronuclear NMR experiments. After the acquisition of 2D NMR spectra, the study indicated the assignments of two spin systems (Fig. 29, Table 4).

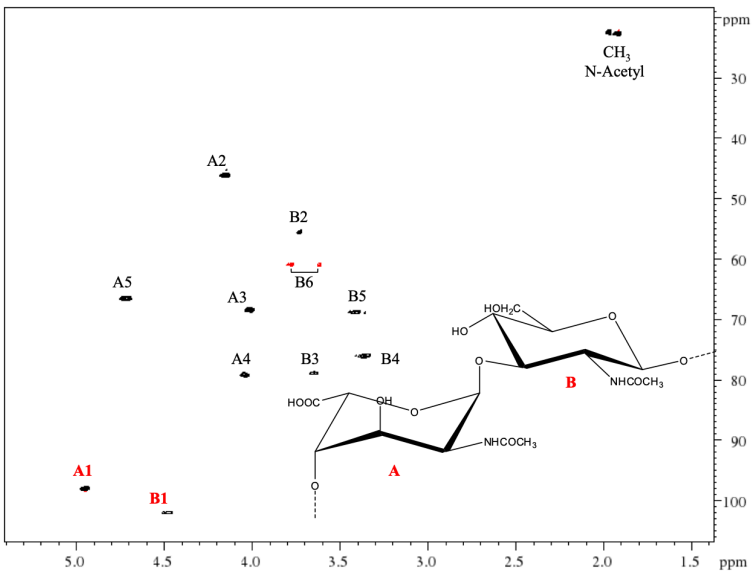

Figure 29. Selected region of ^1H, ^{13}C DEPT-HSQC spectrum of the O-deacetylated EPS. The spectrum was recorded at 298 K, in D_2O.

Residue **A** was recognised as a 2-acetamido-2-deoxy-gulopyranuronic acid (GulNAcA). The total spin system was assigned through the COSY and TOCSY spectra connectivity. Starting from the H-1 in the COSY spectrum, the H-2 proton at δ 4.16 ppm was found. This proton, in turn, correlated in the DEPT-HSQC experiment with a C-2 resonance occurring at δ 45.8 ppm, which was typical of *gulo*-configured monosaccharide (Di Guida, Casillo, & Corsaro, 2020). Moreover, in the HMBC experiment, the H-5 proton signal at δ 4.82 ppm showed a long-range scalar connectivity with the C-6 carboxyl signal at δ 174.0 ppm, thus confirming the presence of a uronic acid residue. Finally, the carbon chemical shifts were indicative of a substitution at C-4, as demonstrated by a downfield shift of this carbon signal at δ 78.7 ppm when compared with that of the unsubstituted residue (Bock & Pedersen, 1983).

Residue **B**, with H-1/C-1 signals at δ 4.45/101.8, was identified as a 3-substituted GlcNAc residue. The occurrence of strong scalar correlations in both COSY and TOCSY experiments suggested *gluco*-configuration. The $^{1}H,^{13}C$-HSQC spectrum revealed that the H-2 signal at 3.74 ppm correlated with a nitrogen-bearing carbon at 55.4 ppm (Table 4). The downfield chemical shift of the C-3 resonance to 78.7 ppm identified its substituted position (Zhang et al., 2017). The sequence of residues was obtained by the long-range scalar correlations observed in the HMBC spectrum between C-1 of **A** and H-3 of **B**, and H-4 of **A** and C-1 of **B**.

Table 4.$^{1}H,^{13}C$-NMR assignments of the O-deacetylated extracellular polysaccharide obtained from A. macleodii Mo169. All the chemical shifts are referred to acetone used as an external standard (δ_H = 2.225 ppm; δ_C = 31.45 ppm). The spectra were recorded at 298K.

	Residue	H-1 C-1	H-2 C-2	H-3 C-3	H-4 C-4	H-5 C-5	H-6a,b C-6
A	4-α-L-GulNAcA	4.95	4.16	4.03	4.04	4.82	-
		97.7	45.8	67.6	78.7	65.8	174.0
B	3-β-D-GlcNAc	4.45	3.74	3.61	3.40	3.36	3.61, 3.76
		101.8	55.4	78.7	68.3	75.6	60.3

The difference between the chemical shift of H-3 of residue **A** in the polymer before and after the alkaline treatment definitively indicated the *O*-acetylation at this position. The HMBC spectrum of the native polymer confirmed this assignment since a long-range connectivity was found between the signal at δ 5.25 and the carbonyl signal at δ 173.2 ppm (Table 3).

The collected data indicated that the EPS isolated from *A. macleodii* Mo169 consists of a disaccharide repeating unit reported below:

→4)-α-L-GulNAc3OAcA-(1→3)-β-D-GlcNAc-(1→.

4.3 Conclusion

In this chapter, EPS produced by *Alteromonas macleodii* Mo169 was isolated and structurally characterized through a combination of chemical, chromatographic, and spectroscopic approaches.

Chemical analyses of the purified EPS showed that it is composed exclusively of glucosamine and gulaminuronic acid, with D- and L-configurations, respectively. The combination of 1D and 2D NMR spectroscopy, performed before and after de-*O*-acetylation, enabled the assignment of the monosaccharide residues, their substitution positions, and the sequence within the repeating unit. NMR data also demonstrated the presence of an *O*-acetyl group located at position O-3 of the gulaminuronic acid residue.

Based on the collected data, the EPS produced by *A. macleodii* Mo169 was shown to consist of a linear disaccharide repeating unit with the structure →4)-α-L-GulNAc3OAcA-(1→3)-β-D-GlcNAc-(1→. These results provide a coherent and complete structural characterization of this marine bacterial EPS and contribute to the broader understanding of the chemical diversity of extracellular polysaccharides produced by *Alteromonas* species.

Chapter 5

Ellisolandia elongata cell-wall polysaccharides

5.1 Ellisolandia elongata

Ellisolandia elongata is an articulated, calcified red macroalga belonging to the family *Corallinaceae*, a taxonomic placement supported by molecular phylogenetic analyses of the Corallineae (Hind & Saunders, 2013). The species is widely distributed in the Mediterranean Sea and along temperate Northeast Atlantic coasts. It commonly forms dense intertidal and shallow subtidal turfs, thus contributing to the habitat complexity (Nannini et al., 2015). Morphologically, the species produces segmented articulated thalli composed of calcified intergenicula, which are composed of densely calcified cell walls made of high-Mg calcite deposited onto the organic polysaccharide wall; and flexible genicula made of one row of elongate cells composed of polysaccharides, cellulose, phenolics, proteins, and very low $CaCO_3$ content compared to intergenicula (Fig. 30). This articulated architecture confers both mechanical resistance and flexibility under hydrodynamic forcing, and contributes to the structural complexity of shallow coastal ecosystems, where it supports diverse benthic assemblages (Couto et al., 2014; Ragazzola et al., 2017).

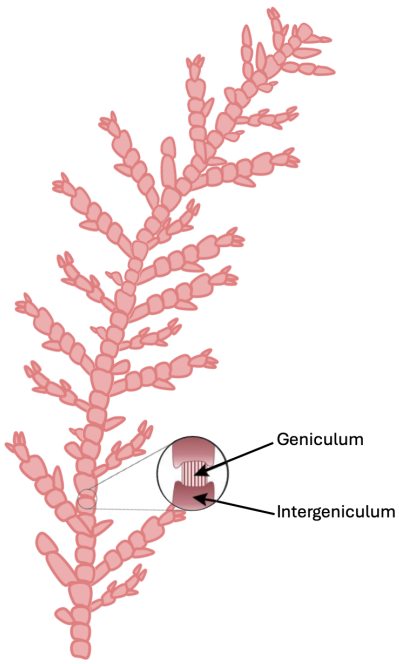

Figure 30. Graphical representation and morphological characteristics of Ellisolandia elongata.

In addition to its ecological relevance, *E. elongata* exhibits a complex cell wall architecture enriched in sulfated galactans as reported in Corallineae algae (previously described in section 1.3.1), whose composition and sulfation degree may vary with environmental conditions and tissue differentiation. These polysaccharides are increasingly recognized for their biological and functional properties, making them of interest in multiple biotechnological fields. Sulfated polysaccharides from red algae have been widely reported to exhibit bioactivities such as antioxidant activity and, in some cases, antibiofilm or antimicrobial effects. Despite their

biological relevance, algal polysaccharides often present significant challenges for structural characterization. Their complexity is influenced by multiple factors, including algal taxonomy, cellular localization, extraction and purification procedures, and the occurrence of secondary modifications such as methylation and acetylation, which can generate a wide diversity of structural motifs (Wijesekara et al., 2011).

E. elongata samples analysed in this study were collected in the Marine Protected Area "Parco Sommerso della Gaiola" (Naples, Italy) during an exceptional low-tide event, which enabled direct access to intertidal patches dominated by *E. elongata*. In this work, cell wall polysaccharides extracted from *E. elongata* were purified and structurally characterized. Their biological activity was evaluated through antioxidant and antibiofilm assays, and their film-forming potential was preliminarily assessed via casting experiments to explore possible applications in biomaterials development.

This study aims to provide a comprehensive characterization of *E. elongata* polysaccharides, linking their chemical features to potential biological activities and functional properties, in order to explore their suitability for future biotechnological applications.

5.2 Results and discussion

5.2.1 Polysaccharides extraction

Three samples of *E. elongata* were collected in the 'Parco Sommerso di Gaiola', a Marine Protected area in Naples, Italy (40°47′36.5″N, 14°11′18.2″E), during an unusual low tide event. The samples were collected two times: the first sampling was conducted in February 2023 by collecting submerged (***S***) and exposed (***E***) algae at the end of the low tide event. The second sampling was conducted in May 2023, when the low tide event ended, and the sea level was restored, submerging the once-exposed algae again (re-submerged **R**) (Fig. 31).

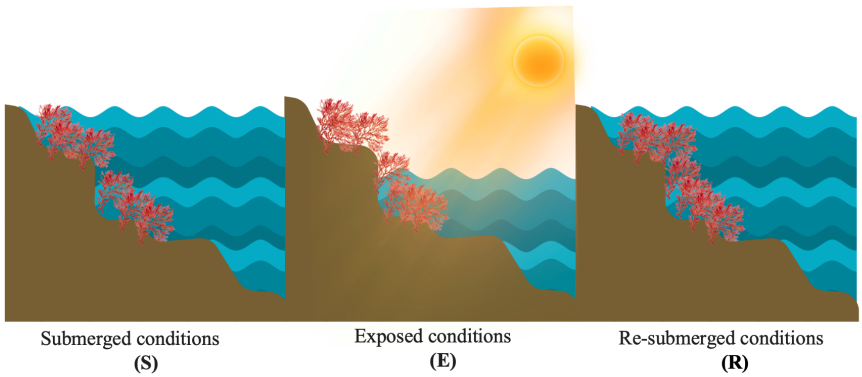

Figure 31. Representation of the collected E. elongata samples. From left to right: Submerged conditions (S), Exposed conditions (E), Re-submerged conditions (R).

All samples were washed, dried, reduced to powder, and subjected to polysaccharide extraction (Fig. 32).

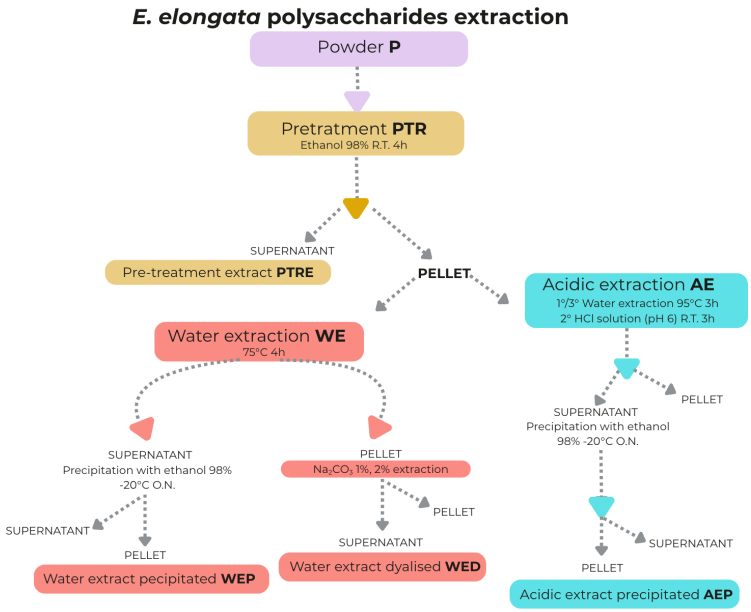

Figure 32. Schematic representation of E. elongata pre-treatment and polysaccharides extraction techniques.

The samples were first subjected to a pretreatment (PTR) with ethanol to remove lipids, pigments, and apolar compounds. GC-MS chromatogram of fatty acids obtained during PTRE procedure, showed the presence of several fatty acids (Table 5) including, tetradecanoic acid (C14:0), pentadecanoic (C15:0), hexadecenoic acid (C16:1), hexadecanoic acid (C16:0), octadecenoic acid (C18:1 oleic acid), octadecanoic acid (C18:0), eicosanoic acid (C20:0) and the presence of eicosapentaenoic acid (C20:5 EPA) and arachidonic acid (C20:4). In all conditions the fatty acid composition was largely dominated by C16:0, which accounted for approximately 46–51% of total fatty acids. However, variations were observed within the

unsaturated fraction in response to the different environmental conditions. In the exposed (**E**) samples, oleic acid (C18:1) and arachidonic acid (C20:4) increased, reaching 13.67% and 13.55%, respectively, compared to **S** conditions (8.14% and 10.42%). Conversely, EPA (C20:5) decreased markedly in **E** (5.39%) compared with **S** thalli samples (12.62%). Following in the **R** samples, EPA showed a strong increase, reaching the highest value among the tested conditions (15.59%), while arachidonic acid decreased again (9.77%). At the same time, a reduction in several saturated fatty acids, including C18:0 and C20:0, was observed, suggesting a re-adjustment of lipid metabolism during recovery. These results indicate that environmental stress and subsequent re-submersion influence fatty acid composition, particularly long-chain polyunsaturated fatty acids.

Table 5. Presence of several fatty acids in E. elongata PTRE in S (blue), E (red), and R (green) conditions.

	Submerged (S) %	**Exposed (E) %**	**Re-submerged (R) %**
C:14:0	3.13	3.03	5.43
C15:0	1.53	1.64	1.61
C16:1	2.98	3.27	6.59
C16:0	50.86	49.70	45.90
C18:1	8.14	13.67	8.47
C18:0	8.17	8.08	5.72
C20:5	12.62	5.39	15.59
C20:4	10.42	13.55	9.77
C20:0	2.15	1.70	0.92

After the pretreatment, two different parallel extractions were performed on all three samples to extract polysaccharides: a water extraction (WE) and an acidic extraction (AE) (Fig.32). The two extraction methods showed no significant differences in terms of extracted polysaccharides, as confirmed by ^{1}H NMR spectra and AMG showing the same profile and the same monosaccharide composition, respectively. Therefore, the structural characterization will be discussed only for the polysaccharide obtained through the acidic extraction.

After the AE extraction, the supernatant was subjected to an ethanol precipitation (AEP), and the collected pellets were analysed. The yields of polysaccharides extracted from *E. elongata* AEP under different conditions ranged from 1.09% (**S**), 1.15% (**E**), up to 1.46% (**R**) of the initial dry biomass. The highest yields were obtained under **R** conditions.

Figure 33. 14% DOC PAGE analysis. Silver staining showed high bands indicating polysaccharides presence in all three samples: a) S conditions; b) E conditions; c) R conditions.

14% DOC PAGE analysis visualised after silver staining (Fig. 33) showed the presence of bands at high molecular weight, suggesting the presence of high molecular weight polymers, mainly for condition **E**.

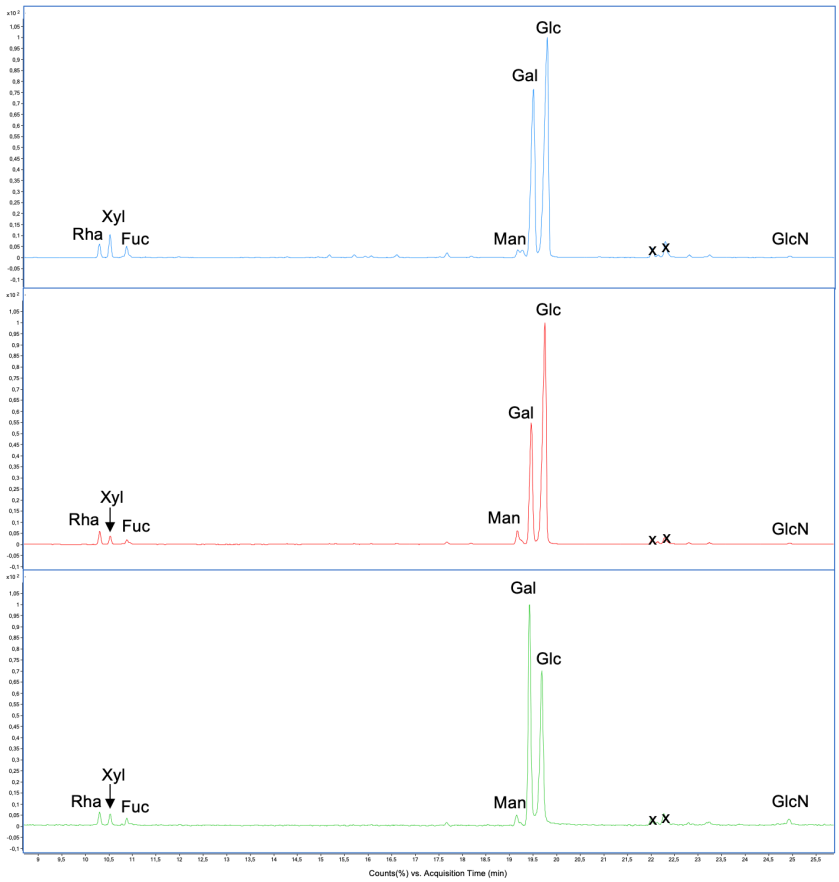

Figure 34. AMG spectra of E. elongata AEP polysaccharide extracts in S (blue), E (red), and R (green) conditions.

Monosaccharide composition of the AEP extracts of the three conditions was obtained by GC-MS analyses after derivatization into acetylated *O*-methyl glycosides (AMG) (Fig. 34). The chromatograms of the AEP polysaccharides in all three conditions show the presence of glucose (Glc) and galactose (Gal) as the main monosaccharides, and traces of rhamnose (Rha), xylose (Xyl), fucose (Fuc), mannose (Man), and 2-acetamido-2-deoxy-glucose (GlcN). The relative amount of Glc and Gal varies among the conditions; notably, in the **R** conditions (green spectra), galactose (56%) is slightly more abundant than glucose (46%). In the **S** and **E** conditions, Glc is more abundant with 59% and 69%, respectively, compared to Gal, which reaches 43% in **S** and 30% in **E** conditions. The AEP samples were analysed by ^{1}H NMR spectra, revealing the same profile for all conditions (Fig.35).

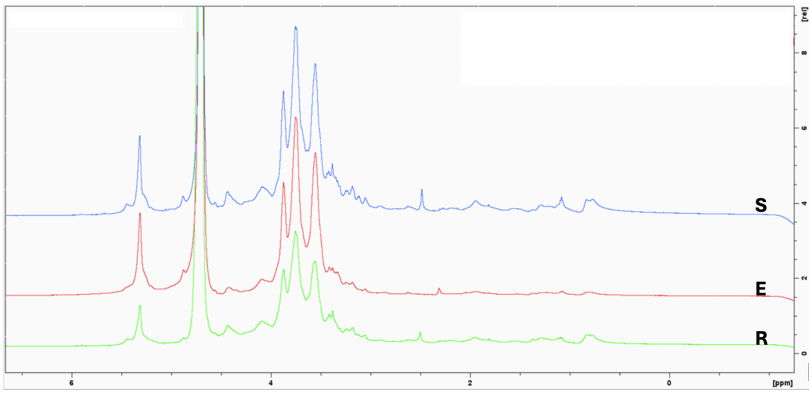

Figure 35. ^{1}H NMR spectra, recorded in D_2O, of E. elongata AEP polysaccharides in S (blue), E (red), and R (green).

5.2.2 Structural characterization of E. elongata CWPS in R condition

Since the highest yield was obtained in **R** condition (1.46 % of the powder) and since the ^{1}H NMR spectra of AEP of all conditions showed no significant differences, along with the AMG monosaccharides analysis, the structural characterization was performed on the re-submerged AEP extract (R-AEP).

R-AEP extract was analysed by homo- and heteronuclear 2D NMR spectra (Fig.36).

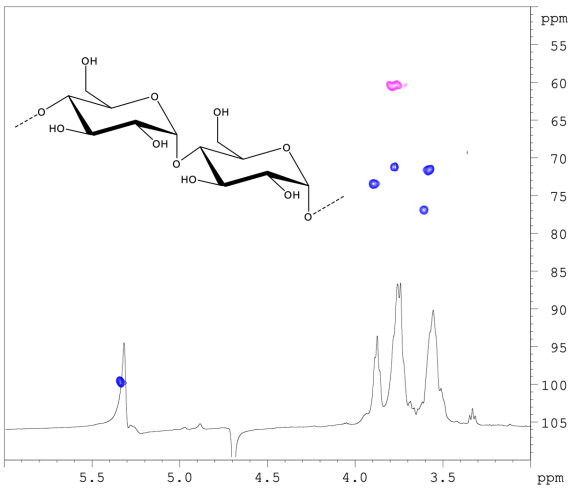

Figure 36. ^{1}H Selected region of ^{1}H, ^{13}C DEPT-HSQC spectrum of E. elongata R-AEP α-1,4-glucan.

The inspection of ^{1}H and ^{1}H, ^{13}C HSQC spectra indicated the presence of one anomeric signal at δ 5.33 ppm attributable to glucose unit. Starting from the anomeric signal at δ 5.33 ppm, all ^{1}H resonances were assigned on the basis of COSY and TOCSY experiments. Based on the ^{13}C chemical shifts, the residue was identified as an α-glucose, substituted at C-4 (77.0 ppm) (Table 6).

Table 6. ^{1}H and ^{13}C NMR chemical shifts (ppm) of E. elongata R-AEP a-1,4-glucan. Spectra were recorded in D_2O solution at 298 K (600 MHz).

Residue	**H-1/C-1** **$^{1}J_{CH}$**	**H-2** **C-2**	**H-3** **C-3**	**H-4** **C-4**	**H-5** **C-5**	**H-6a,b** **C-6**
A 4-α-D-Glc	5.33 99.7 (170 Hz)	3.55 71.7	3.88 73.1	3.57 77.0	3.75 71.7	3.78, 3.70 60.2

This polysaccharide is identified as Floridean starch, a storage polysaccharide already found in red algae (Navarro & Stortz, 2008), but has never been identified in *E. elongata* so far.

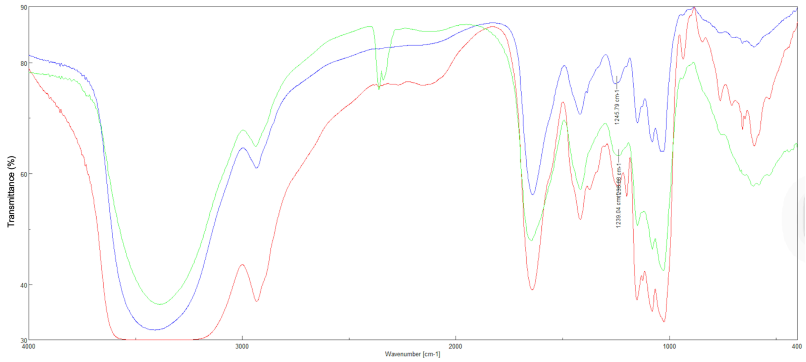

Figure 37. FT-IR spectra of E. elongata AEP polysaccharides extract in S (blue), E (red), and R (green). Absorbing bands around 1260 cm⁻¹ highlight the presence of sulfate in all conditions.

The polysaccharide obtained after AEP extraction for all three conditions was further analysed by FT-IR, showing the typical absorption features of marine algal polysaccharides, confirming the carbohydrate nature of the extracts (Fig. 37). In all samples, a broad absorption band in the 3600-3200 cm^{-1} region was observed, corresponding to O-H stretching vibrations associated with extensive intra- and intermolecular hydrogen bonding, characteristic of polysaccharides. The intensity and breadth of this band varied among conditions, being more pronounced in the **E**, suggesting differences in hydration and hydrogen-bonding networks likely associated with stress-induced modifications of the cell-wall polysaccharides. Weak bands in the 3000-2800 cm^{-1} region were attributed to C-H stretching vibrations of the sugar ring. Absorption bands in the 1650-1600 cm^{-1} regions were assigned to H-O-H bending of the residual water. A distinct absorption band in the 1260-1220 cm^{-1} region was detected in all conditions and attributed to the asymmetric stretching vibration of sulfate ester groups (S=O). Additional bands in the 850-820 cm^{-1} region further supported sulfate substitution on the sugar rings. Notably, the **E** condition exhibited the highest intensity of sulfate-related bands, while a partial decrease was observed in the **R** condition, indicating a modulation of sulfation degree in response to environmental stress. Lastly, strong absorption bands between 1150 and 1000 cm^{-1} were assigned to C-O-C and C-O stretching vibrations of glycosidic linkages and pyranose rings, confirming the integrity of the polysaccharidic backbone (Gieroba et al., 2023).

All the analyses performed on AEP extracts clearly indicated that the Floridian starch was not the only polymer produced. To purify the other polysaccharides, an α-amylase hydrolysis was performed to remove the α-1,4-glucan. The sample was then purified through Sephacryl S-300 and P-100 size exclusion chromatography. The occurrence of the reaction was proved by ^{1}H NMR.

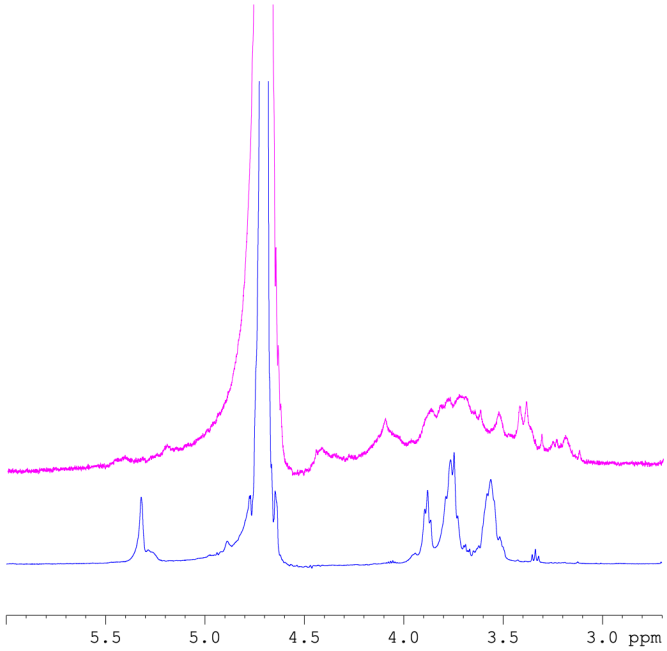

Figure 38. ^{1}H NMR spectra, recorded in D_2O, of E. elongata R-AEP: α-glucan (blue spectrum), and the second polysaccharide uncovered after α-amylase hydrolysis (pink spectrum).

Indeed, ^{1}H NMR revealed a different profile compared to the α-glucan (Fig. 38). The elucidation of the structural features of the second polysaccharide extracted from *E. elongata* R-AEP was achieved by a comprehensive carbohydrate analysis.

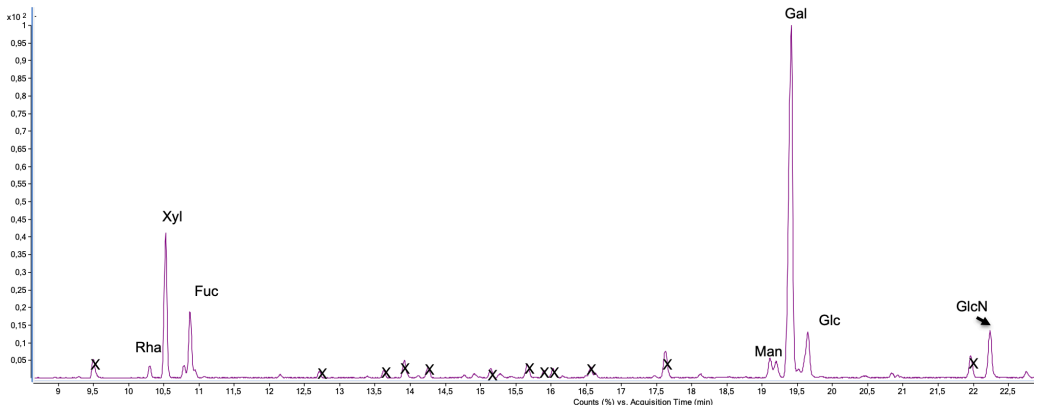

Figure 39. AMG spectra of E. elongata R-AEP polysaccharides post-hydrolysis. All impurities are marked with an X.

Firstly, the GC-MS chromatogram of AMGs disclosed the presence of mainly galactose (Gal) and xylose (Xyl), with traces of 2-amino-2-deoxy-D-glucose (GlcN), fucose (Fuc), glucose (Glc), mannose (Man), and rhamnose (Rha) (Fig. 39).

Furthermore, monosaccharides derivatised as acetylated alditols (AA) revealed that galactose residues were predominantly *O*-methylated at position O-2, and potentially methylated at position O-3, suggesting partial substitution at these hydroxyl groups. The

absolute configuration of the monosaccharides, determined by (+) and (+/-) acetylated 2-octyl glycosides (OGA) analysis, indicated the presence of D-xylose as well as both D- and L-galactose.

Linkage analysis by PMAA showed a complex and heterogeneous distribution of glycosidic linkages. Terminal xylose (t-Xyl, 12.9%) and terminal galactose (t-Gal 3.4%) residues were detected, together with several substituted galactose units, including 4-linked Gal (19,7%), 3-linked Gal (12.9%), 6-linked Gal (2.4%), 3,4-linked Gal (7.2%), 2,4-linked Gal (12.8%), 3,6-linked Gal (22.8%), 3,4,6-linked Gal (2.9%), and 2,3,6-linked Gal residues (3%) (Table 7).

Table 7. Linkage analysis of E. elongata R-AEP second polysaccharides based on GC–MS analysis of PMAAs.

Monosaccharides	**Glycosidic linkage**	**PMAAs derivates**	**Percentage (%)**
Xyl	terminal	2,3,4-tri-*O*-methyl 1,5 di-*O*-acetyl-xylopyranose	12.9%
Gal*p*	terminal	2,3,4,6-tetra-*O*-methyl 1,5 di-*O*-acetyl-galactopyranose	3.4%
Gal*p*	→4)-linked	2,3,6-tri-*O*-methyl-1,4,5-tri-*O*-acetyl-galactopyranose	19.7%
Gal*p*	→3)-linked	2,4,6-tri-*O*-methyl-1,3,5-tri-*O*-acetyl-galactopyranose	12.9%
Gal*p*	→6)-linked	2,3,4-tri-*O*-methyl-1,5,6-tri-*O*-acetyl-galactopyranose	2.4%
Gal*p*	→3,4)-linked	2,6-di-*O*-methyl-1,3,4,5-tetra-*O*-acetyl-galactopyranose	7.2%
Gal*p*	→2,4)-linked	3,6-di-*O*-methyl-1,2,4,5-tetra-*O*-acetyl-galactopyranose	12.8%
Gal*p*	→3,6)-linked	2,4-di-*O*-methyl-1,3,5,6-tetra-*O*-acetyl-galactopyranose	22.8%
Gal*p*	→3,4,6)-linked	2-*O*-methyl-1,3,4,5,6-penta-*O*-acetyl-galactopyranose	2.9%
Gal*p*	→2,3,6)-linked	4-*O*-methyl-1,2,3,5,6-penta-*O*-acetyl-galactopyranose	3%

The linkage distribution indicates that the polysaccharide is highly branched, with the most abundant 3,6-linked galactose residues (22.8%) defining the main branching points. Additional multiply substituted residues, such as 2,4-linked Gal (12.8%) and minor tri-substituted units, further contribute to the complexity. The backbone is primarily composed of 4-linked (19.7%) and 3-linked Gal (12.9%), while terminal xylose (12.9%) residues are confined to the branches, highlighting the structural heterogeneity of the polysaccharide. Comparable patterns, including β-(1→3), α-(1 → 4) backbones, 3,6-linked side chains, D and L-Gal with, and additional sulfate

or methoxy modifications, have been documented for sulfated xylogalactans isolated from *Jania rubens* and *Lithothamnion heterocladum*, supporting the relevance of these linkage types in coralline red algal polysaccharides (Navarro et al., 2011; Navarro & Stortz, 2008). Moreover, comparable backbone and branching features, together with sulfate and methoxy substitutions, have also been reported for xylogalactans isolated from *Jania adhaerens*, further supporting the assignment of the R-AEP polysaccharide from *E. elongata* as a structurally complex and highly branched xylogalactan (Hentati, Delattre, et al., 2020).

The purified sample was then analysed by ^{1}H,^{1}H COSY, TOCSY, NOESY, and ^{1}H,^{13}C DEPT-HSQC NMR experiments (Fig.40).

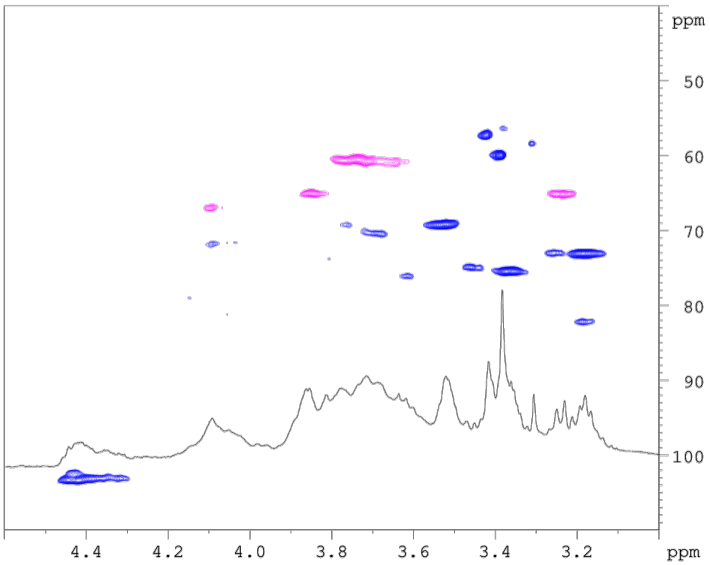

Figure 40. ^{1}H Selected region of ^{1}H, ^{13}C DEPT-HSQC spectrum of E. elongata R-AEP xylogalactan.

The 2D NMR experiments further highlighted the structural complexity of the polysaccharide, which hampers the definition of a unique and fully resolved repeating unit. The spectra displayed multiple overlapping correlations in both the anomeric and ring regions, consistent with the heterogeneous linkage pattern revealed by the PMAA analysis. In agreement with the chemical data, additional resonances attributable to methoxy groups at δ 3.41/60.2 and δ 3.45/58.1 ppm were found. Sulfate substitution of C6 of galactose residues was revealed by the signal of CH_2 at δ 4.10/67 ppm. Altogether, the combined NMR and chemical analyses describe a highly heterogeneous galactan, characterized by variable substitution, branching, and chemical modifications.

Despite extensive linkage, configuration analyses, and 2D NMR analysis, the high degree of heterogeneity, the coexistence of multiple linkage types, and the lack of a dominant repeating unit prevent the assignment of a precise and regular repeating structure. The data suggest a polysaccharide composed of a β-galactan backbone variably substituted with xylose residues and branched with galactose units.

Lastly, the α-amylase hydrolysis was also performed on the **E** and **S** conditions AEP extract and FT-IR spectra were obtained to detect differences in sulfate content in the xylogalactan. As shown in Fig. 41, the FT-IR spectra of the xylogalactan obtained from *E. elongata* AEP under the three experimental conditions displayed even stronger typical sulfate absorption bands around 1260-1220 cm^{-1} compared to the AEP crude extract**,** which is attributed to the S=O stretching vibration**.** The presence of these bands confirms that the xylogalactan backbone is highly sulfated**,** which is a characteristic feature in some of the red algal polysaccharides (Pei et al., 2021; Soto-Vásquez et al., 2022). Moreover, the intensity of the absorption band corresponding to the S=O stretching vibration of sulfate esters was found to be higher in the sample obtained under **E** conditions. This increased band intensity suggests that a higher sulfation of the xylogalactan occurs during the **E** condition, while the **R** condition showed intermediate features between **S** and **E**.

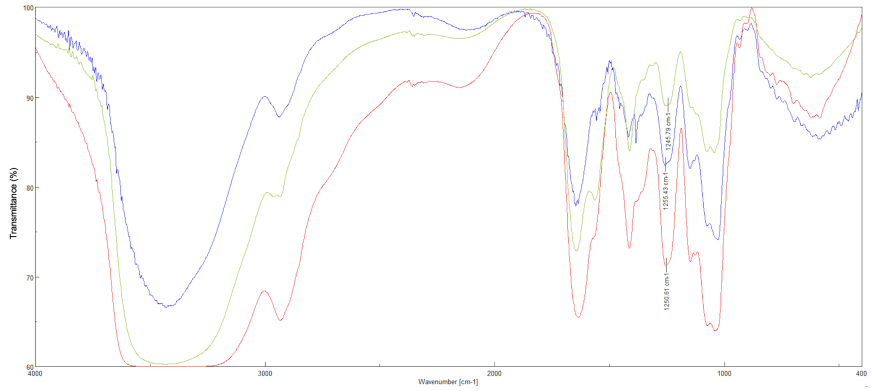

Figure 41. FT-IR spectra of E. elongata AEP second polysaccharides in S (blue); E (red), and R (green). Absorbing bands around 1260 cm^{-1} highlight the presence of a strong band due to the sulfate groups in E condition.

3.3 Functional characterization and application-oriented assessment

5.3.1 Antibiofilm assays

The antibiofilm activity of *E. elongata* samples was evaluated against two different strains of *Staphylococcus epidermidis* O47, an *agr*-mutant characterized by enhanced biofilm production, and RP62A, a reference strain. The samples tested are powders (P), pre-treated extracts (PTRE), and acid extraction precipitated polysaccharides (AEP), obtained from submerged (S), emerged (E), and re-submerged (R) algal conditions (Fig. 42).

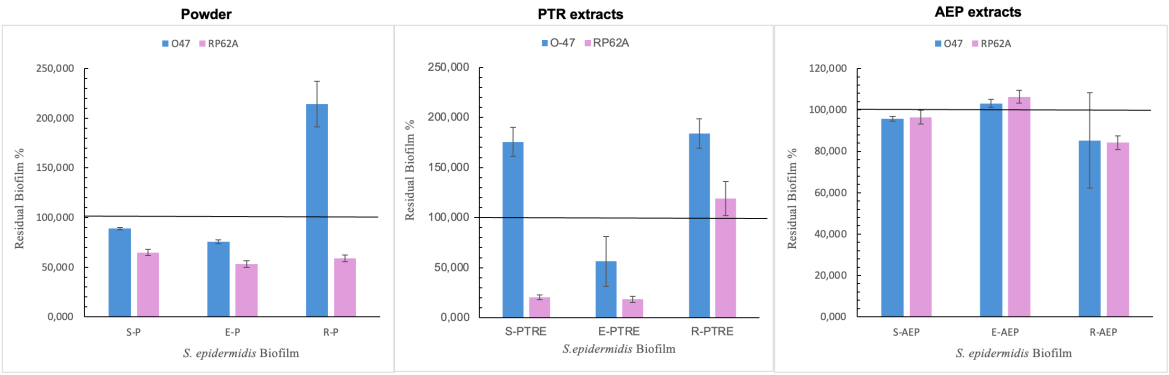

Figure 42. Antibiofilm activity of E. elongata samples: powder (P), pre-treated extracts (PTR), and acid extraction precipitated polysaccharides (AEP) obtained from submerged (S), exposed (E), and re-submerged (R) algal conditions, tested against S. epidermidis reference strain O47, and the clinical isolate RP62A biofilms in formation.

All powder samples showed a moderate antibiofilm effect, with stronger inhibition observed against *S. epidermidis* RP62A strain compared to the O47 strain. In S-P RP62A, biofilm formation was reduced to approximately 40%, whereas O47 showed only a moderate decrease. In contrast, the E-P induced a reduction of 50% of biofilm for the RP62A strain. Finally, for R-P conditions, the reduction in biofilm formation was observed only against RP62A. This suggests that R-P shows an activity that is strain-specificity. PTRE samples exhibited the strongest antibiofilm activity across all conditions, particularly against the RP62A strain, for which residual biofilm values dropped to very low levels in both S-PTRE and E-PTRE conditions. The O47 strain was also significantly inhibited, though to a lesser extent. Notably, the R-PTRE showed reduced antibiofilm performance against both strains, indicating that the **R** condition negatively affects the antibiofilm components preserved during pre-treatment. AEP fractions showed limited or strain-dependent antibiofilm activity. For both strains, S-AEP and E-AEP displayed residual biofilm values close to 100%, indicating the absence of an inhibitory effect. However, R-AEP induced a moderate reduction in biofilm formation for both strains, with a slight effect against RP62A.

The results revealed a clear strain-dependent response, with the RP62A strain being systematically more sensitive to the algal samples than the reference strain O47. Moreover, these findings highlight the selective antibiofilm potential of *E. elongata* PTRE against clinically relevant *S. epidermidis* strains, supporting their possible application as antibiofilm agents and a potential anti-adhesive in biomedical materials to prevent the biofilm formation of *S. epidermidis*.

5.3.2 Antioxidant assays

The antioxidant activity of *E. elongata* samples was evaluated using both H_2O_2 scavenging activity and 2,2-diphenyl-1-picrylhydrazyl (DPPH) radical scavenging assays (Fig. 43), at three incubation times (T0, T15, T30).

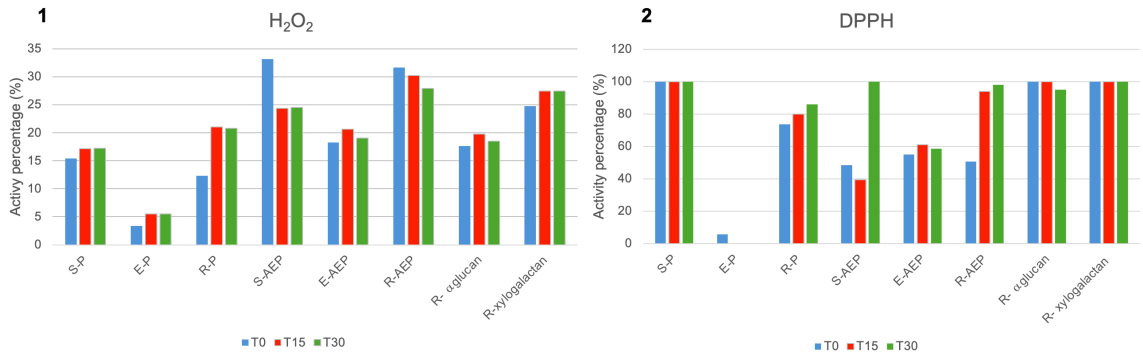

Figure 43. Antioxidant activities 1) hydrogen peroxide (H_2O_2) scavenging and 2) DPPH radical scavenging assays of E. elongata samples: powder samples (P), acid extraction precipitated polysaccharides (AEP), obtained from submerged (S), exposed (E), and re-submerged (R) conditions; and purified polysaccharide fractions (α-glucan and xylogalactan) obtained from re-submerged (R) condition.

All samples exhibited moderate to significant H_2O_2 scavenging activity (Fig. 43-1), with clear differences among environmental conditions and level of purification. The antioxidant activity generally increased from powders (P) to AEP extracts. S-AEP and R-AEP showed the highest scavenging efficiencies, reaching values above 30% at longer incubation times. The re-submerged α-glucan (R-α-glucan) and xylogalactan (R-xylogalactan) fractions also displayed remarkable antioxidant activity, comparable to AEP extracts. Powder samples showed the lowest antioxidant effectiveness, especially in the E-P, suggesting that polysaccharide extraction significantly enhances antioxidant performance. Time-dependent behaviour was observed for most samples, indicating a progressive interaction between the polysaccharides and reactive oxygen species. The DPPH assay revealed a strong activity observed for AEP fractions and purified re-submerged polysaccharides (Fig. 43-2). While S-P showed high scavenging values, E-P exhibited almost no activity, suggesting that environmental exposure strongly affects the antioxidant behaviour of raw biomass. AEP extracts displayed consistently high inhibition percentages, particularly R-AEP, R-α-glucan, and R-xylogalactan, which reached values close to 100% already at early time points.

These results confirm that structural purification enhances redox activity, likely due to higher accessibility of electron-donating groups within the polysaccharide backbone. Moreover, it is possible to assume that environmental stress associated with **E** and subsequent **R** stimulates the biosynthesis of protective polysaccharides, potentially involved in oxidative stress defence and structural reinforcement of the algal cell wall.

5.3.3 Physicochemical characterization and Film-forming properties

The thermal behaviour of *E. elongata* powder (P) samples and their AEP extracts was investigated by Differential Scanning Calorimetry (DSC) to evaluate the effect of physiological condition and purification on their thermal properties.

During the first heating run, all P samples exhibited a broad endothermic event associated with water evaporation (Fig. 44a).

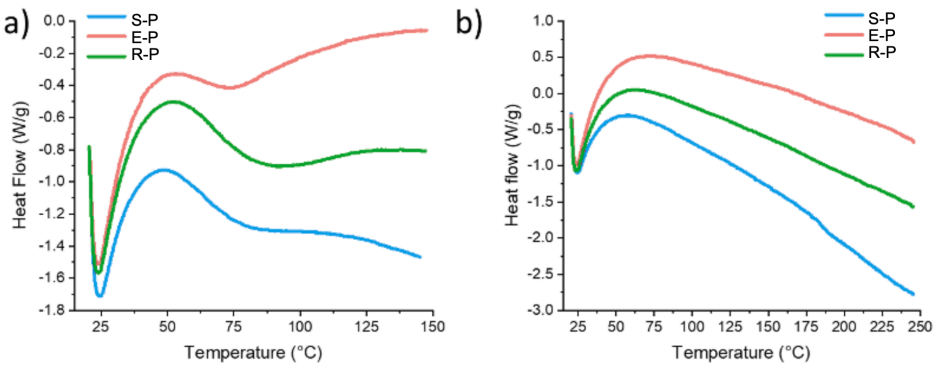

Figure 44. DSC thermograms of ground E. elongata samples: S-P, E-P, R-P recorded during the first (I) heating run (a), and the second (II) heating run (b).

However, clear differences were observed among samples. In particular, the E-P sample showed a slightly lower evaporation temperature and a reduced evaporation enthalpy compared to S-P and R-P (Table 8), suggesting a lower stability of bound water.

Table 8. Evaporation temperature (Tev) and enthalpy of evaporation (ΔHev) of E. elongata S-P, E-P, and R-P, determined by DSC during the first (I) heating run, representing the energy associated with water loss from the samples.

	T_{ev} (°C)	ΔH_{ev} (J/g)
S-P	82	6.99
E-P	75	4.41
R-P	91	11.56

This indicates that water molecules in E-P are less strongly associated with the algal matrix and are therefore more readily released. Following water removal, the second heating run did not show the endothermic band related to water evaporation, confirming its complete elimination during the first run (Fig. 44b). No significant differences were observed among samples, except for S-P, where a possible glass transition around 188 °C was detected, which may suggest the presence of residual amorphous organic material.

DSC analysis was also performed on the *E. elongata* AEP extracts, and more pronounced differences were observed. During the first heating run, all extracts displayed a similar endothermic event related to water evaporation (Fig. 45a), with comparable evaporation temperatures.

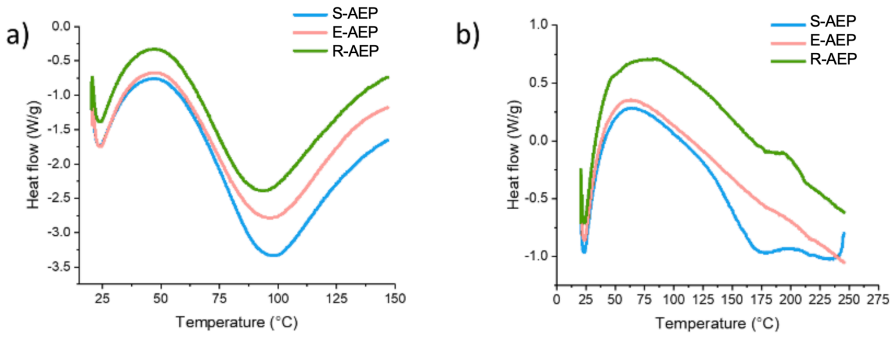

Figure 45. DSC thermograms of E. elongata extracts recorded during the first (I) heating run (a), highlighting water evaporation, and the second (II) heating run (b), showing melting and thermal degradation events.

However, a lower evaporation enthalpy was observed for R-AEP (Table 9), suggesting a reduced amount or a different organization of retained water.

Table 9. Evaporation temperature (Tev), evaporation enthalpy (ΔHev), melting temperature (Tf), and decomposition temperature (Td) of S-AEP, E-AEP, and R-AEP, determined by DSC during the first (I run) and second (II run) heating runs. Tev and ΔHev correspond to water evaporation in the first run, while Tf and Td represent melting and thermal degradation events observed in the second run.

	I run		II run	
	T_{ev} (°C)	**ΔH_{ev} (J/g)**	**Tf (°C)**	**Td (°C)**
S-AEP	97.3	184.6	173.2	199.5
E-AEP	95.5	182.0	-	199.6
R-AEP	94.6	174.9	176.0	195.8

Significant distinctions emerged during the second heating run (Fig. 45b). S-AEP exhibited an intense endothermic peak followed by an exothermic event, which can be attributed to the melting of organic components enriched during purification and their subsequent thermal degradation. In contrast, R-AEP displayed only the exothermic transition, while no significant thermal events were detected for E-AEP, indicating the absence or depletion of thermally active components under stress conditions.

Although *E. elongata* does not possess intrinsic gel- or film-forming properties, the observed thermal behaviour prompted further investigation of its incorporation into a polymeric matrix. Based on the DSC results, which highlighted more defined and reproducible thermal transitions for S-P and S-AEP, these samples were selected for subsequent film preparation. Both S-P and S-AEP were therefore incorporated into a sodium alginate matrix as a model biopolymer to evaluate their compatibility and potential applicability in film-based formulations. Representative images of the obtained films are reported in Fig. 46.

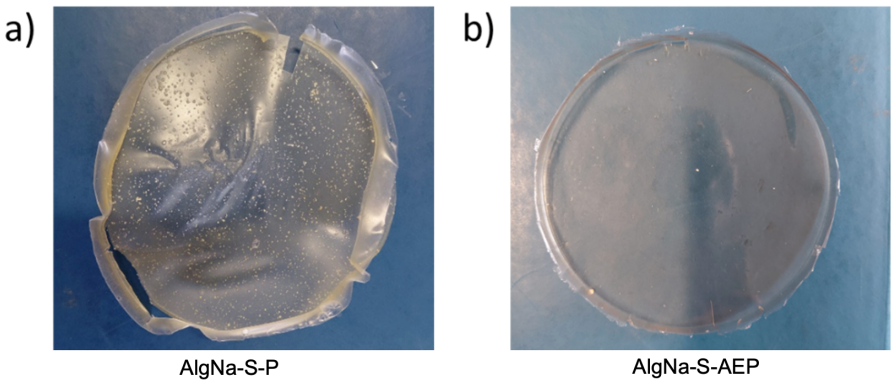

Figure 46. Representative images of sodium alginate (AlgNa) films loaded with E. elongata S-P(a) and S-AEP (b) at 5 wt% with respect to alginate (w/w).

The AlgNa-S-P (Fig. 46a) film showed a relatively homogeneous dispersion of insoluble algal particles within the polymeric matrix, whereas the AlgNa-S-AEP (Fig. 46b) film appeared transparent and highly uniform, reflecting the complete solubility of the extract and its improved compatibility with alginate.

To further investigate the effect of purification and physiological condition on the material properties, the samples were subjected to thermal and structural characterization by DSC and FTIR-ATR, in order to evaluate their thermal behaviour and the nature of chemical interactions within the material. FTIR-ATR spectra of *E. elongata* S-P, S-AEP, and alginate-based films loaded with both components (AlgNa-S-P, AlgNa-S-AEP) are shown in Fig. 47. The comparison between the powder (S-P) and its purified extract (S-AEP) (Fig. 47a) highlights marked compositional changes induced by the purification process.

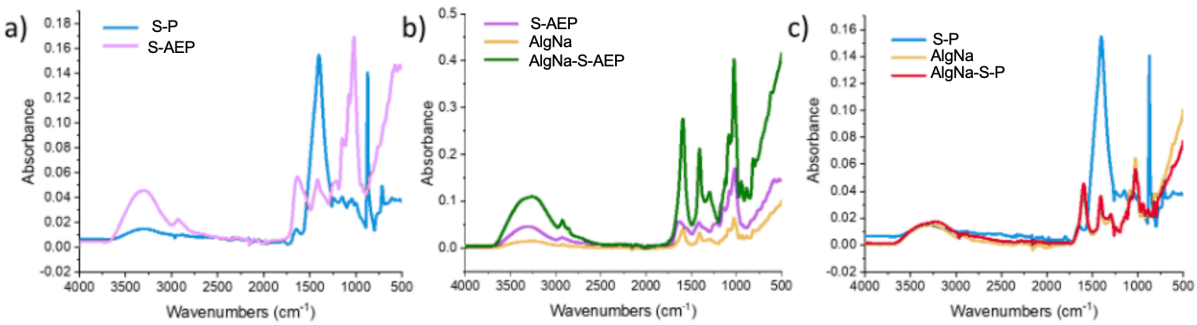

Figure 47. FTIR-ATR spectra of a) the S-P and S-AEP samples; b) the S-AEP sample, neat sodium alginate (AlgNa), and AlgNa film loaded with S-AEP; c) the S-P sample, neat sodium alginate (AlgNa), and AlgNa film loaded with S-P, highlighting the main vibrational features of the organic and inorganic components and their interactions within the polymeric matrix.

The spectrum of S-P is characterized by broad NH and OH stretching bands at approximately 3309 cm^{-1}, associated with amino acids and polysaccharides, and weak aliphatic C-H stretching bands at around 2929 cm^{-1}, attributable to $-CH_3$ and $-CH_2$ groups. A band at 1652 cm^{-1} can be assigned to C=O stretching and asymmetric N=O stretching of ester groups and pectic

complexes (El-Sayed & Ismail, 2022). The spectrum is dominated by the inorganic matrix, as evidenced by intense absorption bands at approximately 1401, 877, and 721 cm^{-1}, corresponding to the fundamental vibrational modes of carbonate ions in calcite (Al-Hosney & Grassian, 2005).

In contrast, the FTIR-ATR spectrum of the purified extract S-AEP shows a substantial reduction of the mineral component and a clear enrichment of the organic fraction. A sharp and intense band at approximately 1022 cm^{-1}, assigned to C-O and C-C stretching vibrations of pyranose rings, indicates an increased polysaccharide content. This is further supported by the broad and intense OH stretching band around 3300 cm^{-1}. Compared to the S-P, the extract also exhibits improved resolution in protein-related regions, with a more clearly defined Amide I band at ~1650 cm^{-1}. The appearance of bands in the aliphatic C-H stretching region (2920–2850 cm^{-1}) further supports the enrichment in organic components, including possible lipid fractions or hydrocarbon chains of cell wall polymers. As widely reported in the literature, the FTIR-ATR spectrum of sodium alginate (AlgNa) is characterized by a broad OH stretching band in the 3600-3000 cm^{-1} region, typical carboxylate absorption bands with asymmetric and symmetric C=O stretching at 1596 and 1408 cm^{-1}, respectively, and a characteristic C-O-C saccharide band at approximately 1026 cm^{-1} (Flórez-Fernández et al., 2019). In alginate films loaded with S-P and S-AEP (Figure 47b), a slight shift of the alginate carbonyl band toward higher wavenumbers was observed (1592, 1594, and 1595 cm^{-1} for AlgNa, AlgNa-S-P, and AlgNa-S-AEP, respectively), suggesting a partial modification of the hydrogen-bonding network between alginate chains and residual water upon incorporation of the algal components.

Lastly, DSC thermograms of alginate-based films, both unloaded and loaded with S-P and S-AEP, are shown in Fig. 48.

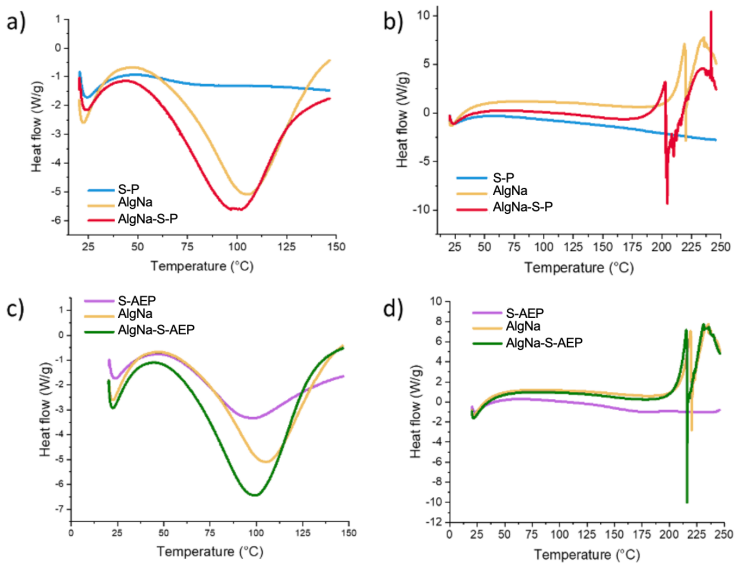

Figure 48. DSC thermograms of E.elongata S-P and S-AEP samples, neat sodium alginate (AlgNa) films, and AlgNa films loaded with S-P and S-AEP at 5 wt%, recorded during the first heating run (a, c) and the second heating run (b, d).

During the first heating run, all alginate-containing films exhibited a pronounced endothermic peak associated with water evaporation, which was markedly more intense than that observed for S-P alone, reflecting the higher water affinity of the alginate matrix. Upon the second heating run, the endothermic evaporation peak was no longer detected, confirming the complete removal of water during the first run. At higher temperatures, thermal events appearing around 200 °C were observed for all alginate-based films and can be attributed to the onset of polymer degradation. The presence of S-P or S-AEP did not introduce additional thermal transitions in this temperature range, indicating that the thermal behaviour of the films is mainly governed by the alginate matrix.

5.4 Conclusion

In this study, *Ellisolandia elongata* samples collected under three different environmental conditions, submerged (**S**), exposed (**E**), and re-submerged (**R**), were investigated to evaluate the impact of environmental stress on lipid and polysaccharide composition, yield, and structural features. Polysaccharides were extracted using both aqueous (WE) and acidic procedures (AEP), revealing comparable monosaccharide compositions and spectroscopic profiles. However, AEP provided higher purity and polysaccharide recovery and was therefore selected for subsequent analyses. Polysaccharide yields ranged from 1.09% (**S**) and 1.15% (**E**) to 1.46% (**R**) of the initial dry biomass, with the highest yield consistently obtained under **R** conditions. Significant compositional differences among the three conditions were observed. Lipid analysis revealed marked variations in long-chain polyunsaturated fatty acids. In particular, exposed samples (**E**) were characterized by higher relative amounts of arachidonic acid (C20:4) and oleic acid (C18:1), while eicosapentaenoic acid (EPA, C20:5) decreased compared to submerged (**S**) thalli. Conversely, re-submerged samples (**R**) showed the highest

EPA content together with a reduction of arachidonic acid, suggesting a recovery-associated remodelling of membrane lipids.

Given the higher polysaccharide yield and, at the same time, the absence of major structural differences among the AEP extracts as assessed by AMG analysis and ^{1}H NMR spectroscopy, the R-AEP extract was selected for detailed structural characterization. Structural analyses revealed the co-extraction of two polysaccharides: an α-1,4-glucan, reported in literature as Floridean starch, and a sulfated heteropolysaccharide. Enzymatic removal of the α-1,4-glucan allowed the isolation and characterization of the second polysaccharide, which was identified as a structurally heterogeneous xylogalactan. The combinations of FT-IR, linkage, and configuration analyses demonstrated a branched galactan backbone variably substituted with xylose residues, multiple galactose linkage types, the coexistence of both D- and L-galactose, and the sulfated substitutions. The high degree of heterogeneity and the lack of a dominant repeating unit prevented the definition of a single, well-defined structural motif. FT-IR analysis confirmed the sulfated nature of the xylogalactan and revealed condition-dependent differences in sulfate content. Polysaccharides obtained under **E** conditions showed a higher degree of sulfation compared to those extracted from **S** and **R** samples, indicating that environmental stress influences not only polysaccharide yield but also chemical features such as sulfation.

E. elongata samples were tested for antibiofilm and antioxidant activities. Assays against *S.epidermidis* demonstrated a strain-dependent response, with the clinical isolate RP62A being consistently more sensitive than the reference strain O47. Pre-treated extracts (PTRE) exhibited the strongest antibiofilm activity across all conditions, particularly against the clinical isolate, while AEP fractions showed limited or moderate, condition-dependent effects. Notably, PTR-R samples displayed reduced antibiofilm activity, suggesting that the sample negatively affects the antibiofilm-active components preserved during the pre-treatment step.

Antioxidant assays further highlighted the functional relevance of polysaccharide extraction and purification. While powder samples exhibited limited scavenging activity, especially under exposed conditions, AEP extracts and purified polysaccharides showed significantly enhanced antioxidant performance. R-AEP, R-α-glucan, and R-xylogalactan displayed high DPPH radical scavenging activity, reaching near-complete inhibition at early incubation times, and moderate to strong hydrogen peroxide scavenging capacity. These results indicate that **R** favours the production of highly bioactive antioxidant polysaccharides and that purification enhances redox activity, likely by increasing the accessibility of electron-donating functional groups within the polysaccharide backbone.

In addition to the biological activities, the thermal and structural characterization provided further insight into the material properties of *E. elongata*. DSC analyses revealed condition-dependent differences in water organization and thermal transitions, highlighting the submerged condition (**S**) as the most thermally defined and reproducible, both for the powder and the corresponding AEP extract. FTIR-ATR analyses confirmed that purification effectively reduced the inorganic fraction and enriched the organic components, improving the

compatibility of the extracts with polymeric matrices. Although *E. elongata* does not exhibit intrinsic gel- or film-forming properties, its incorporation into a sodium alginate matrix resulted in homogeneous and stable films, particularly when using the purified extract. These results support the suitability of *E. elongata* polysaccharides as functional additives in biopolymer-based films and further strengthen the link between environmental conditions, extraction strategy, and potential material applications.

This study demonstrates that environmental stress and subsequent re-submerged significantly influence the chemical composition, structural features, thermal behaviour, and biological activities of *E. elongata* polysaccharides. The observed correlations between environmental conditions, polysaccharide sulfation, structural heterogeneity, and bioactivity provide new insights into the adaptive role of algal polysaccharides and support their potential application as antioxidant and antibiofilm agents in biomedical and biotechnological contexts. In addition, preliminary thermal and structural investigations, together with film-forming assays, indicate that *E. elongata* derived polysaccharides, although not intrinsically film-forming, can be effectively incorporated into biopolymeric matrices such as sodium alginate, yielding homogeneous and stable films. These results further expand the functional relevance of *E. elongata* polysaccharides and highlight their potential as bioactive components in multifunctional, sustainable material formulations.

Chapter 6

Tetraselmis exopolysaccharides

6.1 Tetraselmis

Tetraselmis is a genus of unicellular eukaryotic marine and freshwater microalgae that belongs to the family of *Chlorodedroaceae*, first described in 1959 by Robert William Butcher (Lund & Butcher, 1960). These flagellated green microalgae display a distinctive morphology as described in detail in section 1.4.1 and a widespread ecological distribution across marine and freshwater environments, where they act as primary producers in the photic zones of the water column (Zhou et al., 2022).

This genus is widely used as a model organism in marine research and bioremediation, and also in aquaculture. For instance, *Tetraselmis* species can absorb heavy metals, showcasing their potential in restoring ecosystem health (Goswami et al., 2022), are used as live feed for larval fish and shellfish, thanks to their fatty acids and protein content (Martino et al., 2023; Sandeep et al., 2021), and promising in the field of biotechnology, particularly in biofuel production, due to their lipid content. Furthermore, microalgae of the genus *Tetraselmis* have garnered considerable scientific and industrial interest due to their metabolic versatility. Species belonging to this genus can adjust their metabolism in response to environmental prompts, switching between autotrophic, heterotrophic, and mixotrophic growth modes, which enables them to optimise carbon utilisation and biomass accumulation under varying nutrient and light conditions (Azma et al., 2010). This metabolic plasticity, paired with rapid growth rates, makes *Tetraselmis* valuable for studies in marine physiology, carbon cycling, and sustainable production systems. Finally, *Tetraselmis* species are known to produce a complex array of extracellular and cell wall-associated polysaccharides as previously described in section 1.4, which contribute to cellular defence mechanisms, mediate interactions with the surrounding environment, and exhibit promising bioactivities (Parra-Riofrío et al., 2020). Despite increasing interest in their biological roles, detailed structural characterisation of *Tetraselmis* polysaccharides remains limited, particularly regarding linkage patterns, monosaccharide composition, and functional groups, which are critical for understanding their functional properties and potential applications.

Three different *Tetraselmis* strains were purchased from Culture Collection of Algae and Protozoa (CCAP) and investigated in this study: *Tetraselmis suecica* (CCAP 66/4) isolated from 10 miles south of La Spezia, Italy; *Tetraselmis suecica* (CCAP 66/22D) isolated from Bembridge, Isle of Wight, England, UK; and *Tetraselmis chuii* (CCAP 8/6) collected in Millport, Isle of Cumbrae, Scotland, UK. This strain selection enables a comparative analysis of polysaccharide secretion and composition under autotrophic, heterotrophic, and mixotrophic conditions.

The main objective of this chapter is to characterize the polysaccharides from the three *Tetraselmis* species under autotrophic, heterotrophic, and mixotrophic conditions, isolated from three different habitats. The aim was to evaluate how the growth conditions influence both the

production and structural complexity of *Tetraselmis* polysaccharides. Furthermore, polysaccharides would be further analysed for their potential immunomodulatory activity.

6.2 Result and discussion

6.2.1 Strains growth

Three *Tetraselmis* strains were purchased from Culture Collection of Algae and Protozoa (CCAP) SAMS Limited in axenic conditions: *Tetraselmis suecica* 66/4 (isolated from Italy), *Testraselmis suecica* 66/22D (isolated from the UK), and *Tetraselmis chuii* 8/6 (isolated from the UK) (Fig.49).

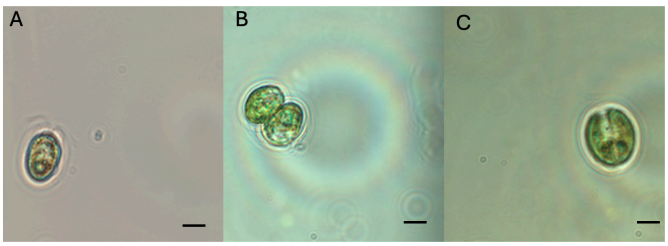

Figure 49. A) Tetraselmis suecica 66/4; B) Tetraselmis suecica 66/22D; C) Tetraselmis chuii 8/6. Scale bar of 5µm.

T. suecica 66/4*, T. chuii* 8/6, and *T. suecica* 66/22D were grown in Nutribloom medium. Each strain was inoculated in three conditions: heterotrophic conditions (HC), mixotrophic conditions (MixC), both with glucose as a carbon source, and autotrophic conditions (AC) as a control. The growth rates were controlled by measuring the OD at 750 nm. The structural and morphological changes expected in different growth conditions were analysed by using an Inverted Fluorescence Microscope**.** The microalgae from autotrophic to heterotrophic conditions presented some visible morphological differences. More specifically, in heterotrophic conditions, the cells appeared with no flagella visible, a round cell shape, and a green to yellowish color due to the absence of light and degradation of pigments (Lu et al., 2017).

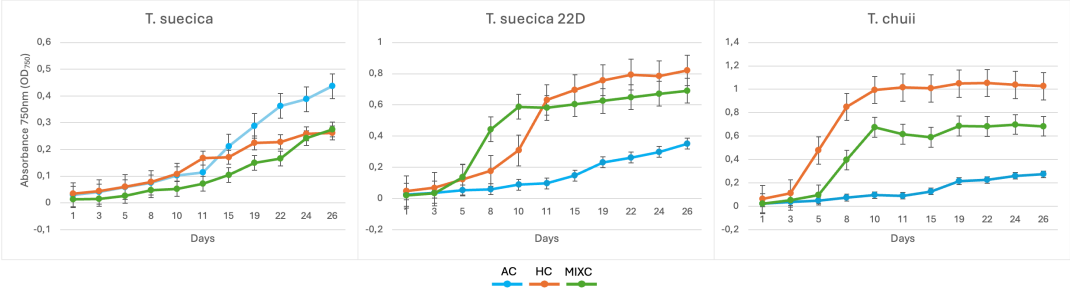

Figure 50. Growth of T. suecica, T. suecica 22D, T. chuii in three conditions was monitored by measuring absorbance at 750nm.

The growth curves of *T. suecica*, *T. suecica* 22D, and *T. chuii* cultivated in flasks under AC, HC, and MixC conditions revealed distinct species and condition-dependent trends (Fig. 50). It is important to note that all heterotrophic cultures (HC) were subjected to a progressive reduction of the photoperiod, from L:D (Light: Dark) 12:12 → 8:16 → 4:20 → 2:22 → 0:24, a strategy designed to shift the cells towards full heterotrophy gradually. This reduction in light availability directly influenced the growth behaviour observed under HC and must be considered when comparing the three trophic regimes (Azma et al., 2010). For *T. suecica*, the three trophic conditions produced clearly distinct growth profiles. The AC culture showed the most pronounced increase over time, with a steady rise in OD_{750} that became more marked after the mid-experiment phase, ultimately reaching the highest final absorbance. The MixC condition also supported sustained growth, although at a slower rate, resulting in intermediate OD_{750} values throughout the cultivation period. In contrast, the HC curve displayed an initial increase followed by a much slower progression, stabilizing at significantly lower OD_{750} values compared to both AC and MixC. This reduced performance is consistent with the progressive removal of light, which likely decreased the photosynthetic contribution over time in a species that remains predominantly photoautotrophic. *T. suecica* 22D showed a markedly different response. The HC condition supported the most rapid and substantial increase in OD_{750}, with cells reaching a plateau earlier and at a higher density than both AC and MixC. The strong heterotrophic performance of this strain suggests an enhanced ability to metabolize organic carbon efficiently, allowing sustained growth even as illumination was progressively reduced. MixC displayed an intermediate pattern, whereas AC resulted in the slowest growth, indicating that the 22D strain relies predominantly on external carbon sources to maximize cell proliferation. Finally, *T. chuii* demonstrated the highest heterotrophic performance among the three species. Under HC, the culture showed a steep increase in OD_{750} during the first week, rapidly reaching a high-density plateau despite the sequential reduction of the photoperiod. MixC followed a similar early trend but stabilised at slightly lower values. Conversely, the AC culture exhibited very limited biomass accumulation throughout the experiment, confirming the species' strong preference for heterotrophic metabolism and its limited efficiency under purely photoautotrophic conditions. It should be noted that these growth profiles are presented for descriptive purposes only, to provide context for the polysaccharide extraction. No statistical comparisons were performed on the OD_{750} data, since the focus of this study is the chemical

characterization of the extracted polysaccharides rather than the growth differences among species or trophic conditions.

The medium of each culture was recovered and treated to extract Extracellular polymeric material (EPMs).

Table 10. Amount (mg) of EPMs by T. suecica, T. sucecica 22D, and T. chuii (500 ml) in three different growth conditions.

EPM (mg)	***T.suecica***	***T. suecica* 22D**	***T. chuii***
AC	33.2	12.3	35.2
HC	45.2	88.3	93
MixC	116.6	180	153.6

EPM production varied considerably with both strain and growth condition (Table 10). AC produced the lowest amounts of EPM, ranging from 12.3 mg (*T. suecica 22D*) to 45.2 mg (*T. suecica*). Under HC, EPM content increased markedly, with values up to 93 mg (*T. chuii AC*), indicating that organic carbon availability enhances polysaccharide secretion. MixC led to the highest overall EPM production (116.6-180 mg), suggesting a synergistic effect of combined autotrophic and heterotrophic metabolism on EPM synthesis.

Table 11. Biomass (mg) by T. suecica, T. sucecica 22D, and T. chuii (500 ml) in three different growth conditions.

BIOMASS (mg)	***T. suecica***	***T. suecica* 22D**	***T. chuii***
AC	251.2	142.1	89.7
HC	153.3	375.4	339.8
MixC	99.2	304.5	304.1

The three microalgal strains displayed distinct growth patterns depending on the cultivation conditions (Table 11). In AC, biomass ranged from 89.7 mg for *T. chuii* to 251.2 mg for *T. suecica*, whereas HC generally promoted higher biomass accumulation, reaching up to 375.4 mg in *T. suecica 22D*. MixC resulted in intermediate to high biomass levels (99.2–304.5 mg) across the strains, suggesting that both organic and inorganic carbon sources contributed to growth.

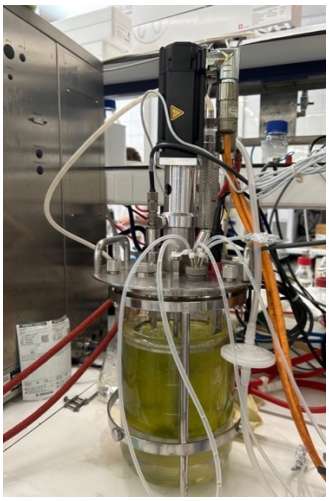

Figure 51. T. chuii cultivation in a 2-L bench-top bioreactor (Biostat B-plus Exclusive Flow, Sartorius Stedim, Germany) MixC.

As a next step, *T. suecica* 22D and *T. chuii* were the two species selected for bioreactor scale-up (Fig. 51). The MixC was chosen as the trophic condition for both species since it proved to be the fastest method to achieve more EPM.

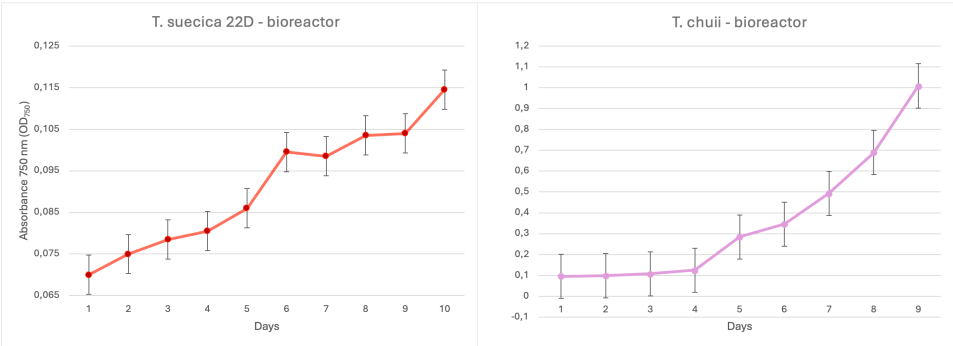

Figure 52. Growth curves of T. suecica 22D and T. chuii in 2L bioreactors.

In Fig. 52, the OD_{750} of *T. suecica* 22D increased gradually, reaching a final value of approximately 0.12 by Day 10. The growth trend was linear and steady, with no evident exponential phase. This suggests that, during the growth in the bioreactor, the strain experienced moderate but stable growth, likely limited by light availability and/or carbon supply. The absence of a sharp increase in biomass indicates that the strain may have adapted slowly to the controlled environment or maintained a predominantly autotrophic metabolic regime. In contrast, *T. chuii* exhibited a markedly different behaviour. After a slow initial phase, the culture entered a clear exponential growth phase starting from Day 7, ultimately reaching an OD_{750} of ~1.0 by Day 9. This indicates that *T. chuii* responded much more efficiently to the bioreactor conditions than *T. suecica* 22D. The sharper growth curve suggests higher

photosynthetic efficiency, better adaptation to mixing and aeration, or a greater ability to utilize the carbon supplied through aeration. The amount of EPM extracted from the two bioreactors is reported in Table 12.

Table 12. Amount (g) of EPS extracted from T. suecica 22D and T. chuii after two weeks of bioreactor assays.

Bioreactors MixC	***T.suecica* 22D 2L**	***T. chuii* 2L**
Biomass (g)	1,660	2,280
EPM (g)	0.7	1.2

6.2.2 T. chuii EPMs in three trophic conditions

Based on the results obtained at both flask and bioreactor scale, *T. chuii* was selected for further investigation since it showed the most consistent and robust performance under MixC and HC conditions, combining high biomass productivity with the highest EPM yields. The EPM obtained from the three trophic conditions of *T.chuii* were dialysed against water. The EPMs of *T. chuii*, were preliminarily analysed by 14% DOC PAGE. The gel was visualised after Alcian blue and silver nitrate and showed the presence of well visible bands at low molecular weight polysaccharides and less pronounced bands at higher molecular weight in all conditions (Fig. 53).

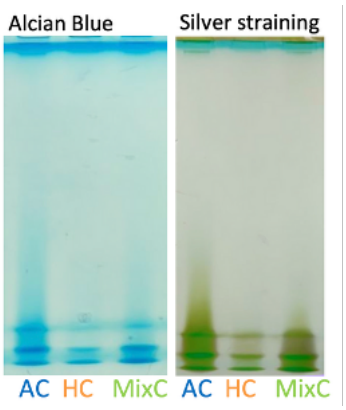

Figure 53. 14% DOC PAGE of T. chuii EPMs grown in AC (blue), HC (orange), and MixC (green). Dyed with A) alcian blue staining, B) silver staining.

An inspection of the ^{1}H NMR spectra of all EPM samples revealed the same profile for HC and MixC polysaccharides in the anomeric and carbinolic regions. Instead, the ^{1}H NMR profile of AC was found to be different (Fig. 54).

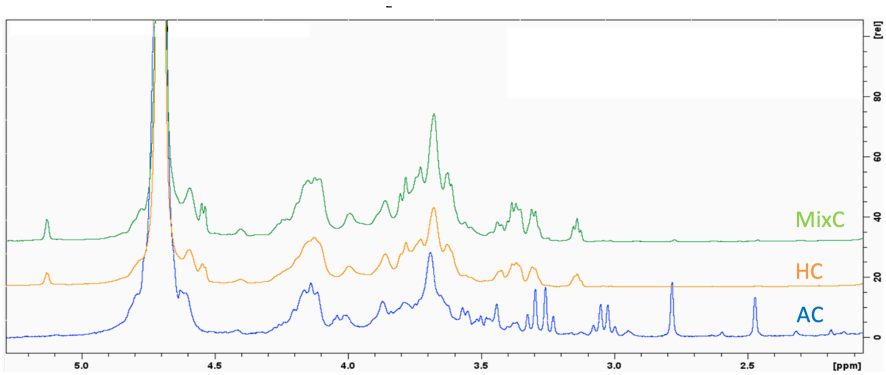

Figure 54. ^{1}H NMR spectra, recorded in D_2O, of T. chuii EPMs crude extract from AC (blue), HC (orange), and MixC (green).

The FTIR spectra of the EPM extracted from *T. chuii* cultivated under AC, MixC, and HC exhibited the characteristic features of polysaccharidic materials, confirming the carbohydrate nature of the extracts (Figure 55).

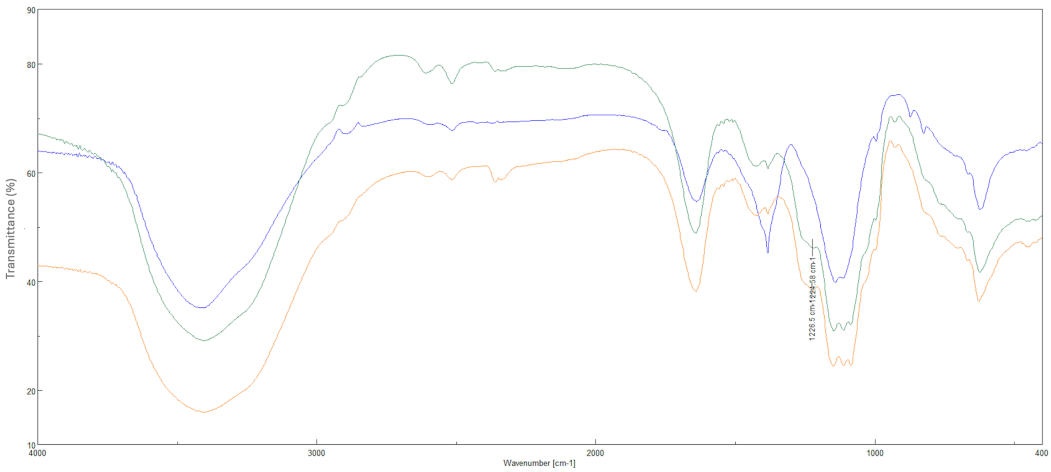

Figure 55. FT-IR spectra of T. chuii EPMs in AC (blue), HC (orange), and MixC (green). Absorbing bands around 1260 cm^{-1} highlight the presence of sulfate in HC (orange) and MixC (green).

All spectra showed a broad absorption band in the 3600-3000 cm^{-1} region, attributed to the stretching vibrations of hydroxyl (-OH) groups, indicative of extensive intra- and intermolecular hydrogen bonding typical of polysaccharides. Minor differences in band intensity and width among the samples suggest variations in hydration depending on the trophic condition. Weak bands observed in the 3000-2800 cm^{-1} range correspond to C-H stretching vibrations of the polysaccharide ring, confirming the aliphatic backbone. Absorption features in the 1600-1400 cm^{-1} region were assigned to the asymmetric and symmetric stretching vibrations of carboxylate groups ($-COO^{-}$), indicating the presence of acidic functionalities within the EPM, which may contribute to their overall negative charge. A characteristic band detected in the 1270-1200 cm^{-1} region was attributed to the asymmetric stretching vibration of sulfate ester groups ($-OSO_3^{-}$), and additional bands in the 900-800 cm^{-1} region are consistent with C-O-S vibrations as already reported by (Fimbres-Olivarria et al., 2023), confirming the

presence of sulfated polysaccharides in MixC and HC conditions, whereas no significant absorption sulfate bands were shown in AC. Variations in band intensity suggest that the trophic regime influences the degree of sulfation. Moreover, the intense absorption bands between 1150 and 1000 cm^{-1} are associated with C-O-C and C-O stretching vibrations of glycosidic linkages and pyranose rings, confirming the integrity of the polysaccharide backbone.

The EPM samples from *T. chuii* were analysed by HPLC with RID detection to assess their carbohydrate profiles (Fig. 56).

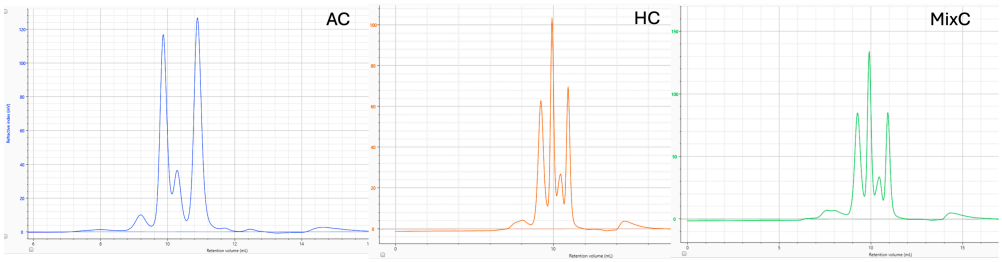

Figure 56. HPLC profiles of T.chuii EPMs in AC (blue) HC (orange), and MixC (green).

The chromatograms showed that the EPM from HC and MixC conditions exhibited highly similar profiles, with overlapping peaks and comparable retention times, suggesting that the polysaccharide composition is conserved under these two culture conditions. In contrast, the AC's EPM has a different chromatographic pattern, characterized by shifts in peak retention times and the presence of unique peaks not observed in HC or MixC samples. In all cases, the broad, multi-peak profiles revealed a high degree of heterogeneity across the EPM fractions, but differences likely reflect the influence of trophic conditions on EPM production. The altered retention times in AC samples may indicate variations in molecular weight distribution or monosaccharide composition, possibly resulting from changes in metabolic pathways under different nutritional regimes.

6.2.3 Structural characterization of T. chuii EPS in MixC

Based on the comparative analyses of EPM production and composition across trophic conditions, the EPM produced by *T. chuii* under MixC was selected for detailed structural characterization, as it provided sufficient, reproducible material and also displayed a comparable compositional profile to the EPM obtained under heterotrophic conditions.

A sugar analysis on *T. chuii* EPM in MixC was performed using GC-MS techniques after derivatization of monosaccharides as acetylated methyl glycosides (AMGs) (Fig. 57).

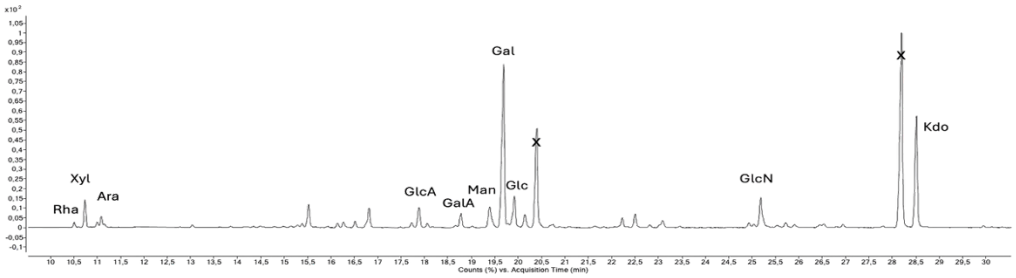

Figure 57. AMG spectrum of T. chuii EPM in MixC.

GC-MS analysis revealed the presence of mannose (Man), galactose (Gal), glucose (Glc), and 2-amino-2-deoxy-D-glucose (GlcN). Traces of rhamnose (Rha), xylose (Xyl), glucuronic acid (GlcA), and galacturonic acid (GalA) were detected. Lastly, 3-Deoxy-D-manno-oct-2-ulosonic acid (Kdo) was observed, which is reported to be a known component of *Tetraselmis* cell wall (Kermanshahi-pour et al., 2014).

To purify the sample, P-10 gel filtration chromatography was performed.

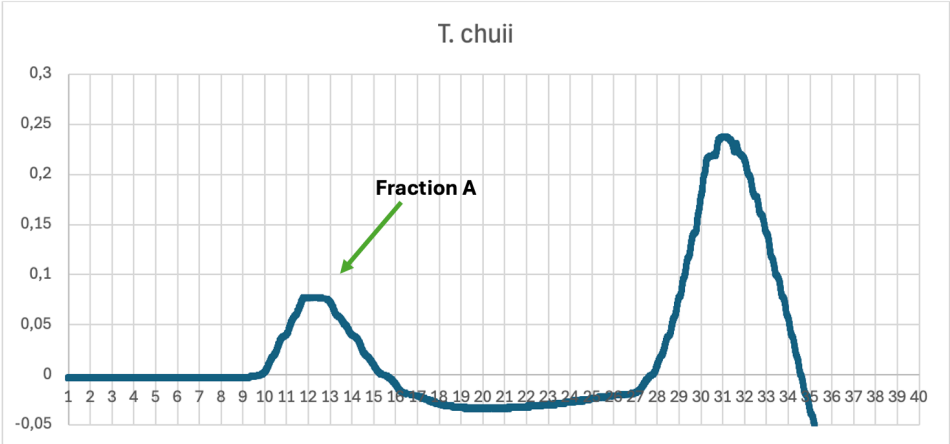

Figure 58. P-10 chromatographic column spectrum of T. chuii EPM in MixC. The green arrow highlights the presence of the purified EPS sample.

Figure 58 shows the chromatogram obtained from the gel filtration chromatography. The green arrow highlights the presence of the purified EPS (Fraction A), while the second peak is attributed to the presence of salts. For the same fraction, a 14% DOC-PAGE electrophoresis on polyacrylamide gel was performed (Fig. 59).

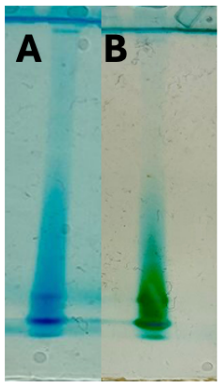

Figure 59. 14% DOC PAGE analysis on T.chuii P10 Fraction A. A) dyed with Alcian blue, B) dyed with silver staining.

The sample was dyed first with Alcian blue (A) and then with silver staining (B). The sample showed low molecular weight bands visible both in Alcian and silver staining, and high molecular weight bands more visible in Alcian blue (A). The FT-IR spectra of the EPM and the EPS after purification were obtained and compared; the EPS revealed clear differences attributable to the purification process (Fig. 60).

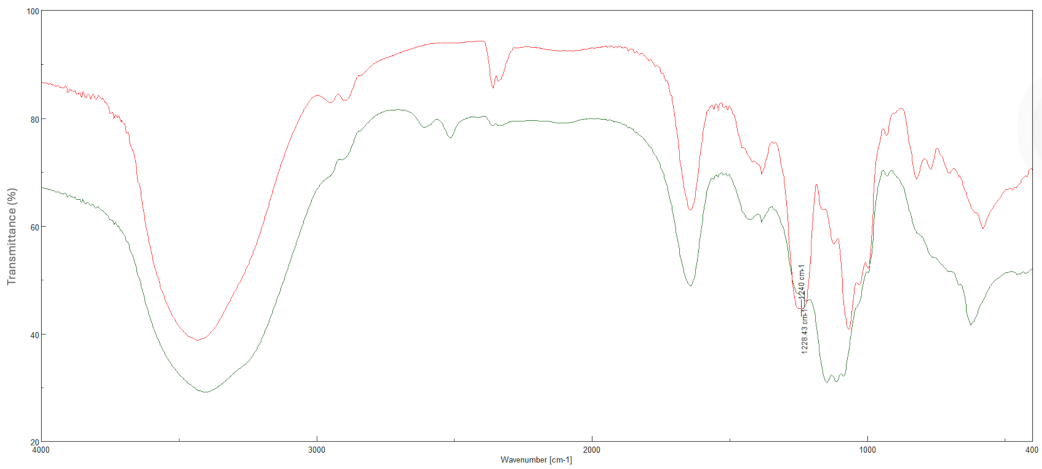

Figure 60. FT-IR spectra of the T. chuii EPSs (MixC). Crude EPM (green) and the purified EPS (red) showing an intense sulfated absorbing band at around 1240 cm $^{-1}$.

Precisely, the absorption bands associated with sulfate ester groups in the 1270-1200 cm^{-1} and 900-800 cm^{-1} regions were more clearly defined in the purified EPS, suggesting an enrichment of sulfated polysaccharide fractions following purification. The persistence and sharpening of the intense bands between 1150 and 1000 cm^{-1}, attributed to C-O-C and C-O stretching vibrations of glycosidic linkages, further confirmed the structural integrity of the polysaccharide backbone.

The HPLC profile in Fig. 61 of the purified EPS exhibited multiple absorption peaks, indicating a still unresolved mixture rather than a single homogeneous component.

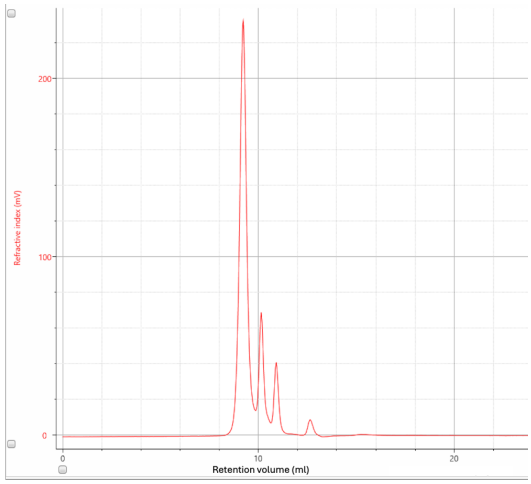

Figure 61. HPLC profile of T.chuii purified EPS (MixC).

The presence of distinct peaks signals across the chromatogram clearly reflects the heterogeneity of the sample. Nonetheless, the AMG analysis of the purified EPS showed the only presence of galactose (Fig. 62), suggesting that *T. chuii* EPS is a galactan.

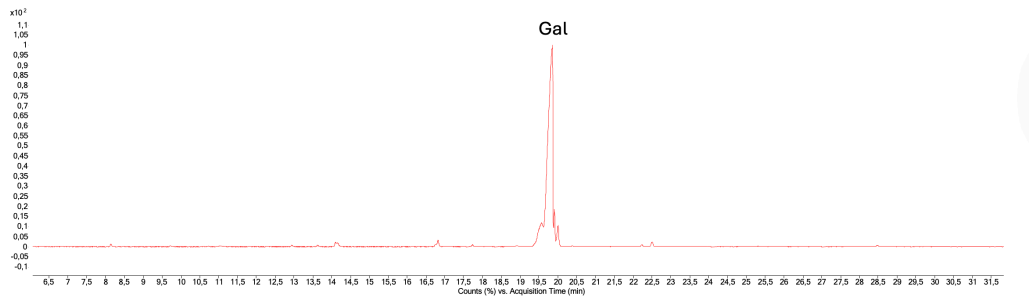

Figure 62. AMG spectrum of T. chuii purified EPS in MixC.

To better identify the structural features of this EPS, a desulfation was performed, and a ^{1}H NMR spectrum was obtained to verify the occurrence of the reaction (Fig. 63).

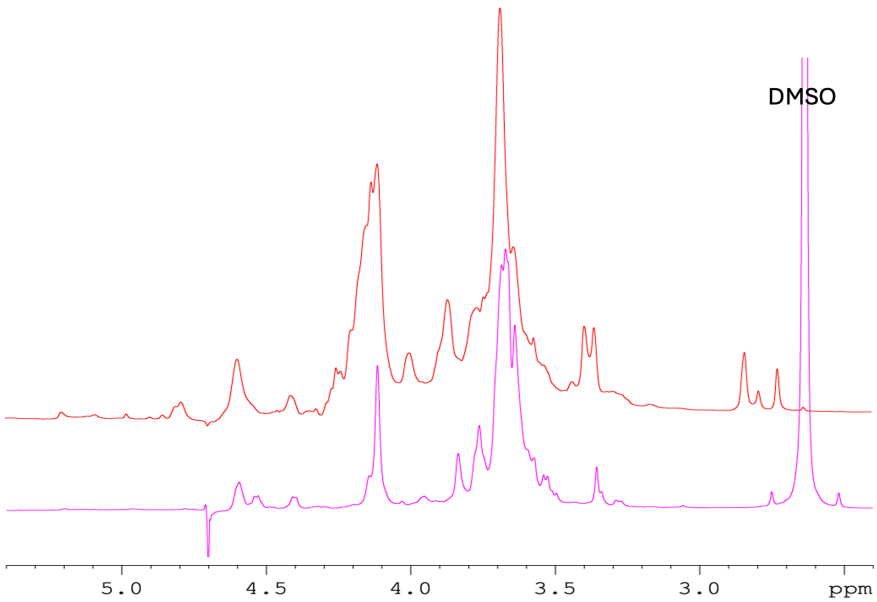

Figure 63.[1]H NMR spectrum of T.chuii purified EPS (red) and desulfated sample (pink). Dimethyl sulfoxide (DMSO) is present as a contaminant after desulfation.

The NMR spectrum after the elimination of the sulfate groups appeared to be less complex (pink line in Fig. 63). The lack of signals at 4.8 ppm suggested that these protons could be on a carbon carrying an O-sulfate group. Acetylated octyl glycosides (AOG) chemical analysis allowed to obtain the sugars' absolute configuration which resulted in only the D-galactose configuration. Lastly, PMAA's chemical analysis of the samples was performed, and Table 13 shows that the galactose present in the sample is linked as follows: t-D-Gal, D-Gal-3-linked, and D-Gal-3,6-linked.

Table 13. Linkage analysis of the EPS from Tetraselmis chuii based on GC–MS analysis of PMAAs.

Monosaccharides	Glycosidic linkage	PMAAs derivates
Gal*p*	terminal	2,3,4,6-tetra-*O*-methyl 1,5 di-*O*-acetyl-galactopyranose
Gal*p*	→3-linked	2,4,6-tri-*O*-methyl-1,3,5-tri-*O*-acetyl-galactopyranose
Gal*p*	→3,6-linked	2,4-di-*O*-methyl-1,3,5,6-tetra-*O*-acetyl-galactopyranose

The $^{1}H,^{1}H$ COSY, TOCSY, NOESY and $^{1}H,^{13}C$ DEPT-HSQC NMR experiments of purified EPS were collected (Fig. 64) and confirmed the presence of a galactan polysaccharide.

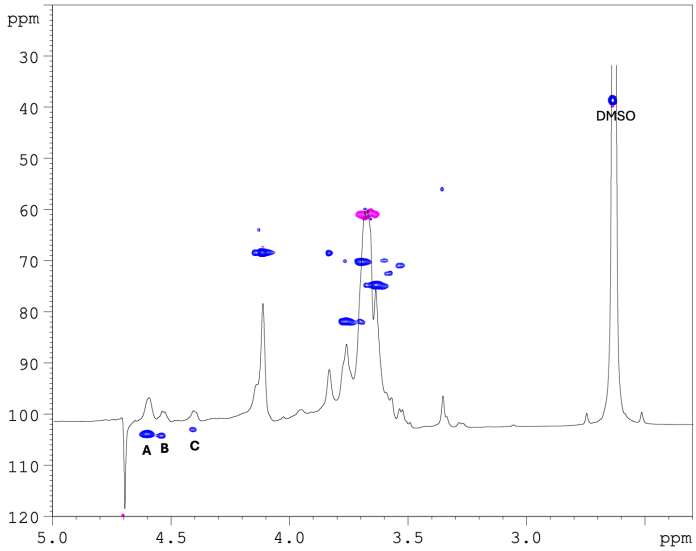

Figure 64. [1]H Selected region of [1]H, [13]C DEPT-HSQC spectrum of T. chuii desulfated EPS (MixC). DMSO is highlighted as a contaminant after chemical desulfation.

The presence of anomeric signals at 103-104 ppm indicated β anomeric configurations for all the residues (Table 14). All the chemical shifts of the three different galactose units were identified. The downfield shift of the C-3 signals for units **A** at 82.0 ppm indicated its substitution (Bock & Pedersen, 1983). Residues **C** were recognised to be 3,6-substituted units due to the downfield shifts of both C3 and C6, at 82.0 and 69.0 ppm, respectively. Residues **B** were found to be terminal non-reducing ends since none of the carbons were downfield shifted. The study of the 2D NMR also revealed that some of the 3-linked galactose units are substituted at position O-2 by a methyl group (A' units, Table 14). This was revealed by the signal at δ 3.36 ppm that displayed a long-range correlation with the shifted C2 of the **A**' units at 81.6 ppm. Integration of the ^{1}H NMR signals suggested an approximate ratio of one methylated galactose unit every six galactose residues. These structural features deduced from the NMR analysis are aligned with previously described extracellular polysaccharides from marine microalgae, which are commonly reported as β-galactans or galactose-rich polymers dominated by 3-linked and 3,6-substituted β-D-galactopyranose residues (Laroche, 2022). For instance, EPS produced by red microalgae such as *Porphyridium* spp. have been extensively described as high-molecular-weight, anionic polysaccharides with significant galactose content and structural features comparable to marine algal galactans (Percival & Foyle, 1979). In addition, substituents such as methyl ethers, sulfate groups, and other functional groups have been reported as recurrent modifications in algal and marine polysaccharides, supporting the identification of methyl-substituted galactose units in the present EPS (Ciancia et al., 2020).

Table 14. [1]H and [13]C NMR chemical shifts (ppm) of EPS from T. chuii in MixC. Spectra were recorded in D_2O solution at 298 K (600 MHz)

Residue	H-1/C-1 $^1J_{CH}$	H-2 C-2	H-3 C-3	H-4 C-4	H-5 C-5	H-6 a,b C-6	*O*-CH_3
A 3-β-D-Gal*p*	4.60 103.8	3.69 70.2	3.76 82.0	4.11 68.3	3.63 74.6	3.63 60.9	-
A' 3-β-D-Gal*p* 2-OCH_3	4.60 103.8	3.69 81.6	3.76 82.0	4.11 68.3	3.63 74.6	3.63 60.9	3.36 58.1
B t-β-D-Gal*p*	4.54 104.2	3.53 70.9	3.58 72.5	3.84 66.8	3.84 73.3	3.59 72.0	-
C 3,6-β-D-Gal*p*	4.41 103.0	3.60 70.1	3.83 82.0	4.11 68.4	3.82 73.9	3.95 69.0	-

Linkage analysis via PMAA and the analysed 2D NMR spectra indicated that the EPS from *T. chuii* is a β-galactan, composed predominantly of 1,3-linked galactose units forming a linear backbone. Occasional 3,6-linked galactose residues introduce branch points, with approximately one branch per five backbone units. A schematic representation of the EPS using the symbol nomenclature for glycans SNFG (Fig. 65) highlights the galactan backbone and its sparse branching, illustrating the overall architecture of this polysaccharide.

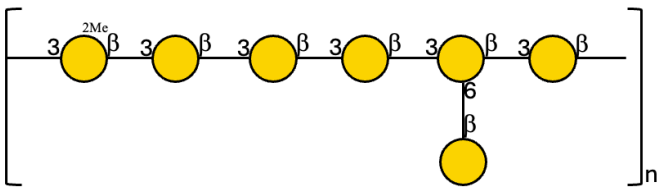

Figure 65. Final structure of T. chii EPS using symbol nomenclature for glycans (SNFG), highlighting the 1,3-linked β-D-galactan backbone, occasional 3,6-linked branching points, and the presence of 2-O-methylated galactose units.

6.3 Conclusion

Across the three *Tetraselmis* strains, the results of this study demonstrate a clear strain- and trophic mode-dependent variability in all growth and EPS production. AC favoured *T. suecica*, whereas *T. suecica* 22D and *T. chuii* performed better under HC, reflecting their stronger reliance on organic carbon sources. The progressive reduction of light in HC likely amplified these differences by limiting photosynthetic contribution and promoting strains with robust heterotrophic metabolism. EPM production was markedly influenced by both strain and growth conditions. MixC consistently yielded the highest EPM amounts, suggesting a synergistic effect of combined autotrophic and heterotrophic metabolism on polysaccharide synthesis. While AC cultures produced lower EPM amounts, HC significantly enhanced secretion. In MixC bioreactor cultivations, the strain-dependent response was further confirmed under controlled conditions, with *T. chuii* showing higher biomass and EPS yields (2.28 g and 1.2 g, respectively) compared to *T. suecica* 22D (1.66 g biomass and 0.8 g EPS), reflecting the

differential growth dynamics and polysaccharide production observed across cultivation systems. Overall, these findings highlight the metabolic plasticity of *Tetraselmis* strains and underscore how trophic mode, light availability, and cultivation system jointly shape biomass accumulation and, more specifically, polysaccharide production.

The preliminary data of *T. chuii* EPMs revealed a highly heterogeneous polysaccharide composition that varies according to the cultivation conditions. DOC-PAGE analysis highlighted the presence of both low and high molecular weight components under all conditions, whereas ^{1}H NMR and FT-IR spectra indicated that EPMs obtained under HC and MixC conditions share similar structural features, while the AC-derived polysaccharides displayed different profiles, suggesting a diverse composition and/or sulfation pattern. In particular, the absence of significant sulfate bands in AC EPM, compared to HC and MixC, indicates that organic carbon availability and combined trophic growth influence the chemical features of *T. chuii* EPM.

Purification of *T. chuii* MixC EPS by gel filtration, DOC-PAGE analysis, and HPLC revealed an intrinsic heterogeneity of the sample; however, monosaccharide analysis identified galactose as the sole monosaccharide, confirming the galactan nature of the EPS. Further structural elucidation, including desulfation and PMAA linkage analysis, demonstrated that the polysaccharide is a β-galactan mainly composed of 1,3-linked galactose units forming a linear backbone, with occasional 3,6-linked residues introducing branch points at approximately one branch every five backbone units. 2D NMR experiments further confirmed the galactan structure and revealed the presence of 2-*O*-methylated galactose units, occurring approximately once every six galactose residues. Overall, the combined NMR and linkage analysis data indicate that the EPS consists of a linear 1,3-β-D-galactan backbone with sparse branching and minor structural modifications, consistent with reported extracellular galactans from marine microalgae.

These findings indicate that *T. chuii* EPS grown in MixC exhibits a galactan backbone with controlled branching, and that its structural features, such as sulfation, are influenced by cultivation conditions, highlighting the interaction between metabolism and polysaccharide biosynthesis. Since *T. chuii* EPM grown in HC showed the most similar HPLC and ^{1}H NMR profiles compared to MixC, it is possible to speculate that no significant differences in its backbone are present. On the other hand, *T. chuii* EPM grown in AC can be further studied to identify the punctual structural differences. This chemical characterization provides a foundation for understanding the potential functional and biotechnological applications of these EPSs.

Chapter 7

Experimental

7.1 Shewanella vesiculosa

7.1.1 Bacterial cells growth

The cells of *S. vesiculosa* HM13 *nfnB* mutant strain (Chen et al., 2020) were grown at 18°C in an LB medium, and the cells at the stationary phase (OD_{600} = 2.0-3.0) were recovered after centrifugation. A rifampin-resistant mutant of this strain (HM13-Rif^r) was used as the parental strain for the construction of gene-disrupted mutants.

7.1.2 Isolation and purification of capsular polysaccharide

Dried cells (1.5 g) were first extracted with phenol/chloroform/petroleum ether (PCP) procedure and then by hot water/phenol extraction, as already reported (Galanos et al., 1969; Hendrickson & Ward, 1975). The water extract was extensively dialyzed against milli-Q water (cut-off 3500 Da) and freeze-dried (150 mg). The water extract was firstly subjected to enzymatic digestion with DNase, RNase, and protease, and dialysed against water (cut-off 1000 Da) (Di Guida et al., 2022). Then, it was hydrolyzed with 1% aqueous CH_3COOH (9 mL, 100 °C, 3 h), and the resulting suspension was centrifuged (11.5 g, 4 °C, 30 min). The pellet was washed twice with water, and the supernatant layers were combined and fractionated on a Biogel P-10 column (Bio-Rad, 1.50 cm X 90 cm, fraction volume 2.5 mL), eluted with water. The CPS fraction (1 mg) was lyophilized and analysed using chemical analyses and NMR spectroscopy.

7.2 Vibrio crassostreae

7.2.1 Bacterial cells growth

Vibrio crassostreae isolates were cultivated under laboratory conditions in LB medium supplemented with NaCl (35 g L^{-1}) to mimic marine salinity. Cultures were incubated overnight at 25-28 °C under aerobic conditions. Cells were harvested by centrifugation and immediately stored at low temperature before further analyses.

7.2.2 CPS and LPS extraction and purifications

1,4 g of *V. crassostreae* bacterial dried cells were extracted using the PCP (phenol/chloroform/petroleum ether, 2:5:8 v/v/v) method (Galanos et al., 1969). After removing chloroform and petroleum ether, LPS was precipitated by adding water. The cell debris was then extracted using the hot phenol-water method (Hendrickson & Ward, 1975). The obtained aqueous phase (WP) was purified from proteins and nucleic acids by treatment with DNase and RNase from bovine pancreas at 37°C for 16 h, followed by Proteinase K from *Streptomyces griseus* (Sigma Aldrich®, St. Louis, MO, USA) at 60 °C for 2 h (Nguyen et al., 2019). The mixture was dialyzed against water (cut-off 1000 Da) and freeze-dried. The sample

was then hydrolysed with 1% aqueous CH_3COOH (15 mL, 100° C, 3 h). The resulting suspension was then centrifuged (4° C, 60min), and the supernatant portion was fractionated on a Sephacryl S-400HR (Sigma, 110 × 0.75 cm, flow rate 10.0 mL/h, fraction volume 2.5 mL), eluted with 0.05 M ammonium bicarbonate. The elution was monitored with a refractive index detector (Knauer K-2301).

7.3 Alteromonas macleodii

7.3.1 Bacterial cells growth

The EPS was produced by the bacterium *Alteromonas macleodii* Mo169 (CNCM I-5374), cultivated in a 2 L bioreactor, using (60 g/L) as a carbon source, as described by Concórdio-Reis et al. (Concórdio-Reis et al., 2023). At the end of the cultivation run, the EPS was recovered from the cell-free supernatant, obtained by centrifugation (13,000 ×g, 45 min, 4°C), through dia/ultrafiltration (Sartocon Slide Holder equipped with a 100 kDa Hydrosart ultrafiltration cassette, Sartorius), as previously described (Concórdio-Reis et al., 2020).

7.3.2 EPS purification

To eliminate residual lipopolysaccharides (LPS) present in the sample, mild acid hydrolysis was performed with 1% aqueous CH_3COOH (10 mg mL^{-1}, 100 °C, 3 h) (Fresno et al., 2007). The resulting suspension was centrifuged (4500 *g*, 4 °C, 30 min), and the supernatant was purified through a Biogel P-10 column (Bio-Rad, 78 × 0.50 cm, flow rate 9.6 mL h^{-1}, fraction volume 2.5 mL) eluted with water. The fraction eluted in the void volume was further purified on a Sephacryl S-300 (Sigma, 176 × 0.75 cm, flow rate 10.8 mL h^{-1}, fraction volume 2.5 mL) eluted with ammonium hydrogen bicarbonate 50 mM. The purified EPS was subjected to an alkaline treatment with aq. NH_3 for 1 h at room temperature and purified through Sephacryl S-400 column (Sigma, 176 × 0.75cm, flow rate 10.8 mL h^{-1}, fraction volume 2.5 mL) eluted with ammonium bicarbonate 50 mM.

7.4 Ellisolandia elongata

7.4.1 Sampling

The samples were collected and kept in marine water to prevent degradation. Then each sample was washed with milli-Q water to remove epiphytes and other organisms that are usually located on the algae. Samples were dried in an oven at 37°C for 48 h and reduced to powder using liquid nitrogen.

7.4.2 Polysaccharides extraction and purification

A pretreatment (PTR) was performed by adding 98% ethanol 10 $g \cdot L^{-1}$ to the powder, followed by magnetic stirring at room temperature for 4 hours. Subsequently, the solution underwent centrifugation at 7000 rpm at 4°C for 30 minutes.

After the pretreatment, a water extraction (WE) was performed on the pellet. The polysaccharides were extracted from 4g of cells using 50 $g \cdot L^{-1}$ water at 75°C for 4 hours under magnetic stirring. Then the solution was centrifuged at 4°C, 7000 rpm for 30 minutes. The supernatant was collected, and 4 volumes of ethanol 98% (v/v), -20°C, O.N. (WEP). The extraction was performed another two times by adding a solution of Na_2CO_3 1% at 60°C the first time, and 2% the second time. The second and third supernatants were collected, unified, and this time they were put on a dialysis bag (cut-off of 3.5KDa) against water (WED).

The acidic extraction (AE) was performed by adding water to the pellet 100 $g \cdot L^{-1}$ and keeping them at 95°C, with magnetic stirring for 3 hours. The cells were resuspended with HCl solution (pH 6), R.T., on magnetic stirring for 3h. The last time the extraction was performed by adding water again to the cells at 95°C for 3h. To facilitate polysaccharide precipitation, two volumes of absolute ethanol 98% (v/v) were added to the supernatant, and the mixture was incubated at -20°C overnight. The solution was then centrifuged, and the polysaccharides (AEP) were freeze-dried. The samples were then purified through a Sephacryl S-400 (Sigma, 78x 0.50cm, flow rate 8,4 mL/h, fraction volume 2.5 mL) eluted with ammonium bicarbonate 50 mM.

Enzymatic hydrolysis was performed using α-amylase to cleave the α-(1→4) glycosidic linkages of α-glucans. An enzymatic solution was prepared at a concentration of 30 $g \cdot L^{-1}$ α-amylase from *Aspergillus oryzae* (Sigma Aldrich®, St. Louis, MO, USA), in distilled water. This solution was then added to approximately 20 mg of the sample, and the mixture was incubated at 40 °C for 2 h under continuous stirring. After incubation, the enzyme was inactivated by heating the mixture at 90 °C, and the sample was subsequently loaded onto a Sephacryl S-300 chromatographic column (Sigma, 40 x 0.50cm, flow rate 8,4 mL/h, fraction volume 2.5 mL) eluted with ammonium bicarbonate 50 mM for isolation of the other polysaccharide. The fraction eluted in the void volume was further purified on a Biogel P-100 column (Bio-Rad, 78 x 0.75 cm, flow rate 9.6 mL/h, fraction volume 2.5 mL) eluted with water.

7.5 Tetraselmis strains

Three *Tetraselmis* strains were purchased from Culture Collection of Algae and Protozoa (CCAP) SAMS Limited in axenic conditions: *Tetraselmis suecica* 66/4 (isolated from Italy), *Testraselmis suecica* 66/22D (isolated from the UK), and *Tetraselmis chuii* 8/6 (isolated from the UK)

50 ml of *T. suecica* 66/4 and *T. chuii* 8/6 arrived on liquid media F/2, and under a flow chamber, 10 ml of each culture were immediately inoculated in 100ml T-flasks with air caps in two different media: F/2 and a media solution with 1ml of Nutribloom Plus (Necton S.A., Portugal). *T. suecica* 66/22D arrived on an agar plate; in this case, a small number of cells were taken and added to the two media in 100ml T-flasks. 1mL of *T. suecica* 66/4 and *T. chuii* 8/6, and a small amount of cells from *T. suecica* 66/22D were added to the agar plates. All samples were located under autotrophic conditions at 12:12 light and dark (L:D) cycle. All optical

density (OD) measurements were acquired using a Single Beam Scanning UV–Vis M509T spectrophotometer, monitoring absorbance at 750 nm.

T. suecica 66/4 and *T. chuii* 8/6 growing on Nutribloom medium showed higher OD than the inocula growing on F/2 media. At this stage, *T. suecica* 66/4 and *T. chuii* were moved to 1L T-flasks, adding 100ml of media, and the L:D cycle was increased to 18:6. *T. suecica* 66/22D OD was still low due to the lower amount of cell inoculated, so no scale-up in T-flasks was performed, and the L:D cycle was increased to 18:6.

7.5.1 Microalgae cells growth in different trophic conditions

Microalgae were cultivated in 500-mL flasks with a working volume of 500 mL. For each condition (autotrophic, heterotrophic, and mixotrophic), 25 mL of an actively growing pre-culture were inoculated into fresh Nutrbloom medium. Autotrophic cultures were grown in sterile seawater with a decrease in salinity from 36 to 30 to facilitate the future EPS purification steps, enriched with Nutribloom at a final concentration of 1 $mL \cdot L^{-1}$. No external organic carbon source was added. Cultures were maintained under constant shaking (150 rpm). Cultures were illuminated with 8 W T5 LED lamps (T5 TUVE 8W/32, 0.5 W/LED, 30 cm) with a color temperature of 3500 K following a 12:12 L:D photoperiod. Lamps were positioned above the cultures to provide uniform illumination. Heterotrophic cultures were supplemented with glucose as the carbon source. A stock solution of 20 g glucose in 100 mL was prepared, and 4.2 mL were added to each 500-mL flask to obtain a C/N ratio of 24, based on the nitrate content of Nutribloom (2.800% in 5 L). To minimise bacterial contamination, ampicillin (1 $mg \cdot mL^{-1}$ in sterile water) and rifampicin (1 $mg \cdot mL^{-1}$ dissolved in 2 mL ethanol) were added at the respective working concentrations. Cultures were kept in complete darkness and shaken at 150 rpm. Mixotrophic cultures received the same glucose supplementation and antibiotic treatment as the heterotrophic ones. In addition, they were subjected to a gradual reduction of light availability, following the sequence of photoperiods: L:D 12:12 → 8:16 → 4:20 → 2:22 → 0:24. Each photoperiod was maintained for an equal duration before transitioning to the next. Cultures were continuously shaken at 150 rpm. Once a week, a small amount of each culture was sampled to measure the OD at 750nm, and all cultures were checked under Zeiss AXIO Observer Z1 Inverted Fluorescence Microscope (100x) to compare the expected changing cell morphology of the microalgae in three different conditions. Biomass was harvested only at the end of the assay, and no statistical analyses were performed on growth data, since the primary objective of this work is the extraction and chemical characterization of polysaccharides. All EPMs were recovered from each strain by centrifuging at 4°C, 11000 ×g for 45 minutes. The pellet was washed with ammonium formate 0.5 M solution, and the supernatant was sequentially concentrated, dialyzed with dialysis bags (cut-off 3.5KDa), and freeze-dried.

7.5.2 Bioreactor scale-up

Microalgal cultures were grown in a 2-L bench-top bioreactor (Biostat B-plus Exclusive Flow, Sartorius Stedim, Germany). 2 mL of NutriBloom was added to 1.7 L of autoclaved Milli-Q water, along with 200 mL of each culture. Lastly, 30 mL of HEPES buffer (10 g/L)

was added to prevent foaming, 100 mL of glucose (200 g/L) was used as a carbon source, and 20 mL of Penicillin and Streptomycin solution (Gibco Thermo Fisher, USA) was added to prevent contamination. The culture temperature was set at 25 °C, and stable thermal conditions were maintained with a Julabo CORIO CD-BC4 immersion circulator. The pH was controlled at 8 through automatic addition of HCl 1M and NaOH 1M. Mixing was provided by magnetic stirring at 200 rpm. Cultures were exposed to natural light throughout the experiment. Aeration was supplied at 1 SLPM (Standard Liters Per Minute) (0.5 vvm) through a sterile PTFE 0.22-µm filter; this aeration rate corresponds to 0.5 volumes of air per volume of culture per minute for a 2-L working volume. All parameters were continuously recorded through the integrated bioreactor control system. All EPMs were recovered from each strain by centrifuging at 4°C, 11000 ×g for 45 minutes. The pellet was washed with ammonium formate 0.5 M solution, and the supernatant was sequentially concentrated, dialyzed with dialysis bags (cut-off 3.5KDa), and freeze-dried.

7.5.3 T. chuii EPS in MixC extraction and purification

The EPS was recovered from each strain by centrifuging at 4°C, 11000 ×g for 45 minutes. The pellet was washed with ammonium formate 0.5 M solution, and the supernatant was sequentially concentrated, dialyzed with dialysis bags (cut-off 3.5KDa), and freeze-dried. The sample was then purified through P-10 gel filtration chromatography (BioRad, 160 × 1.50 cm, flow rate 9.6 mL h^{-1}, fraction volume 2.5 mL) eluted with degassed water. The sample was then desulfated as already described (Farias et al., 2000).

7.6 Other analysis

7.6.1 Deoxycholate-Polyacrylamide Gel Electrophoresis (DOC-PAGE)

Polyacrylamide gel electrophoresis (PAGE) was performed using the system of Laemmli (Laemmli & Favre, 1973) with sodium deoxycholate (DOC) as detergent. Polysaccharide bands were visualized after Alcian blue staining and silver staining (Tsai & Frasch, 1982). The separating gel contained final concentrations of 14% acrylamide, 0.1% DOC, and 375 mM Tris/HCl (pH 8.8); the stacking gel contained 4% acrylamide, 0.1% DOC, and 125 mM Tris/HCl (pH 6.8). All samples were prepared at a concentration of 0.05% in the sample buffer (2% DOC and 60 mM Tris/HCl [pH 6.8], 25% glycerol, 14.4 mM 2-mercaptoethanol, and 0.1% bromophenol blue). All concentrations are expressed as mass/vol percentage. The electrode buffer was composed of sodium dodecyl sulfate (SDS) (1 g·L-1), glycine (14.4 g·L-1), and Tris (3.0 g·L-1). Electrophoresis was performed at a constant amperage of 30 mA. Gels were fixed in an aqueous solution of 40% ethanol and 5% acetic acid.

7.6.2 FT-IR

FT-IR spectra were recorded using a Jasco 3000 FT-IR spectrometer. For each measurement, 1 mg of dried sample was thoroughly mixed with approximately 100 mg of

potassium bromide (KBr, EMSURE®, ACS reagent, Ph. Eur. grade; Merck KGaA) and pressed into transparent pellets using a hydraulic press. Spectra were collected in the range of 4000-400 cm^{-1}, with a resolution of 4 cm^{-1} and an average of 32 scans per sample.

7.6.3 FT-ATR

E. elongata samples and alginate-based films were analyzed using the Attenuated Total Reflectance (ATR) mode. FTIR-ATR spectra were recorded using a Thermo Fischer Scientific Nicolet 6700 spectrometer equipped with a universal-ATR accessory, featuring a diamond crystal and ZnSe focusing elements. Measurements were performed at room temperature with a single reflection at an incident angle of 45°. For each sample, 16 scans were collected over the 4000-650 cm^{-1} spectral range at a resolution of 4 cm^{-1}.

7.6.4 High-performance liquid chromatography (HPLC)

HPLC analyses were performed using an Agilent 1100 Series system equipped with a G1312A binary pump and a refractive index detector (RID). Separation was carried out on an A6000 aqueous column (300 × 8 mm). The eluent consisted of 0.1 M $NaNO_3$ containing 0.02% (w/v) NaN_3, delivered at a flow rate of 0.5 $mL \cdot min^{-1}$. Samples were filtered prior to analysis, and an injection volume of 100 µL was used for all runs.

7.7 Chemical analysis

7.7.1 Acetylated O-methyl glycosides (AMG)

Monosaccharides were derivatized as acetylated methyl glycosides (AMGs) and analyzed by gas chromatography-mass spectrometry (GC-MS). Samples (1 mg) were methanolyzed in HCl/MeOH (1.25 M, 1 mL) at 80°C for 16 h (Abid et al., 2019), followed by hexane extraction. The hexane layer was directly analyzed for fatty acid methyl esters (FAMEs), while the methanol phase was dried and acetylated (Ac_2O/pyridine, 100°C, 30 min). GC-MS was conducted on an Agilent 7820A instrument with a 5977B MS detector and HP-5 capillary column (30 m×0.25 mm i.d.; He, 1 mL/min) (Artini et al., 2019).

7.7.2 Acetylated Alditols (AA)

A portion of the freeze-dried material (1 mg) was subjected to hydrolysis with 2 M TFA at 120 °C for 2 h. The hydrolysate was evaporated under a gentle air stream, and the released monosaccharides were reduced in ethanol using $NaBH_4$ to generate alditols. These were subsequently acetylated with acetic anhydride (25 µL) in pyridine (25 µL) at 80 °C for 30 min. After removal of solvents under airflow, the acetylated alditols were resuspended in 100 µL of acetone and analyzed by GC-MS (Corsaro et al., 1997).

7.7.3 Octyl-glycosides (OGA)

The absolute configuration of the sugars was determined by gas-chromatography analysis of their acetylated (-)-2-octyl glycosides (Leontein et al., 1978). Acetylated octyl glycosides were then analysed at the GC-MS.

7.7.4 Partially Methylated Alditol Acetates (PMAA)

Linkage positions were determined after derivatization of the sample into partially methylated acetylated alditols. The sample was methylated with 100 µL of CH_3I and subsequently hydrolyzed with 2 M TFA at 120 °C for 2 h. Following neutralization, the hydrolysate was reduced with $NaBD_4$, acetylated, and injected into the GC-MS system.

7.7.5 Dephosphorylation of LPS by hydrofluoric acid (HF) treatment

LPS (1 mg) was treated with 100 µL of 48% aqueous hydrofluoric acid (HF) (Sigma Aldrich®, St. Louis, MO, USA) at 4 °C for 16 h in order to remove phosphate groups. The reaction mixture was kept in an ice bath throughout the treatment. After incubation, the HF was carefully evaporated to dryness under a fume hood at low temperature. The HF-treated residue was then dissolved in distilled water and lyophilized.

The resulting dephosphorylated sample was subsequently analyzed as acetylated methyl glycosides (AMG), following the procedure described in section 7.7.1. This treatment enables the detection of phosphorylated Kdo and heptose residues by GC-MS, since HF cleavage efficiently removes phosphate groups without degrading the sugar backbone.

7.7.6 Gas Chromatography Mass Spectrometry (GC-MS)

All analyses were performed using an Agilent Technologies 7820A Gas Chromatograph equipped with a 5977B mass selective detector and an HP-5 capillary column (Agilent, Milan, Italy; 30 m×0.25 mm). Helium was used as the carrier gas at a flow rate of 1 mL/min.

For AMG and OGA analysis, the temperature program was set as follows: initial temperature of 140°C held for 3 min, followed by a ramp from 140 °C to 240°C at 3°C/min.

For PMAA analysis, the program was: 90°C for 1 min, ramped from 90 C to 140°C at 25°C/min, then from 140°C to 200°C at 5°C/min, followed by an increase from 200°C to 280°C at 10°C/min, with a final hold at 280°C for 10 min.

For FAMEs analysis, the temperature program was: 150°C for 5 min, ramped from 150°C to 280°C at 3°C/min, with a final hold at 280°C for 5 min.

7.8 Nuclear Magnetic Resonance spectroscopy (NMR)

7.8.1 NMR spectroscopy in solution

One- and two-dimensional ^{1}H and ^{13}C NMR spectra were recorded in deuterium oxide (D_2O) at pD 7.0. Experiments were performed at 298 K using a Bruker DRX-600 MHz spectrometer equipped with a cryoprobe, and at 307 K using a Bruker Avance 600 MHz

instrument. ^{13}C NMR experiments were also carried out on a Bruker DRX-400 MHz spectrometer. Chemical shifts were calibrated using acetone as an internal reference ($\delta_H = 2.225$ ppm; $\delta_C = 31.45$ ppm).

A complete set of 2D NMR experiments was acquired to assign spin systems and establish connectivity. Homonuclear spectra included double-quantum-filtered correlation spectroscopy (DQF-COSY), total correlation spectroscopy (TOCSY), and Nuclear Overhauser enhancement spectroscopy (NOESY) or rotating frame Overhauser enhancement spectroscopy (ROESY). TOCSY experiments were acquired with mixing (spin-lock) times of 100 ms, while NOESY/ROESY experiments used mixing times ranging from 100 to 300 ms (typically 150 ms), acquiring 16 scans per increment.

Data sets ($t_1 \times t_2$) consisted of 4096 × 256 points for TOCSY and NOESY/ROESY, and 4096 × 512 points for DQF-COSY. The t_1 and t_2 time domains were converted by double Fourier transformation into the F1 (indirect) and F2 (direct) frequency axes, producing 2D spectra in which cross-peaks indicate correlations between nuclei. Homonuclear experiments (COSY, TOCSY) reveal scalar couplings, whereas NOESY and ROESY highlight through-space proximities. In NOESY/ROESY, the intensity of cross-peaks is inversely proportional to the sixth power of the internuclear distance:

$$I_{NOE} \propto \frac{1}{r^6}$$

This relationship provides qualitative distance information, which is particularly useful for mapping spatial proximities within the oligosaccharide structure.

The data matrix for all homonuclear experiments was zero-filled to 4K×2K points and resolution-enhanced in both dimensions using a cosine-bell window function prior to Fourier transformation. Coupling constants were determined from phase-sensitive DQF-COSY spectra.

Heteronuclear experiments included ^1H, ^{13}C HSQC, and HMBC. HSQC spectra were recorded in phase-sensitive mode using echo/antiecho gradient selection and multiplicity editing during the selection step. HMBC experiments were optimized for long-range coupling constants and employed a low-pass J-filter to suppress one-bond correlations, using gradient pulses for selection. A 60-ms relay was used for the evolution of long-range correlations. Data sets for HSQC and HMBC consisted of 2048 × 256 points, with proton detection and broadband decoupling in the ^{13}C domain. DEPT-HSQC and F2-coupled HSQC were also acquired for improved assignment of proton–carbon connectivities.

All spectra were processed using standard Bruker software with zero-filling and apodization to enhance resolution. Experimental conditions and acquisition parameters were chosen according to established procedures.

7.9 Functional Characterization and Application-Oriented Assessment

The biological experiments were conducted as a preliminary; no additional statistical analyses were carried out. Future work will include independent replicates and statistical analyses to confirm the observed trends.

7.9.1 Antibiofilm assays

Biofilm formation was assessed according to Christensen et al., with minor modifications. Sterile 96-well flat-bottom polystyrene plates were inoculated with *S. epidermidis* RP62A (Gowrishankar & Pandian, 2017) or O-47 (Raue et al., 2020) at initial OD_{600} values of approximately 0.1 and 0.001, respectively, in BHI medium.

The analysed samples were resuspended in different buffers according to their nature. The crude sample was resuspended in bidistilled water, the polysaccharidic extract in BHI medium, and the lipid extract in 8% DMSO diluted in water. All samples were sterilised by filtration through a 0.22 μm pore-size filter and tested at final concentrations of 0.5 or 0.25 mg/mL.

Plates were incubated at 37 °C for 24 h. Biofilm biomass was quantified by crystal violet staining, and the bound dye was solubilised in a solution of 20% (v/v) glacial acetic acid and 80% (v/v) ethanol before measuring absorbance at 590 nm using a microplate reader (Benchmark Plus Microplate Spectrophotometer). All conditions were tested in six technical replicates and repeated at least twice in independent experiments.

7.9.2 Hydrogen Peroxide Scavenging Assay

The hydrogen peroxide stability was measured by following the absorbance at 240 nm of 1 mL of fresh hydrogen peroxide solution (50 mM Potassium Phosphate Buffer, pH 7.0; 0.036% (*w*/*w*) H_2O_2). Quantitative determination of H_2O_2 scavenging activity of all samples was measured by the loss of absorbance at 240 nm as previously described (Vittoria et al., 2023). More specifically, 1mg/ml of each sample were incubated in 1 mL of 0.036% hydrogen peroxide solution at RT. After 15 and 30 minutes, the hydrogen peroxide concentration in the supernatant was determined by measuring the absorbance at 240 nm. The percentage of peroxide removed was calculated as reported below:

$$H_2O_{2\ \text{removed}}\ (\%) = (1 - A_{\text{sample}}/A_{\text{control}}) \times 100$$

7.9.3 α,α-diphenyl-β-picrylhydrazyl (DPPH) Assay

The α,α-diphenyl-β-picrylhydrazyl (DPPH) free radical scavenging method was used to evaluate the potential antioxidant activity of all samples following the protocol reported in (Vittoria et al., 2023), with some modifications. 2mg/ml of each sample was incubated in a final volume of 1 mL of 50 mM citrate phosphate buffer (pH 7) containing 0.1 mM of freshly prepared DPPH (giving absorbance ≤ 1.0). The reaction was allowed to proceed in the dark at room temperature, taking different times at 15, 30, 60, and 90 minutes. The DPPH free radical scavenging activity was then monitored by determining the absorbance at 515 nm and calculated according to the following equation:

$$\text{DPPH}_{\text{radical scavenging activity}}\ (\%) = (1 - A_{sample}/A_{control}) \times 100$$

where A_{sample} is the absorbance of the reacted mixture of DPPH with the extract sample, and $A_{control}$ is the absorbance of the DPPH solution.

7.9.4 Differential Scanning Calorimetry (DSC)

Thermal properties of *Ellisolandia elongata* samples and their corresponding extracts were investigated by Differential Scanning Calorimetry (DSC) using a Q2000 TA Instruments apparatus equipped with a TA Instruments DSC cooling system, under a nitrogen flow rate of 20 mg/mL. Approximately 5 mg of each sample was sealed in aluminum pans and analyzed under an inert nitrogen (N_2) atmosphere. Heating/cooling rate was fixed to 10 °C/min in all the measurements.

The thermal program was set as follows:

- First heating run (I run): 20 → 150 °C at 10 °C·min^{-1}
- Cooling: 150 → 20 °C at 10 °C·min^{-1}
- Second heating run (II run): 20 → 150 °C at 10 °C·min^{-1}

7.9.5 Alginate-Based Films

The samples were added to a 2% (w/v) aqueous sodium alginate solution at a concentration of 5% (w/w) with respect to alginate. Due to its insolubility, *E. elongata* **S** was dispersed using an Ultra-Turrax® T25 homogenizer (Janke & Kunkel, Germany) for 30 s at 16,000 rpm to ensure a homogeneous distribution within the polymeric matrix, whereas S-AEP was dissolved under magnetic stirring until complete solubilization.

The AlgNa-S dispersion and the AlgNa-S-AEP solution were cast into Petri dishes, and films were obtained by solvent casting. Mild heating was applied to facilitate solvent evaporation and to remove air bubbles formed during mixing.

Chapter 8

Final remarks and future perspective

This PhD work was focused on the isolation, purification, and structural characterization of marine polysaccharides derived from different biological sources, including Gram-negative bacteria, red macroalgae, and microalgae. By integrating chemical, chromatographic, and spectroscopic approaches, this study highlights the extraordinary structural diversity of marine glycans and their close relationship with environmental adaptation and potential biological functionality.

The investigation of *Shewanella vesiculosa* HM13 nfnb mutant provided insight into the plasticity of bacterial surface polysaccharides in response to genetic and physiological variations. In addition to the previously described CPS corona, the *nfnB* mutant strain produced an additional capsular polysaccharide composed of a disaccharide repeating unit never been reported so far. This finding underlines the remarkable capacity of marine bacteria to modulate their surface glycan architecture and suggests a potential role of CPS structural variability in membrane vesicle formation and cargo loading, opening new perspectives for functional and mechanistic studies.

The capsular polysaccharide of *Vibrio crassostreae*, was structurally elucidated for the first time. The CPS consists of a well-defined trisaccharide repeating unit composed of fucose, N-acetylfucosamine, and mannose, all in α-configuration. In parallel, preliminary analyses of the lipooligosaccharide revealed phosphorylated Kdo residues, providing the first molecular information on the surface glycoconjugates of this species. Together, these results establish a chemical framework for understanding the role of surface polysaccharides in host-pathogen interactions and represent a necessary step toward future in vivo and functional studies addressing *V. crassostreae* pathogenicity in BSUD.

The extracellular polysaccharide produced by *Alteromonas macleodii* Mo169 was fully characterized and shown to consist of a linear disaccharide repeating unit composed of *N*-acetylglucosamine and *O*-acetylated gulaminuronic acid. The presence of specific substitutions, such as *O*-acetyl groups, further emphasizes the chemical diversity of EPSs produced by marine bacteria and their potential to mimic glycosaminoglycan-like structures. These results support the relevance of marine microbial EPSs as promising alternatives to animal- or pathogen-derived glycans, with potential biotechnological and biomedical applications.

The study of the red coralline alga *Ellisolandia elongata* demonstrated how environmental conditions strongly influence polysaccharide yield, composition, sulfation degree, and biological activity. Structural analyses revealed the coexistence of Floridean starch and a highly heterogeneous sulfated xylogalactan, characterized by complex branching patterns, mixed D- and L-galactose configurations, and variable sulfation. Although the high structural heterogeneity prevented the definition of a unique repeating unit, the observed correlations between environmental stress, sulfation degree, and antioxidant and antibiofilm activities highlight the adaptive role of algal polysaccharides and support their potential application in biomedical and biotechnological fields. Furthermore, preliminary thermal analyses (DSC) and

incorporation of purified extracts into sodium alginate films demonstrated well-defined thermal transitions and good compatibility with polymeric matrices, suggesting additional opportunities for the development of functional materials and bioactive formulations.

Finally, the investigation of EPSs secreted by *Tetraselmis* species demonstrated the strong influence of strain selection, trophic mode, and cultivation conditions on biomass accumulation and polysaccharide production. *Tetraselmis chuii* emerged as the most promising strain in terms of EPS yield and structural consistency. Detailed analyses showed that its EPS is a β-galactan with a mainly linear 1,3-linked backbone and sparse 3,6-linked branching points, whose chemical features are modulated by cultivation conditions. These findings confirm microalgae as a versatile and tenable source of marine polysaccharides and highlight the tight interplay between metabolism and glycan biosynthesis.

The results presented in this thesis open several avenues for future research. From a chemical standpoint, further fractionation strategies and advanced analytical approaches could help to better resolve the intrinsic heterogeneity of complex marine polysaccharides, particularly those derived from macroalgae and microalgae. New approaches may also assist in elucidating structure-function relationships, enabling a deeper understanding of how specific structural features contribute to biological activity. From a biological and biotechnological perspective, the structurally characterized bacterial CPSs and EPSs provide a solid foundation for functional studies. In particular, *Vibrio crassostreae* CPS and LPS will be evaluated through in vivo assays to determine their direct role in Bald Sea Urchins Disease and to clarify whether these surface polysaccharides are contributing agents of pathogenicity. Additionally, immunomodulatory assays will be conducted to assess the potential activity of *Tetraselmis chuii* EPS, investigating its ability to modulate immune responses and highlighting its relevance as a biotechnological and biomedical tool. Algal extracts and polysaccharides, including sulfated galactans and xylogalactans, demonstrated significant antibiofilm and antioxidant activities, respectively, highlighting their potential as functional biomaterials. Preliminary investigations into film formation by solvent casting using *Ellisolandia elongata* polysaccharides are ongoing, and it can be speculated that the combination of antioxidant, antibiofilm, and film-forming properties may open promising avenues for biotechnological applications, including biomedical coatings, functional materials, and sustainable bio-based products. Further studies are expected to elucidate the structure-activity relationships and optimize these properties for practical implementation.

Overall, this work contributes to expanding current knowledge on marine glycobiology by providing new structural and functional data on underexplored bacterial, algal, and microalgal polysaccharides. It highlights that structural heterogeneity, rather than being a limitation, represents an intrinsic and functionally relevant feature of marine glycans. The integration of chemical characterization with functional and application-oriented research demonstrates the potential of these molecules not only as bioactive compounds but also as versatile materials for biotechnological applications. In the broader context of the blue economy, this work

underscores the valorisation of marine biodiversity as a sustainable source of novel polymers, bridging rigorous chemical analysis with practical applications in biotechnology, biomedicine, and sustainable materials development.

Bibliography

Abid, Y., Azabou, S., Joulak, I., Casillo, A., Lanzetta, R., Corsaro, M. M., Gharsallaoui, A., & Attia, H. (2019). Potential biotechnological properties of an exopolysaccharide produced by newly isolated Bacillus tequilensis-GM from spontaneously fermented goat milk. *LWT*, *105*, 135–141. https://doi.org/10.1016/j.lwt.2019.02.005

Abinaya, M., Vaseeharan, B., Divya, M., Vijayakumar, S., Govindarajan, M., Alharbi, N. S., Khaled, J. M., Al-anbr, M. N., & Benelli, G. (2018). RETRACTED ARTICLE: Structural characterization of Bacillus licheniformis Dahb1 exopolysaccharide—antimicrobial potential and larvicidal activity on malaria and Zika virus mosquito vectors. *Environmental Science and Pollution Research*, *25*(19), 18604–18619. https://doi.org/10.1007/s11356-018-2002-6

Abou Zeid, A. H., Aboutabl, E. A., Sleem, A. A., & El-Rafie, H. M. (2014). Water soluble polysaccharides extracted from Pterocladia capillacea and Dictyopteris membranacea and their biological activities. *Carbohydrate Polymers*, *113*, 62–66. https://doi.org/10.1016/j.carbpol.2014.06.004

Agoun, N. A., & Avci, F. G. (2025). Phycoremediation: A path towards heavy metal bioremediation from wastewater. *Journal of Chemical Technology & Biotechnology*, *100*(1), 13–23. https://doi.org/10.1002/jctb.7745

Alexander, M., & Dalgleish, D. G. (2007). The interaction of casein micelles with κ-carrageenan studied by diffusing wave spectroscopy. *Food Hydrocolloids*, *21*(1), 128–136. https://doi.org/10.1016/j.foodhyd.2006.03.003

Alfinaikh, R. S., Alamry, K. A., & Hussein, M. A. (2025). Sustainable and biocompatible hybrid materials-based sulfated polysaccharides for biomedical applications: A review. *RSC Advances*, *15*(6), 4708–4767. https://doi.org/10.1039/D4RA07277D

Alharbi, M. A., Alrehaili, A. A., Albureikan, M. O. I., Gharib, A. F., Daghistani, H., Bakhuraysah, M. M., Aloraini, G. S., Bazuhair, M. A., Alhuthali, H. M., & Ghareeb, A. (2023). *In vitro* studies

on the pharmacological potential, anti-tumor, antimicrobial, and acetylcholinesterase inhibitory activity of marine-derived *Bacillus velezensis* AG6 exopolysaccharide. *RSC Advances*, *13*(38), 26406–26417. https://doi.org/10.1039/D3RA04009G

Al-Hosney, H. A., & Grassian, V. H. (2005). Water, sulfur dioxide and nitric acid adsorption on calcium carbonate: A transmission and ATR-FTIR study. *Physical Chemistry Chemical Physics*, *7*(6), 1266. https://doi.org/10.1039/b417872f

Al-Hussaniy, H. A., Mahan, S. J., Redha, Z. M., AlSaeedi, A. H., Almukram, A. M. A., Oraibi, A. I., Abdalrahman, M. A., Jabbar, A. A., Al-Ani, A. A. I., Hamed, H. E., & Jawad, M. A. (2025). Marine-derived bioactive molecules as modulators of immune pathways: A molecular insight into pharmacological potential. *Pharmacia*, *72*, 1–10. https://doi.org/10.3897/pharmacia.72.e141923

Alldredge, A. L., & Silver, M. W. (1988). Characteristics, dynamics and significance of marine snow. *Progress in Oceanography*, *20*(1), 41–82. https://doi.org/10.1016/0079-6611(88)90053-5

Amna Kashif, S., Hwang, Y. J., & Park, J. K. (2018). Potent biomedical applications of isolated polysaccharides from marine microalgae Tetraselmis species. *Bioprocess and Biosystems Engineering*, *41*(11), 1611–1620. https://doi.org/10.1007/s00449-018-1987-z

Angelis, S., Novak, A. C., Sydney, E. B., Soccol, V. T., Carvalho, J. C., Pandey, A., Noseda, M. D., Tholozan, J. L., Lorquin, J., & Soccol, C. R. (2012). Co-Culture of Microalgae, Cyanobacteria, and Macromycetes for Exopolysaccharides Production: Process Preliminary Optimization and Partial Characterization. *Applied Biochemistry and Biotechnology*, *167*(5), 1092–1106. https://doi.org/10.1007/s12010-012-9642-7

Araki, C., Arai, K., & Hirase, S. (1967). Studies on the Chemical Constitution of Agar-agar. XXIII. Isolation of D -Xylose, 6- *O* -Methyl- D -galactose, 4- *O* -Methyl- L -galactose and *O* -Methylpentose. *Bulletin of the Chemical Society of Japan*, *40*(4), 959–962. https://doi.org/10.1246/bcsj.40.959

Arnosti, C., Wietz, M., Brinkhoff, T., Hehemann, J.-H., Probandt, D., Zeugner, L., & Amann, R. (2021). The Biogeochemistry of Marine Polysaccharides: Sources, Inventories, and Bacterial

Drivers of the Carbohydrate Cycle. *Annual Review of Marine Science*, *13*(1), 81–108. https://doi.org/10.1146/annurev-marine-032020-012810

Artini, M., Papa, R., Vrenna, G., Lauro, C., Ricciardelli, A., Casillo, A., Corsaro, M. M., Tutino, M. L., Parrilli, E., & Selan, L. (2019). Cold-Adapted Bacterial Extracts as a Source of Anti-Infective and Antimicrobial Compounds against *Staphylococcus Aureus*. *Future Microbiology*, *14*(16), 1369–1382. https://doi.org/10.2217/fmb-2019-0147

Arun, J., Selvakumar, S., Sathishkumar, R., Moovendhan, M., Ananthan, G., Maruthiah, T., & Palavesam, A. (2017). In vitro antioxidant activities of an exopolysaccharide from a salt pan bacterium Halolactibacillus miurensis. *Carbohydrate Polymers*, *155*, 400–406. https://doi.org/10.1016/j.carbpol.2016.08.085

Arunkumar, K., Raja, R., Kumar, V. B. S., Joseph, A., Shilpa, T., & Carvalho, I. S. (2021). Antioxidant and cytotoxic activities of sulfated polysaccharides from five different edible seaweeds. *Journal of Food Measurement and Characterization*, *15*(1), 567–576. https://doi.org/10.1007/s11694-020-00661-4

Atanasov, A. G., Zotchev, S. B., Dirsch, V. M., the International Natural Product Sciences Taskforce, Orhan, I. E., Banach, M., Rollinger, J. M., Barreca, D., Weckwerth, W., Bauer, R., Bayer, E. A., Majeed, M., Bishayee, A., Bochkov, V., Bonn, G. K., Braidy, N., Bucar, F., Cifuentes, A., D'Onofrio, G., … Supuran, C. T. (2021). Natural products in drug discovery: Advances and opportunities. *Nature Reviews Drug Discovery*, *20*(3), 200–216. https://doi.org/10.1038/s41573-020-00114-z

Axpe, E., & Oyen, M. (2016). Applications of Alginate-Based Bioinks in 3D Bioprinting. *International Journal of Molecular Sciences*, *17*(12), 1976. https://doi.org/10.3390/ijms17121976

Azam, F., Fenchel, T., Field, J., Gray, J., Meyer-Reil, L., & Thingstad, F. (1983). The Ecological Role of Water-Column Microbes in the Sea. *Marine Ecology Progress Series*, *10*, 257–263. https://doi.org/10.3354/meps010257

Azaman, S. N. A., Nagao, N., Yusoff, F. M., Tan, S. W., & Yeap, S. K. (2017). A comparison of the morphological and biochemical characteristics of *Chlorella sorokiniana* and *Chlorella zofingiensis* cultured under photoautotrophic and mixotrophic conditions. *PeerJ*, *5*, e3473. https://doi.org/10.7717/peerj.3473

Azma, M., Mohamad, R., Rahim, R. A., & Ariff, A. B. (2010). Improved Protocol for the Preparation of Axenic Culture and Adaptation to Heterotrophic Cultivation. *The Open Biotechnology Journal*, *4*(1), 36–46. https://doi.org/10.2174/1874070701004010036

Baudelet, P.-H., Ricochon, G., Linder, M., & Muniglia, L. (2017). A new insight into cell walls of Chlorophyta. *Algal Research*, *25*, 333–371. https://doi.org/10.1016/j.algal.2017.04.008

Becker, B., Lommerse, J. P. M., Melkonian, M., Kamerling, J. P., & Vliegenthart, J. F. G. (1995). The structure of an acidic trisaccharide component from a cell wall polysaccharide preparation of the green alga Tetraselmis striata Butcher. *Carbohydrate Research*, *267*(2), 313–321. https://doi.org/10.1016/0008-6215(94)00300-5

Becker, B., Melkonian, M., & Kamerling, J. P. (1998). THE CELL WALL (THECA) OF *TETRASELMIS STRIATA (CHLOROPHYTA)*: MACROMOLECULAR COMPOSITION AND STRUCTURAL ELEMENTS OF THE COMPLEX POLYSACCHARIDES. *Journal of Phycology*, *34*(5), 779–787. https://doi.org/10.1046/j.1529-8817.1998.340779.x

Belghit, I., Rasinger, J. D., Heesch, S., Biancarosa, I., Liland, N., Torstensen, B., Waagbø, R., Lock, E.-J., & Bruckner, C. G. (2017). In-depth metabolic profiling of marine macroalgae confirms strong biochemical differences between brown, red and green algae. *Algal Research*, *26*, 240–249. https://doi.org/10.1016/j.algal.2017.08.001

Bergstrom, E., Lahnstein, J., Collins, H., Page, T. M., Bulone, V., & Diaz-Pulido, G. (2023). Cell wall organic matrix composition and biomineralization across reef-building coralline algae under global change. *Journal of Phycology*, *59*(1), 111–125. https://doi.org/10.1111/jpy.13290

Beuder, S., & Braybrook, S. A. (2023). Brown algal cell walls and development. *Seminars in Cell & Developmental Biology*, *134*, 103–111. https://doi.org/10.1016/j.semcdb.2022.03.003

Bhuyar, P., Sundararaju, S., Rahim, M. H. Ab., Unpaprom, Y., Maniam, G. P., & Govindan, N. (2021). Antioxidative study of polysaccharides extracted from red (Kappaphycus alvarezii), green (Kappaphycus striatus) and brown (Padina gymnospora) marine macroalgae/seaweed. *SN Applied Sciences*, *3*(4), 485. https://doi.org/10.1007/s42452-021-04477-9

Bilan, M. I., & Usov, A. I. (2001). Polysaccharides of Calcareous Algae and Their Effect on the Calcification Process. *Russian Journal of Bioorganic Chemistry*, *27*(1), 2–16. https://doi.org/10.1023/A:1009584516443

Blanchard, G. (1990). Overlapping microscale dispersion patterns of meiofauna and microphytobenthos. *Marine Ecology Progress Series*, *68*, 101–111. https://doi.org/10.3354/meps068101

Bock, K., & Pedersen, C. (1974). A study of 13CH coupling constants in hexopyranoses. *Journal of the Chemical Society, Perkin Transactions 2*, (3), 293. https://doi.org/10.1039/p29740000293

Bock, K., & Pedersen, C. (1983). Carbon-13 Nuclear Magnetic Resonance Spectroscopy of Monosaccharides. In *Advances in Carbohydrate Chemistry and Biochemistry* (Vol. 41, pp. 27–66). Elsevier. https://doi.org/10.1016/S0065-2318(08)60055-4

Bock, K., & Pedersen, C. (1985). Determination of one-bond carbon-proton coupling constants through 13C-satellites in 1H-n.m.r. Spectra. *Carbohydrate Research*, *145*(1), 135–140. https://doi.org/10.1016/S0008-6215(00)90420-8

Bomberger, J. M., MacEachran, D. P., Coutermarsh, B. A., Ye, S., O'Toole, G. A., & Stanton, B. A. (2009). Long-Distance Delivery of Bacterial Virulence Factors by Pseudomonas aeruginosa Outer Membrane Vesicles. *PLoS Pathogens*, *5*(4), e1000382. https://doi.org/10.1371/journal.ppat.1000382

Boonchai, R., Kaewsuk, J., & Seo, G. (2015). Effect of nutrient starvation on nutrient uptake and extracellular polymeric substance for microalgae cultivation and separation. *Desalination and Water Treatment*, *55*(2), 360–367. https://doi.org/10.1080/19443994.2014.939501

Borjas Esqueda, A., Gardarin, C., & Laroche, C. (2022). Exploring the Diversity of Red Microalgae for Exopolysaccharide Production. *Marine Drugs*, *20*(4), 246. https://doi.org/10.3390/md20040246

Bowman, J. P., McCammon, S. A., Brown, J. L., Nichols, P. D., & McMeekin, T. A. (1997). Psychroserpens burtonensis gen. Nov., sp. Nov., and Gelidibacter algens gen. Nov., sp. Nov., Psychrophilic Bacteria Isolated from Antarctic Lacustrine and Sea Ice Habitats. *International Journal of Systematic Bacteriology*, *47*(3), 670–677. https://doi.org/10.1099/00207713-47-3-670

Bracchi, V. A., Piazza, G., & Basso, D. (2021). A stable ultrastructural pattern despite variable cell size in *Lithothamnion corallioides*. *Biogeosciences*, *18*(22), 6061–6076. https://doi.org/10.5194/bg-18-6061-2021

Brennan, L., & Owende, P. (2010). Biofuels from microalgae—A review of technologies for production, processing, and extractions of biofuels and co-products. *Renewable and Sustainable Energy Reviews*, *14*(2), 557–577. https://doi.org/10.1016/j.rser.2009.10.009

Bruto, M., James, A., Petton, B., Labreuche, Y., Chenivesse, S., Alunno-Bruscia, M., Polz, M. F., & Le Roux, F. (2017). *Vibrio crassostreae* , a benign oyster colonizer turned into a pathogen after plasmid acquisition. *The ISME Journal*, *11*(4), 1043–1052. https://doi.org/10.1038/ismej.2016.162

Burg, A., & Oshrat, L.-O. (2015). Salt Effect on the Antioxidant Activity of Red Microalgal Sulfated Polysaccharides in Soy-Bean Formula. *Marine Drugs*, *13*(10), 6425–6439. https://doi.org/10.3390/md13106425

Cambon-Bonavita, M.-A., Raguenes, G., Jean, J., Vincent, P., & Guezennec, J. (2002). A novel polymer produced by a bacterium isolated from a deep-sea hydrothermal vent polychaete annelid. *Journal of Applied Microbiology*, *93*(2), 310–315. https://doi.org/10.1046/j.1365-2672.2002.01689.x

Campo, V. L., Kawano, D. F., Silva, D. B. D., & Carvalho, I. (2009). Carrageenans: Biological properties, chemical modifications and structural analysis – A review. *Carbohydrate Polymers*, *77*(2), 167–180. https://doi.org/10.1016/j.carbpol.2009.01.020

Cao, R., Jin, W., Shan, Y., Wang, J., Liu, G., Kuang, S., & Sun, C. (2018). Marine Bacterial Polysaccharide EPS11 Inhibits Cancer Cell Growth via Blocking Cell Adhesion and Stimulating Anoikis. *Marine Drugs*, *16*(3), 85. https://doi.org/10.3390/md16030085

Carella, F., Correggia, M., Cordone, A., Iacovino, O., Maresca, F., Villari, G., Roque, A., & Vico, G. D. (2025). Bald disease in a natural population of the purple sea urchin Paracentrotus lividus of the Mediterranean Sea: From spines to tissues. *Journal of Invertebrate Pathology*, *213*, 108415. https://doi.org/10.1016/j.jip.2025.108415

Carillo, S., Casillo, A., Pieretti, G., Parrilli, E., Sannino, F., Bayer-Giraldi, M., Cosconati, S., Novellino, E., Ewert, M., Deming, J. W., Lanzetta, R., Marino, G., Parrilli, M., Randazzo, A., Tutino, M. L., & Corsaro, M. M. (2015). A Unique Capsular Polysaccharide Structure from the Psychrophilic Marine Bacterium *Colwellia psychrerythraea* 34H That Mimics Antifreeze (Glyco)proteins. *Journal of the American Chemical Society*, *137*(1), 179–189. https://doi.org/10.1021/ja5075954

Carpena, M., Garcia-Perez, P., Garcia-Oliveira, P., Chamorro, F., Otero, P., Lourenço-Lopes, C., Cao, H., Simal-Gandara, J., & Prieto, M. A. (2023). Biological properties and potential of compounds extracted from red seaweeds. *Phytochemistry Reviews*, *22*(6), 1509–1540. https://doi.org/10.1007/s11101-022-09826-z

Casillo, A., Di Guida, R., Carillo, S., Chen, C., Kamasaka, K., Kawamoto, J., Kurihara, T., & Corsaro, M. M. (2019). Structural Elucidation of a Novel Lipooligosaccharide from the Cold-Adapted Bacterium OMVs Producer Shewanella sp. HM13. *Marine Drugs*, *17*(1), 34. https://doi.org/10.3390/md17010034

Casillo, A., Di Guida, R., Cavasso, D., Stellavato, A., Rai, D., Yokoyama, F., Kamasaka, K., Kawamoto, J., Kurihara, T., Schiraldi, C., Kulkarni, S., Paduano, L., & Corsaro, M. M. (2022). Polysaccharide corona: The acetyl-rich envelope wraps the extracellular membrane

vesicles and the cells of Shewanella vesiculosa providing adhesiveness. *Carbohydrate Polymers*, *297*, 120036. https://doi.org/10.1016/j.carbpol.2022.120036

Casillo, A., Lanzetta, R., Parrilli, M., & Corsaro, M. M. (2018). Exopolysaccharides from Marine and Marine Extremophilic Bacteria: Structures, Properties, Ecological Roles and Applications. *Marine Drugs*, *16*(2), 69. https://doi.org/10.3390/md16020069

Casillo, A., Parrilli, E., Sannino, F., Mitchell, D. E., Gibson, M. I., Marino, G., Lanzetta, R., Parrilli, M., Cosconati, S., Novellino, E., Randazzo, A., Tutino, M. L., & Corsaro, M. M. (2017). Structure-activity relationship of the exopolysaccharide from a psychrophilic bacterium: A strategy for cryoprotection. *Carbohydrate Polymers*, *156*, 364–371. https://doi.org/10.1016/j.carbpol.2016.09.037

Casillo, A., Ståhle, J., Parrilli, E., Sannino, F., Mitchell, D. E., Pieretti, G., Gibson, M. I., Marino, G., Lanzetta, R., Parrilli, M., Widmalm, G., Tutino, M. L., & Corsaro, M. M. (2017). Structural characterization of an all-aminosugar-containing capsular polysaccharide from Colwellia psychrerythraea 34H. *Antonie van Leeuwenhoek*, *110*(11), 1377–1387. https://doi.org/10.1007/s10482-017-0834-6

Cha, M., Yan, S., Zhang, Y., & Wang, P. (2025). Progress in the Application of Marine Polysaccharide Drug Delivery Systems in Tumor Immunotherapy: Multiple Mechanisms and Material Forms. *Marine Drugs*, *23*(10), 384. https://doi.org/10.3390/md23100384

Chattopadhyay, M. K., & Jaganandham, M. V. (2015). Vesicles-mediated resistance to antibiotics in bacteria. *Frontiers in Microbiology*, *6*. https://doi.org/10.3389/fmicb.2015.00758

Chen, C., Kawamoto, J., Kawai, S., Tame, A., Kato, C., Imai, T., & Kurihara, T. (2020). Isolation of a Novel Bacterial Strain Capable of Producing Abundant Extracellular Membrane Vesicles Carrying a Single Major Cargo Protein and Analysis of Its Transport Mechanism. *Frontiers in Microbiology*, *10*, 3001. https://doi.org/10.3389/fmicb.2019.03001

Chen, L.-M., Yang, P.-P., Al Haq, A. T., Hwang, P.-A., Lai, Y.-C., Weng, Y.-S., Chen, M. A., & Hsu, H.-L. (2022). Oligo-Fucoidan supplementation enhances the effect of Olaparib on preventing

metastasis and recurrence of triple-negative breast cancer in mice. *Journal of Biomedical Science*, *29*(1), 70. https://doi.org/10.1186/s12929-022-00855-6

Choi, S.-M., Jang, E.-J., & Cha, J.-D. (2015). Synergistic Effect between Fucoidan and Antibiotics against Clinic Methicillin-Resistant <i>Staphylococcus aureus</i> *Advances in Bioscience and Biotechnology*, *06*(04), 275–285. https://doi.org/10.4236/abb.2015.64027

Choix, F. J., de-Bashan, L. E., & Bashan, Y. (2012). Enhanced accumulation of starch and total carbohydrates in alginate-immobilized Chlorella spp. induced by Azospirillum brasilense: II. Heterotrophic conditions. *Enzyme and Microbial Technology*, *51*(5), 300–309. https://doi.org/10.1016/j.enzmictec.2012.07.012

Chong, B. F., Blank, L. M., Mclaughlin, R., & Nielsen, L. K. (2005). Microbial hyaluronic acid production. *Applied Microbiology and Biotechnology*, *66*(4), 341–351. https://doi.org/10.1007/s00253-004-1774-4

Cian, R., Drago, S., De Medina, F., & Martínez-Augustin, O. (2015). Proteins and Carbohydrates from Red Seaweeds: Evidence for Beneficial Effects on Gut Function and Microbiota. *Marine Drugs*, *13*(8), 5358–5383. https://doi.org/10.3390/md13085358

Ciancia, M., Matulewicz, M. C., & Tuvikene, R. (2020). Structural Diversity in Galactans From Red Seaweeds and Its Influence on Rheological Properties. *Frontiers in Plant Science*, *11*, 559986. https://doi.org/10.3389/fpls.2020.559986

Coêlho, D. D. F., Tundisi, L. L., Cerqueira, K. S., Rodrigues, J. R. D. S., Mazzola, P. G., Tambourgi, E. B., & Souza, R. R. D. (2019). Microalgae: Cultivation Aspects and Bioactive Compounds. *Brazilian Archives of Biology and Technology*, *62*, e19180343. https://doi.org/10.1590/1678-4324-2019180343

Concórdio-Reis, P., Alves, V. D., Moppert, X., Guézennec, J., Freitas, F., & Reis, M. A. M. (2021a). Characterization and Biotechnological Potential of Extracellular Polysaccharides Synthesized by Alteromonas Strains Isolated from French Polynesia Marine Environments. *Marine Drugs*, *19*(9), 522. https://doi.org/10.3390/md19090522

Concórdio-Reis, P., Alves, V. D., Moppert, X., Guézennec, J., Freitas, F., & Reis, M. A. M. (2021b). Characterization and Biotechnological Potential of Extracellular Polysaccharides Synthesized by Alteromonas Strains Isolated from French Polynesia Marine Environments. *Marine Drugs*, *19*(9), 522. https://doi.org/10.3390/md19090522

Concórdio-Reis, P., Pereira, C. V., Batista, M. P., Sevrin, C., Grandfils, C., Marques, A. C., Fortunato, E., Gaspar, F. B., Matias, A. A., Freitas, F., & Reis, M. A. M. (2020). Silver nanocomposites based on the bacterial fucose-rich polysaccharide secreted by Enterobacter A47 for wound dressing applications: Synthesis, characterization and in vitro bioactivity. *International Journal of Biological Macromolecules*, *163*, 959–969. https://doi.org/10.1016/j.ijbiomac.2020.07.072

Concórdio-Reis, P., Pereira, J. R., Alves, V. D., Nabais, A. R., Neves, L. A., Marques, A. C., Fortunato, E., Moppert, X., Guézennec, J., Reis, M. A. M., & Freitas, F. (2022). Characterisation of Films Based on Exopolysaccharides from Alteromonas Strains Isolated from French Polynesia Marine Environments. *Polymers*, *14*(20), 4442. https://doi.org/10.3390/polym14204442

Concórdio-Reis, P., Serafim, B., Pereira, J. R., Moppert, X., Guézennec, J., Reis, M. A. M., & Freitas, F. (2023a). Exopolysaccharide production by the marine bacterium Alteromonas macleodii Mo169 using fruit pulp waste as the sole carbon source. *Environmental Technology & Innovation*, *30*, 103090. https://doi.org/10.1016/j.eti.2023.103090

Concórdio-Reis, P., Serafim, B., Pereira, J. R., Moppert, X., Guézennec, J., Reis, M. A. M., & Freitas, F. (2023b). Exopolysaccharide production by the marine bacterium Alteromonas macleodii Mo169 using fruit pulp waste as the sole carbon source. *Environmental Technology & Innovation*, *30*, 103090. https://doi.org/10.1016/j.eti.2023.103090

Conesa, A. L., Dellatorre, F. G., Latour, E., Ponce, N. M. A., Stortz, C. A., Scolaro, L. A., Álvarez, V. A., Lassalle, V. L., & Ayala-Peña, V. B. (2023). *Potential of Fucoidan From Myriogloea Major Asensi as Antiviral Against Herpes Simplex Type 1 and 2 and Bovine Coronavirus*. In Review. https://doi.org/10.21203/rs.3.rs-2947896/v1

Corbett, D., & Roberts, I. S. (2008). Capsular Polysaccharides in Escherichia coli. In *Advances in Applied Microbiology* (Vol. 65, pp. 1–26). Elsevier. https://doi.org/10.1016/S0065-2164(08)00601-1

Corino, C., Di Giancamillo, A., Modina, S. C., & Rossi, R. (2021). Prebiotic Effects of Seaweed Polysaccharides in Pigs. *Animals*, *11*(6), 1573. https://doi.org/10.3390/ani11061573

Corsaro, M. M., De Castro, C., Evidente, A., Lanzetta, R., Lavermicocca, P., Molinaro, A., Sisto, A., Parrilli, M., & Surico, G. (1997). Lipopolysaccharides from three phytopathogenic pseudomonads. *Phytochemistry*, *46*(2), 289–292. https://doi.org/10.1016/S0031-9422(97)00274-4

Costa, J. A. V., Lucas, B. F., Alvarenga, A. G. P., Moreira, J. B., & De Morais, M. G. (2021). Microalgae Polysaccharides: An Overview of Production, Characterization, and Potential Applications. *Polysaccharides*, *2*(4), 759–772. https://doi.org/10.3390/polysaccharides2040046

Costerton, J. W., Cheng, K. J., Geesey, G. G., Ladd, T. I., Nickel, J. C., Dasgupta, M., & Marrie, T. J. (1987). Bacterial Biofilms in Nature and Disease. *Annual Review of Microbiology*, *41*(1), 435–464. https://doi.org/10.1146/annurev.mi.41.100187.002251

Couto, R. P., Rosas-Alquicira, E. F., Rodrigues, A. S., & Neto, A. I. (2014). The genus Ellisolandia (Corallinaceae, Corallinales, Rhodophyta) in the Azores (NE Atlantic): Character expression and taxonomic evaluation. *Phytotaxa*, *190*(1), 5. https://doi.org/10.11646/phytotaxa.190.1.3

Cunha, C., Faria, M., Nogueira, N., Ferreira, A., & Cordeiro, N. (2019). Marine vs freshwater microalgae exopolymers as biosolutions to microplastics pollution. *Environmental Pollution*, *249*, 372–380. https://doi.org/10.1016/j.envpol.2019.03.046

Cunha, L., & Grenha, A. (2016). Sulfated Seaweed Polysaccharides as Multifunctional Materials in Drug Delivery Applications. *Marine Drugs*, *14*(3), 42. https://doi.org/10.3390/md14030042

D'Amico, R., Casillo, A., Olimpo, D., Gallucci, N., D'Angelo, C., Tutino, M. L., Paduano, L., Parrilli, E., & Corsaro, M. M. (2025). Capsular polysaccharide from Psychrobacter sp. TAE2020: An

unusual amino sugar-enriched macromolecule with anti-biofilm and emulsification activities. *Carbohydrate Polymers*, *370*, 124484. https://doi.org/10.1016/j.carbpol.2025.124484

D'Amico, S., Collins, T., Marx, J., Feller, G., Gerday, C., & Gerday, C. (2006). Psychrophilic microorganisms: Challenges for life. *EMBO Reports*, *7*(4), 385–389. https://doi.org/10.1038/sj.embor.7400662

Daus, S., & Heinze, T. (2010). Xylan-Based Nanoparticles: Prodrugs for Ibuprofen Release. *Macromolecular Bioscience*, *10*(2), 211–220. https://doi.org/10.1002/mabi.200900201

De Carvalho, C. C. C. R. (2018). Marine Biofilms: A Successful Microbial Strategy With Economic Implications. *Frontiers in Marine Science*, *5*, 126. https://doi.org/10.3389/fmars.2018.00126

De Clerck, O., Guiry, M. D., Leliaert, F., Samyn, Y., & Verbruggen, H. (2013). Algal taxonomy: A road to nowhere? *Journal of Phycology*, *49*(2), 215–225. https://doi.org/10.1111/jpy.12020

Decho, A. W., & Gutierrez, T. (2017). Microbial Extracellular Polymeric Substances (EPSs) in Ocean Systems. *Frontiers in Microbiology*, *8*, 922. https://doi.org/10.3389/fmicb.2017.00922

Delbarre-Ladrat, C., Salas, M. L., Sinquin, C., Zykwinska, A., & Colliec-Jouault, S. (2017). Bioprospecting for Exopolysaccharides from Deep-Sea Hydrothermal Vent Bacteria: Relationship between Bacterial Diversity and Chemical Diversity. *Microorganisms*, *5*(3), 63. https://doi.org/10.3390/microorganisms5030063

Delbarre-Ladrat, C., Sinquin, C., Lebellenger, L., Zykwinska, A., & Colliec-Jouault, S. (2014a). Exopolysaccharides produced by marine bacteria and their applications as glycosaminoglycan-like molecules. *Frontiers in Chemistry*, *2*. https://doi.org/10.3389/fchem.2014.00085

Delbarre-Ladrat, C., Sinquin, C., Lebellenger, L., Zykwinska, A., & Colliec-Jouault, S. (2014b). Exopolysaccharides produced by marine bacteria and their applications as glycosaminoglycan-like molecules. *Frontiers in Chemistry*, *2*. https://doi.org/10.3389/fchem.2014.00085

Delbarre-Ladrat, C., Sinquin, C., Marchand, L., Bonnetot, S., Zykwinska, A., Verrez-Bagnis, V., & Colliec-Jouault, S. (2022). Influence of the Carbon and Nitrogen Sources on Diabolican

Production by the Marine Vibrio diabolicus Strain CNCM I-1629. *Polymers*, *14*(10), 1994. https://doi.org/10.3390/polym14101994

Deng, Y., Huang, M., Sun, D., Hou, Y., Li, Y., Dong, T., Wang, X., Zhang, L., & Yang, W. (2018). Dual Physically Cross-Linked κ-Carrageenan-Based Double Network Hydrogels with Superior Self-Healing Performance for Biomedical Application. *ACS Applied Materials & Interfaces*, *10*(43), 37544–37554. https://doi.org/10.1021/acsami.8b15385

Di Donato, P., Buono, A., Poli, A., Finore, I., Abbamondi, G. R., Nicolaus, B., & Lama, L. (2018). Exploring Marine Environments for the Identification of Extremophiles and Their Enzymes for Sustainable and Green Bioprocesses. *Sustainability*, *11*(1), 149. https://doi.org/10.3390/su11010149

Di Guida, R., Casillo, A., & Corsaro, M. M. (2020). O-specific polysaccharide structure isolated from the LPS of the Antarctic bacterium Pseudomonas ANT_J38B. *Carbohydrate Research*, *497*, 108125. https://doi.org/10.1016/j.carres.2020.108125

Di Guida, R., Casillo, A., Stellavato, A., Kawai, S., Ogawa, T., Di Meo, C., Kawamoto, J., Kurihara, T., Schiraldi, C., & Corsaro, M. M. (2022). Capsular polysaccharide from a fish-gut bacterium induces/promotes apoptosis of colon cancer cells in vitro through Caspases' pathway activation. *Carbohydrate Polymers*, *278*, 118908. https://doi.org/10.1016/j.carbpol.2021.118908

Di Guida, R., Casillo, A., Yokoyama, F., Kawamoto, J., Kurihara, T., & Corsaro, M. M. (2020). Detailed Structural Characterization of the Lipooligosaccharide from the Extracellular Membrane Vesicles of Shewanella vesiculosa HM13. *Marine Drugs*, *18*(5), 231. https://doi.org/10.3390/md18050231

Dolganyuk, V., Belova, D., Babich, O., Prosekov, A., Ivanova, S., Katserov, D., Patyukov, N., & Sukhikh, S. (2020). Microalgae: A Promising Source of Valuable Bioproducts. *Biomolecules*, *10*(8), 1153. https://doi.org/10.3390/biom10081153

Domozych, C. R., Plante, K., Blais, P., Paliulis, L., & Domozych, D. S. (1993). MUCILAGE PROCESSING AND SECRETION IN THE GREEN ALGA *CLOSTERIUM.* I. CYTOLOGY

AND BIOCHEMISTRY[1]. *Journal of Phycology*, *29*(5), 650–659. https://doi.org/10.1111/j.0022-3646.1993.00650.x

Domozych, D. S., & LoRicco, J. G. (2023). The extracellular matrix of green algae. *Plant Physiology*, *194*(1), 15–32. https://doi.org/10.1093/plphys/kiad384

Domozych, D. S., Stewart, K. D., & Mattox, K. R. (1981). Development of the cell wall in *Tetraselmis:* role of the golgi apparatus and extracellular wall assembly. *Journal of Cell Science*, *52*(1), 351–371. https://doi.org/10.1242/jcs.52.1.351

El-Newary, S. A., Ibrahim, A. Y., Asker, M. S., Mahmoud, M. G., & El Awady, M. E. (2017). Production, characterization and biological activities of acidic exopolysaccharide from marine Bacillus amyloliquefaciens 3MS 2017. *Asian Pacific Journal of Tropical Medicine*, *10*(7), 652–662. https://doi.org/10.1016/j.apjtm.2017.07.005

El-Sayed, A. A. M., & Ismail, M. M. (2022). Physico-chemodiversity variation between the most common calcareous red seaweed, Eastern Harbor, Alexandria, Egypt. *Heliyon*, *8*(12), e12457. https://doi.org/10.1016/j.heliyon.2022.e12457

Falkowski, P. G., Barber, R. T., & Smetacek, V. (1998). Biogeochemical Controls and Feedbacks on Ocean Primary Production. *Science*, *281*(5374), 200–206. https://doi.org/10.1126/science.281.5374.200

Falshaw, R., & Furneaux, R. H. (1995). Carrageenans from the tetrasporic stages of Gigartina clavifera and Gigartina alveata (Gigartinaceae, Rhodophyta). *Carbohydrate Research*, *276*(1), 155–165. https://doi.org/10.1016/0008-6215(95)00153-K

Farias, W. R. L., Valente, A.-P., Pereira, M. S., & Mourão, P. A. S. (2000). Structure and Anticoagulant Activity of Sulfated Galactans. *Journal of Biological Chemistry*, *275*(38), 29299–29307. https://doi.org/10.1074/jbc.M002422200

Fernandes, P. A. R., & Coimbra, M. A. (2023). The antioxidant activity of polysaccharides: A structure-function relationship overview. *Carbohydrate Polymers*, *314*, 120965. https://doi.org/10.1016/j.carbpol.2023.120965

Field, C. B., Behrenfeld, M. J., Randerson, J. T., & Falkowski, P. (1998). Primary Production of the Biosphere: Integrating Terrestrial and Oceanic Components. *Science*, *281*(5374), 237–240. https://doi.org/10.1126/science.281.5374.237

Fimbres-Olivarria, D., Carvajal-Millan, E., Lopez-Elias, J. A., Martinez-Robinson, K. G., Miranda-Baeza, A., Martinez-Cordova, L. R., Enriquez-Ocaña, F., & Valdez-Holguin, J. E. (2018). Chemical characterization and antioxidant activity of sulfated polysaccharides from Navicula sp. *Food Hydrocolloids*, *75*, 229–236. https://doi.org/10.1016/j.foodhyd.2017.08.002

Fimbres-Olivarria, D., Marquez-Escalante, J., Martínez-Robinson, K. G., Miranda-Arizmendi, V., Anda-Flores, Y. D., Rascon-Chu, A., Brown-Bojorquez, F., & Carvajal-Millan, E. (2023). Physicochemical and Microstructural Characteristics of Sulfated Polysaccharide from Marine Microalga. *Analytica*, *4*(4), 527–537. https://doi.org/10.3390/analytica4040036

Flemming, H.-C., & Wingender, J. (2010). The biofilm matrix. *Nature Reviews Microbiology*, *8*(9), 623–633. https://doi.org/10.1038/nrmicro2415

Flórez-Fernández, N., Domínguez, H., & Torres, M. D. (2019). A green approach for alginate extraction from Sargassum muticum brown seaweed using ultrasound-assisted technique. *International Journal of Biological Macromolecules*, *124*, 451–459. https://doi.org/10.1016/j.ijbiomac.2018.11.232

Foster, M. S. (2001). RHODOLITHS: BETWEEN ROCKS AND SOFT PLACES. *Journal of Phycology*, *37*(5), 659–667. https://doi.org/10.1046/j.1529-8817.2001.00195.x

Fresno, S., Jiménez, N., Canals, R., Merino, S., Corsaro, M. M., Lanzetta, R., Parrilli, M., Pieretti, G., Regué, M., & Tomás, J. M. (2007). A Second Galacturonic Acid Transferase Is Required for Core Lipopolysaccharide Biosynthesis and Complete Capsule Association with the Cell Surface in *Klebsiella pneumoniae*. *Journal of Bacteriology*, *189*(3), 1128–1137. https://doi.org/10.1128/JB.01489-06

Fresno, S., Jiménez, N., Izquierdo, L., Merino, S., Corsaro, M. M., De Castro, C., Parrilli, M., Naldi, T., Regué, M., & Tomás, J. M. (2006). The ionic interaction of Klebsiella pneumoniae K2

capsule and core lipopolysaccharide. *Microbiology*, *152*(6), 1807–1818. https://doi.org/10.1099/mic.0.28611-0

Freyria, N. J., Góngora, E., Greer, C. W., & Whyte, L. G. (2024). High Arctic seawater and coastal soil microbiome co-occurrence and composition structure and their potential hydrocarbon biodegradation. *ISME Communications*, *4*(1), ycae100. https://doi.org/10.1093/ismeco/ycae100

Fuhrman, J. A., Steele, J. A., Hewson, I., Schwalbach, M. S., Brown, M. V., Green, J. L., & Brown, J. H. (2008). A latitudinal diversity gradient in planktonic marine bacteria. *Proceedings of the National Academy of Sciences*, *105*(22), 7774–7778. https://doi.org/10.1073/pnas.0803070105

Gaignard, C., Laroche, C., Pierre, G., Dubessay, P., Delattre, C., Gardarin, C., Gourvil, P., Probert, I., Dubuffet, A., & Michaud, P. (2019). Screening of marine microalgae: Investigation of new exopolysaccharide producers. *Algal Research*, *44*, 101711. https://doi.org/10.1016/j.algal.2019.101711

Galanos, C., Lüderitz, O., & Westphal, O. (1969). A New Method for the Extraction of R Lipopolysaccharides. *European Journal of Biochemistry*, *9*(2), 245–249. https://doi.org/10.1111/j.1432-1033.1969.tb00601.x

Gargouch, N., Elleuch, F., Karkouch, I., Tabbene, O., Pichon, C., Gardarin, C., Rihouey, C., Picton, L., Abdelkafi, S., Fendri, I., & Laroche, C. (2021). Potential of Exopolysaccharide from Porphyridium marinum to Contend with Bacterial Proliferation, Biofilm Formation, and Breast Cancer. *Marine Drugs*, *19*(2), 66. https://doi.org/10.3390/md19020066

Gieroba, B., Kalisz, G., Krysa, M., Khalavka, M., & Przekora, A. (2023). Application of Vibrational Spectroscopic Techniques in the Study of the Natural Polysaccharides and Their Cross-Linking Process. *International Journal of Molecular Sciences*, *24*(3), 2630. https://doi.org/10.3390/ijms24032630

Gladue, R. M., & Maxey, J. E. (1994). Microalgal feeds for aquaculture. *Journal of Applied Phycology*, *6*(2), 131–141. https://doi.org/10.1007/BF02186067

Gongi, W., Rube, M., Ben Ouada, Hafedh, Ben Ouada, Hatem, Tamarin, O., & Dejous, C. (2023). Elaboration and Characterization of a New Heavy Metal Sensor Functionalized by Extracellular Polymeric Substances Isolated from a Tunisian Thermophilic Microalga Strain Graesiella sp. *Sensors*, *23*(2), 803. https://doi.org/10.3390/s23020803

Goswami, R. K., Agrawal, K., Mehariya, S., & Verma, P. (2022). Current perspective on wastewater treatment using photobioreactor for Tetraselmis sp.: An emerging and foreseeable sustainable approach. *Environmental Science and Pollution Research*, *29*(41), 61905–61937. https://doi.org/10.1007/s11356-021-16860-5

Gowrishankar, S., & Pandian, S. K. (2017). Modulation of Staphylococcus epidermidis (RP62A) extracellular polymeric layer by marine cyclic dipeptide-cyclo(l -leucyl- l -prolyl) thwarts biofilm formation. *Biochimica et Biophysica Acta (BBA) - Biomembranes*, *1859*(7), 1254–1262. https://doi.org/10.1016/j.bbamem.2017.04.009

Gualtieri, P., & Barsanti, L. (2022). *Algae: Anatomy, Biochemistry, and Biotechnology* (3ª ed.). CRC Press. https://doi.org/10.1201/9781003187707

Gurgel, C. F. D., & Lopez-Bautista, J. (2007). Red Algae. In Wiley, *Encyclopedia of Life Sciences* (1ª ed.). Wiley. https://doi.org/10.1002/9780470015902.a0000335

Guzmán-Murillo, M. A., López-Bolaños, C. C., Ledesma-Verdejo, T., Roldan-Libenson, G., Cadena-Roa, M. A., & Ascencio, F. (2007). Effects of fertilizer-based culture media on the production of exocellular polysaccharides and cellular superoxide dismutase by Phaeodactylum tricornutum (Bohlin). *Journal of Applied Phycology*, *19*(1), 33–41. https://doi.org/10.1007/s10811-006-9108-9

Harris, J., Haward, M., Jabour, J., & Woehler, E. J. (2007). A new approach to selecting Marine Protected Areas (MPAs) in the Southern Ocean. *Antarctic Science*, *19*(2), 189–194. https://doi.org/10.1017/S0954102007000260

Helmke, E., & Weyland, H. (1995). Bacteria in sea ice and underlying water of the eastern Weddell Sea in midwinter. *Marine Ecology Progress Series*, *117*, 269–287. https://doi.org/10.3354/meps117269

Hendrickson, W. A., & Ward, K. B. (1975a). Atomic models for the polypeptide backbones of myohemerythrin and hemerythrin. *Biochemical and Biophysical Research Communications*, *66*(4), 1349–1356. https://doi.org/10.1016/0006-291x(75)90508-2

Hendrickson, W. A., & Ward, K. B. (1975b). Atomic models for the polypeptide backbones of myohemerythrin and hemerythrin. *Biochemical and Biophysical Research Communications*, *66*(4), 1349–1356. https://doi.org/10.1016/0006-291x(75)90508-2

Hentati, F., Delattre, C., Gardarin, C., Desbrières, J., Le Cerf, D., Rihouey, C., Michaud, P., Abdelkafi, S., & Pierre, G. (2020). Structural Features and Rheological Properties of a Sulfated Xylogalactan-Rich Fraction Isolated from Tunisian Red Seaweed Jania adhaerens. *Applied Sciences*, *10*(5), 1655. https://doi.org/10.3390/app10051655

Hentati, F., Tounsi, L., Djomdi, D., Pierre, G., Delattre, C., Ursu, A. V., Fendri, I., Abdelkafi, S., & Michaud, P. (2020). Bioactive Polysaccharides from Seaweeds. *Molecules*, *25*(14), 3152. https://doi.org/10.3390/molecules25143152

Hewson, I. (2025). *When bacteria meet many arms: Autecological insights into* Vibrio pectinicida *FHCF-3 in echinoderms*. Microbiology. https://doi.org/10.1101/2025.08.15.670479

Heymann, D., Ruiz-Velasco, C., Chesneau, J., Ratiskol, J., Sinquin, C., & Colliec-Jouault, S. (2016). Anti-Metastatic Properties of a Marine Bacterial Exopolysaccharide-Based Derivative Designed to Mimic Glycosaminoglycans. *Molecules*, *21*(3), 309. https://doi.org/10.3390/molecules21030309

Hind, K. R., & Saunders, G. W. (2013). A Molecular Phylogenetic Study of the Tribe Corallineae (Corallinales, Rhodophyta) with an Assessment of Genus-Level Taxonomic Features and Descriptions of Novel Genera. *Journal of Phycology*, *49*(1), 103–114. https://doi.org/10.1111/jpy.12019

Hira, J., & Stensvåg, K. (2022). Evidence for association of Vibrio echinoideorum with tissue necrosis on test of the green sea urchin Strongylocentrotus droebachiensis. *Scientific Reports*, *12*(1), 4859. https://doi.org/10.1038/s41598-022-08772-2

Hori, T., Norris, R. E., & Chihara, M. (1982). Studies on the ultrastructure and taxonomy of the genusTetraselmis (Prasinophyceae): I. SubgenusTetraselmis. *The Botanical Magazine Tokyo*, *95*(1), 49–61. https://doi.org/10.1007/BF02493410

Hussein, H. A., Kassim, M. N. I., Maulidiani, M., Abas, F., & Abdullah, M. A. (2022). Cytotoxicity and 1H NMR metabolomics analyses of microalgal extracts for synergistic application with Tamoxifen on breast cancer cells with reduced toxicity against Vero cells. *Heliyon*, *8*(3), e09192. https://doi.org/10.1016/j.heliyon.2022.e09192

Hussein, H. A., Syamsumir, D. F., Radzi, S. A. M., Siong, J. Y. F., Zin, N. A. M., & Abdullah, M. A. (2020). Phytochemical screening, metabolite profiling and enhanced antimicrobial activities of microalgal crude extracts in co-application with silver nanoparticle. *Bioresources and Bioprocessing*, *7*(1), 39. https://doi.org/10.1186/s40643-020-00322-w

Hwang, P.-A., Lin, X.-Z., Kuo, K.-L., & Hsu, F.-Y. (2017). Fabrication and Cytotoxicity of Fucoidan-Cisplatin Nanoparticles for Macrophage and Tumor Cells. *Materials*, *10*(3), 291. https://doi.org/10.3390/ma10030291

Ibrahim, H. A. H., Abou Elhassayeb, H. E., & El-Sayed, W. M. M. (2022). Potential functions and applications of diverse microbial exopolysaccharides in marine environments. *Journal of Genetic Engineering and Biotechnology*, *20*(1), 151. https://doi.org/10.1186/s43141-022-00432-2

Ignatovich, V. F. (1975). Enhancement of the antigenic activity and virulence of the vaccine strain E of Rickettsia prow azeki by passages in cell culture. *Acta Virologica*, *19*(6), 481–485.

Ismail, M. M., & Kanaan, H. M. (2022). Chemodiversity of Galactans from Different Red Seaweed Species with Emphasis on their Antioxidant and Antiproliferative Activities in vitro. *Brazilian Archives of Biology and Technology*, *65*, e22210122. https://doi.org/10.1590/1678-4324-2022210122

Iwamoto, K., & Shiraiwa, Y. (2005). Salt-Regulated Mannitol Metabolism in Algae. *Marine Biotechnology*, *7*(5), 407–415. https://doi.org/10.1007/s10126-005-0029-4

Jang, Y., Shin, H., Lee, M. K., Kwon, O. S., Shin, J. S., Kim, Y., Kim, C. W., Lee, H.-R., & Kim, M. (2021). Antiviral activity of lambda-carrageenan against influenza viruses and severe acute respiratory syndrome coronavirus 2. *Scientific Reports*, *11*(1), 821. https://doi.org/10.1038/s41598-020-80896-9

Jiang, F., Chi, Z., Ding, Y., Quan, M., Tian, Y., Shi, J., Song, F., & Liu, C. (2021). Wound Dressing Hydrogel of *Enteromorpha prolifera* Polysaccharide–Polyacrylamide Composite: A Facile Transformation of Marine Blooming into Biomedical Material. *ACS Applied Materials & Interfaces*, *13*(12), 14530–14542. https://doi.org/10.1021/acsami.0c21543

Jothisaraswathi, S., Babu, B., & Rengasamy, R. (2006). Seasonal studies on alginate and its composition II: Turbinaria conoides (J.Ag.) Kütz. (Fucales, Phaeophyceae). *Journal of Applied Phycology*, *18*(2), 161–166. https://doi.org/10.1007/s10811-006-9089-8

Jovic, T. H., Kungwengwe, G., Mills, A. C., & Whitaker, I. S. (2019). Plant-Derived Biomaterials: A Review of 3D Bioprinting and Biomedical Applications. *Frontiers in Mechanical Engineering*, *5*, 19. https://doi.org/10.3389/fmech.2019.00019

Jun, J.-Y., Jung, M.-J., Jeong, I.-H., Yamazaki, K., Kawai, Y., & Kim, B.-M. (2018). Antimicrobial and Antibiofilm Activities of Sulfated Polysaccharides from Marine Algae against Dental Plaque Bacteria. *Marine Drugs*, *16*(9), 301. https://doi.org/10.3390/md16090301

Jung, S.-H., Zell, N., Boßle, F., Teipel, U., Rauh, C., McHardy, C., & Lindenberger, C. (2022). Influence of Process Operation on the Production of Exopolysaccharides in Arthrospira platensis and Chlamydomonas asymmetrica. *Frontiers in Sustainable Food Systems*, *6*, 883069. https://doi.org/10.3389/fsufs.2022.883069

Juranek, L. W., White, A. E., Dugenne, M., Henderikx Freitas, F., Dutkiewicz, S., Ribalet, F., Ferrón, S., Armbrust, E. V., & Karl, D. M. (2020). The Importance of the Phytoplankton "Middle Class" to Ocean Net Community Production. *Global Biogeochemical Cycles*, *34*(12), e2020GB006702. https://doi.org/10.1029/2020GB006702

Kamasaka, K., Kawamoto, J., Chen, C., Yokoyama, F., Imai, T., Ogawa, T., & Kurihara, T. (2020). Genetic characterization and functional implications of the gene cluster for selective protein

transport to extracellular membrane vesicles of Shewanella vesiculosa HM13. *Biochemical and Biophysical Research Communications*, *526*(2), 525–531. https://doi.org/10.1016/j.bbrc.2020.03.125

Kamenos, N. A., Burdett, H. L., Aloisio, E., Findlay, H. S., Martin, S., Longbone, C., Dunn, J., Widdicombe, S., & Calosi, P. (2013). Coralline algal structure is more sensitive to rate, rather than the magnitude, of ocean acidification. *Global Change Biology*, *19*(12), 3621–3628. https://doi.org/10.1111/gcb.12351

Kamio, Y., & Nikaido, H. (1976). Outer membrane of Salmonella typhimurium: Accessibility of phospholipid head groups to phospholipase C and cyanogen bromide activated dextran in the external medium. *Biochemistry*, *15*(12), 2561–2570. https://doi.org/10.1021/bi00657a012

Kermanshahi-pour, A., Sommer, T. J., Anastas, P. T., & Zimmerman, J. B. (2014). Enzymatic and acid hydrolysis of Tetraselmis suecica for polysaccharide characterization. *Bioresource Technology*, *173*, 415–421. https://doi.org/10.1016/j.biortech.2014.09.048

Ko, S.-C., Lee, S.-H., Ahn, G., Kim, K.-N., Cha, S.-H., Kim, S.-K., Jeon, B.-T., Park, P.-J., Lee, K.-W., & Jeon, Y.-J. (2012). Effect of enzyme-assisted extract of Sargassum coreanum on induction of apoptosis in HL-60 tumor cells. *Journal of Applied Phycology*, *24*(4), 675–684. https://doi.org/10.1007/s10811-011-9685-0

Kolkman, M. A. B., Van Der Zeijst, B. A. M., & Nuijten, P. J. M. (1997). Functional Analysis of Glycosyltransferases Encoded by the Capsular Polysaccharide Biosynthesis Locus of Streptococcus pneumoniae Serotype 14. *Journal of Biological Chemistry*, *272*(31), 19502–19508. https://doi.org/10.1074/jbc.272.31.19502

Kong, D.-X., Jiang, Y.-Y., & Zhang, H.-Y. (2010). Marine natural products as sources of novel scaffolds: Achievement and concern. *Drug Discovery Today*, *15*(21–22), 884–886. https://doi.org/10.1016/j.drudis.2010.09.002

Kronusová, O., Kaštánek, P., Koyun, G., Kaštánek, F., & Brányik, T. (2022). Factors Influencing the Production of Extracellular Polysaccharides by the Green Algae Dictyosphaerium

chlorelloides and Their Isolation, Purification, and Composition. *Microorganisms*, *10*(7), 1473. https://doi.org/10.3390/microorganisms10071473

Laemmli, U. K., & Favre, M. (1973). Maturation of the head of bacteriophage T4. *Journal of Molecular Biology*, *80*(4), 575–599. https://doi.org/10.1016/0022-2836(73)90198-8

Laroche, C. (2022). Exopolysaccharides from Microalgae and Cyanobacteria: Diversity of Strains, Production Strategies, and Applications. *Marine Drugs*, *20*(5), 336. https://doi.org/10.3390/md20050336

Lee, H. E., Lee, J. H., Park, S. M., & Kim, D. G. (2023). Symbiotic relationship between filamentous algae (Halomicronema sp.) and extracellular polymeric substance-producing algae (Chlamydomonas sp.) through biomimetic simulation of natural algal mats. *Frontiers in Microbiology*, *14*, 1176069. https://doi.org/10.3389/fmicb.2023.1176069

Leontein, K., Lindberg, B., & Lönngren, J. (1978). Assignment of absolute configuration of sugars by g.l.c. Of their acetylated glycosides formed from chiral alcohols. *Carbohydrate Research*, *62*(2), 359–362. https://doi.org/10.1016/S0008-6215(00)80882-4

Li, Q., Chen, Y., Liu, X., Li, Y., Xu, J., Li, T., Xiang, W., & Li, A. (2023). Effect of salinity on the biochemical characteristics and antioxidant activity of exopolysaccharide of Porphyridium purpureum FACHB 806. *Frontiers in Marine Science*, *9*, 1097200. https://doi.org/10.3389/fmars.2022.1097200

Li, Z., Liu, Y., Zhou, T., Cao, L., Cai, Y., Wang, Y., Cui, X., Yan, H., Ruan, R., & Zhang, Q. (2022). Effects of Culture Conditions on the Performance of Arthrospira platensis and Its Production of Exopolysaccharides. *Foods*, *11*(14), 2020. https://doi.org/10.3390/foods11142020

Liber, J. A., Bryson, A. E., Bonito, G., & Du, Z. (2020). Harvesting Microalgae for Food and Energy Products. *Small Methods*, *4*(10), 2000349. https://doi.org/10.1002/smtd.202000349

Lipsman, V., Shlakhter, O., Rocha, J., & Segev, E. (2024). Bacteria contribute exopolysaccharides to an algal-bacterial joint extracellular matrix. *Npj Biofilms and Microbiomes*, *10*(1), 36. https://doi.org/10.1038/s41522-024-00510-y

Liu, L., Liu, Y., Li, J., Du, G., & Chen, J. (2011). Microbial production of hyaluronic acid: Current state, challenges, and perspectives. *Microbial Cell Factories*, *10*(1), 99. https://doi.org/10.1186/1475-2859-10-99

Liu, S., Hu, Q., Shen, Z., Krishnan, S., Zhang, H., & Ramalingam, M. (2022). 3D printing of self-standing and vascular supportive multimaterial hydrogel structures for organ engineering. *Biotechnology and Bioengineering*, *119*(1), 118–133. https://doi.org/10.1002/bit.27954

Liyanage, N. M., Nagahawatta, D. P., Jayawardena, T. U., Sanjeewa, K. K. A., Jayawrdhana, H. H. A. C. K., Kim, J.-I., & Jeon, Y.-J. (2023). Sulfated Polysaccharides from Seaweeds: A Promising Strategy for Combatting Viral Diseases—A Review. *Marine Drugs*, *21*(9), 461. https://doi.org/10.3390/md21090461

Llamas, I., Amjres, H., Mata, J. A., Quesada, E., & Béjar, V. (2012). The Potential Biotechnological Applications of the Exopolysaccharide Produced by the Halophilic Bacterium Halomonas almeriensis. *Molecules*, *17*(6), 7103–7120. https://doi.org/10.3390/molecules17067103

Llull, D., Lopez, R., & Garcia, E. (2001). Genetic Bases and Medical Relevance of Capsular Polysaccharide Biosynthesis in Pathogenic Streptococci. *Current Molecular Medicine*, *1*(4), 475–491. https://doi.org/10.2174/1566524013363618

López-Pérez, M., Gonzaga, A., Martin-Cuadrado, A.-B., Onyshchenko, O., Ghavidel, A., Ghai, R., & Rodriguez-Valera, F. (2012). Genomes of surface isolates of Alteromonas macleodii: The life of a widespread marine opportunistic copiotroph. *Scientific Reports*, *2*(1), 696. https://doi.org/10.1038/srep00696

Lu, L., Wang, J., Yang, G., Zhu, B., & Pan, K. (2017). Heterotrophic growth and nutrient productivities of Tetraselmis chuii using glucose as a carbon source under different C/N ratios. *Journal of Applied Phycology*, *29*(1), 15–21. https://doi.org/10.1007/s10811-016-0919-z

Lund, J. W. G., & Butcher, R. W. (1960). Marine Nannoplankton. *The Journal of Animal Ecology*, *29*(1), 192. https://doi.org/10.2307/2279

Malagoli, B. G., Cardozo, F. T. G. S., Gomes, J. H. S., Ferraz, V. P., Simões, C. M. O., & Braga, F. C. (2014). Chemical characterization and antiherpes activity of sulfated polysaccharides from Lithothamnion muelleri. *International Journal of Biological Macromolecules*, *66*, 332–337. https://doi.org/10.1016/j.ijbiomac.2014.02.053

Manivasagan, P., Sivasankar, P., Venkatesan, J., Senthilkumar, K., Sivakumar, K., & Kim, S.-K. (2013). Production and characterization of an extracellular polysaccharide from Streptomyces violaceus MM72. *International Journal of Biological Macromolecules*, *59*, 29–38. https://doi.org/10.1016/j.ijbiomac.2013.04.012

Maray, S. O., Abdel-Kareem, M. S. M., Mabrouk, M. E. M., El-Halmouch, Y., & Makhlof, M. E. M. (2023). In Vitro Assessment of Antiviral, Antimicrobial, Antioxidant and Anticancer Activities of Ulvan Extracted from the Green Seaweed Ulva lactuca. *Thalassas: An International Journal of Marine Sciences*, *39*(2), 779–790. https://doi.org/10.1007/s41208-023-00584-z

Mariani, P., Tolomio, C., & Braghetta, P. (1985). An ultrastructural approach to the adaptive role of the cell wall in the intertidal algaFucus virsoides. *Protoplasma*, *128*(2–3), 208–217. https://doi.org/10.1007/BF01276343

Martino, A., Montero, D., Roo, J., Holt, W. V., Lavorano, S., Narizzano, R., & Otero Ferrer, F. (2023). Live Microalgae-Based Diets as Enrichment to Improve the Nutritional Profile of the Calanoid Copepod Acartia tonsa (Dana, 1849) Nauplii. *Aquaculture Research*, *2023*, 1–12. https://doi.org/10.1155/2023/6622009

Marudhupandi, T., & Kumar, T. T. A. (2013). Antibacterial effect of fucoidan from Sargassum wightii against the chosen human bacterial pathogens. *International Current Pharmaceutical Journal*, *2*(10), 156–158. https://doi.org/10.3329/icpj.v2i10.16408

Maruyama, A., Honda, D., Yamamoto, H., Kitamura, K., & Higashihara, T. (2000). Phylogenetic analysis of psychrophilic bacteria isolated from the Japan Trench, including a description of the deep-sea species Psychrobacter pacificensis sp. Nov. *International Journal of Systematic and Evolutionary Microbiology*, *50*(2), 835–846. https://doi.org/10.1099/00207713-50-2-835

Marx, J. G., Carpenter, S. D., & Deming, J. W. (2009). Production of cryoprotectant extracellular polysaccharide substances (EPS) by the marine psychrophilic bacterium *Colwellia psychrerythraea* strain 34H under extreme conditionsThis article is one of a selection of papers in the Special Issue on Polar and Alpine Microbiology. *Canadian Journal of Microbiology*, *55*(1), 63–72. https://doi.org/10.1139/W08-130

Mata, M. T., Cameron, H., Avalos, V., & Riquelme, C. (2023). Identification and Characterization of a Novel Microalgal Strain from the Antofagasta Coast Tetraselmis marina AC16-MESO (Chlorophyta) for Biotechnological Applications. *Plants*, *12*(19), 3372. https://doi.org/10.3390/plants12193372

Matsuura, M. (2013). Structural Modifications of Bacterial Lipopolysaccharide that Facilitate Gram-Negative Bacteria Evasion of Host Innate Immunity. *Frontiers in Immunology*, *4*. https://doi.org/10.3389/fimmu.2013.00109

Matsuyama, H., Hirabayashi, T., Kasahara, H., Minami, H., Hoshino, T., & Yumoto, I. (2006). Glaciecola chathamensis sp. Nov., a novel marine polysaccharide-producing bacterium. *International Journal of Systematic and Evolutionary Microbiology*, *56*(12), 2883–2886. https://doi.org/10.1099/ijs.0.64413-0

Maue, A. C., Mohawk, K. L., Giles, D. K., Poly, F., Ewing, C. P., Jiao, Y., Lee, G., Ma, Z., Monteiro, M. A., Hill, C. L., Ferderber, J. S., Porter, C. K., Trent, M. S., & Guerry, P. (2013). The Polysaccharide Capsule of Campylobacter jejuni Modulates the Host Immune Response. *Infection and Immunity*, *81*(3), 665–672. https://doi.org/10.1128/IAI.01008-12

Mayer, A. M. S., Rodríguez, A. D., Berlinck, R. G. S., & Fusetani, N. (2011). Marine pharmacology in 2007–8: Marine compounds with antibacterial, anticoagulant, antifungal, anti-inflammatory, antimalarial, antiprotozoal, antituberculosis, and antiviral activities; affecting the immune and nervous system, and other miscellaneous mechanisms of action. *Comparative Biochemistry and Physiology Part C: Toxicology & Pharmacology*, *153*(2), 191–222. https://doi.org/10.1016/j.cbpc.2010.08.008

McCoy, S. J., & Kamenos, N. A. (2015). Coralline algae (Rhodophyta) in a changing world: Integrating ecological, physiological, and geochemical responses to global change. *Journal of Phycology*, *51*(1), 6–24. https://doi.org/10.1111/jpy.12262

Mclachlan, J., & Parke, M. (1967). *Platymonas Impellucida* Sp.Nov. From Puerto Rico. *Journal of the Marine Biological Association of the United Kingdom*, *47*(3), 723–733. https://doi.org/10.1017/S002531540003530X

Methé, B. A., Nelson, K. E., Deming, J. W., Momen, B., Melamud, E., Zhang, X., Moult, J., Madupu, R., Nelson, W. C., Dodson, R. J., Brinkac, L. M., Daugherty, S. C., Durkin, A. S., DeBoy, R. T., Kolonay, J. F., Sullivan, S. A., Zhou, L., Davidsen, T. M., Wu, M., … Fraser, C. M. (2005). The psychrophilic lifestyle as revealed by the genome sequence of *Colwellia psychrerythraea* 34H through genomic and proteomic analyses. *Proceedings of the National Academy of Sciences*, *102*(31), 10913–10918. https://doi.org/10.1073/pnas.0504766102

Mohamed, S., Hashim, S. N., & Rahman, H. A. (2012). Seaweeds: A sustainable functional food for complementary and alternative therapy. *Trends in Food Science & Technology*, *23*(2), 83–96. https://doi.org/10.1016/j.tifs.2011.09.001

Mokrosnop, V. M., & Zolotariova, Ye. K. (2020). Polysaccharides of Seaweeds' Cell Walls: Structure and Features (a Review). *Hydrobiological Journal*, *56*(5), 41–50. https://doi.org/10.1615/HydrobJ.v56.i5.50

Moreira, J. B., Kuntzler, S. G., Bezerra, P. Q. M., Cassuriaga, A. P. A., Zaparoli, M., Da Silva, J. L. V., Costa, J. A. V., & De Morais, M. G. (2022). Recent Advances of Microalgae Exopolysaccharides for Application as Bioflocculants. *Polysaccharides*, *3*(1), 264–276. https://doi.org/10.3390/polysaccharides3010015

Mousavian, Z., Safavi, M., Azizmohseni, F., Hadizadeh, M., & Mirdamadi, S. (2022). Characterization, antioxidant and anticoagulant properties of exopolysaccharide from marine microalgae. *AMB Express*, *12*(1), 27. https://doi.org/10.1186/s13568-022-01365-2

Nakhamchik, A., Wilde, C., Chong, H., & Rowe-Magnus, D. A. (2010). Evidence for the Horizontal Transfer of an Unusual Capsular Polysaccharide Biosynthesis Locus in Marine Bacteria. *Infection and Immunity*, *78*(12), 5214–5222. https://doi.org/10.1128/IAI.00653-10

Nannini, M., De Marchi, L., Lombardi, C., & Ragazzola, F. (2015). Effects of thermal stress on the growth of an intertidal population of Ellisolandia elongata (Rhodophyta) from N–W Mediterranean Sea. *Marine Environmental Research*, *112*, 11–19. https://doi.org/10.1016/j.marenvres.2015.05.005

Nash, M. C., Diaz-Pulido, G., Harvey, A. S., & Adey, W. (2019). Coralline algal calcification: A morphological and process-based understanding. *PLOS ONE*, *14*(9), e0221396. https://doi.org/10.1371/journal.pone.0221396

Navarro, D. A., Ricci, A. M., Rodríguez, M. C., & Stortz, C. A. (2011). Xylogalactans from Lithothamnion heterocladum, a crustose member of the Corallinales (Rhodophyta). *Carbohydrate Polymers*, *84*(3), 944–951. https://doi.org/10.1016/j.carbpol.2010.12.048

Navarro, D. A., & Stortz, C. A. (2008). The system of xylogalactans from the red seaweed Jania rubens (Corallinales, Rhodophyta). *Carbohydrate Research*, *343*(15), 2613–2622. https://doi.org/10.1016/j.carres.2008.06.015

Nguyen, M. P., Tran, L. V. H., Namgoong, H., & Kim, Y.-H. (2019). Applications of different solvents and conditions for differential extraction of lipopolysaccharide in Gram-negative bacteria. *Journal of Microbiology*, *57*(8), 644–654. https://doi.org/10.1007/s12275-019-9116-5

Nichols, C. M., Lardière, S. G., Bowman, J. P., Nichols, P. D., A.E. Gibson, J., & Guézennec, J. (2005). Chemical Characterization of Exopolysaccharides from Antarctic Marine Bacteria. *Microbial Ecology*, *49*(4), 578–589. https://doi.org/10.1007/s00248-004-0093-8

Okazaki, M., Furuya, K., Tsukayama, K., & Nisizawa, K. (1982). Isolation and Identification of Alginic Acid from a Calcareous Red Alga Serraticardia maxima. *Botanica Marina*, *25*(3). https://doi.org/10.1515/botm.1982.25.3.123

Park, G.-T., Go, R.-E., Lee, H.-M., Lee, G.-A., Kim, C.-W., Seo, J.-W., Hong, W.-K., Choi, K.-C., & Hwang, K.-A. (2017). Potential Anti-proliferative and Immunomodulatory Effects of Marine Microalgal Exopolysaccharide on Various Human Cancer Cells and Lymphocytes In Vitro. *Marine Biotechnology*, *19*(2), 136–146. https://doi.org/10.1007/s10126-017-9735-y

Parra-Riofrío, G., García-Márquez, J., Casas-Arrojo, V., Uribe-Tapia, E., & Abdala-Díaz, R. T. (2020). Antioxidant and Cytotoxic Effects on Tumor Cells of Exopolysaccharides from Tetraselmis suecica (Kylin) Butcher Grown Under Autotrophic and Heterotrophic Conditions. *Marine Drugs*, *18*(11), 534. https://doi.org/10.3390/md18110534

Parra-Riofrio, G., Moreno, P., García-Rosado, E., Alonso, M. C., Uribe-Tapia, E., Abdala-Diaz, R. T., & Bejar, J. (2023). Tetraselmis suecica and Porphyridium cruentum exopolysaccharides show anti-VHSV activity on RTG-2 cells. *Aquaculture International*, *31*(6), 3145–3157. https://doi.org/10.1007/s10499-023-01202-8

Pei, Y., Yang, S., Xiao, Z., Zhou, C., Hong, P., & Qian, Z.-J. (2021). Structural Characterization of Sulfated Polysaccharide Isolated From Red Algae (Gelidium crinale) and Antioxidant and Anti-Inflammatory Effects in Macrophage Cells. *Frontiers in Bioengineering and Biotechnology*, *9*, 794818. https://doi.org/10.3389/fbioe.2021.794818

Percival, E., & Foyle, R. A. J. (1979). The extracellular polysaccharides of porphyridium cruentum and porphyridium aerugineum. *Carbohydrate Research*, *72*, 165–176. https://doi.org/10.1016/S0008-6215(00)83932-4

Perez Recalde, M., Canelón, D. J., Compagnone, R. S., Matulewicz, M. C., Cerezo, A. S., & Ciancia, M. (2016). Carrageenan and agaran structures from the red seaweed Gymnogongrus tenuis. *Carbohydrate Polymers*, *136*, 1370–1378. https://doi.org/10.1016/j.carbpol.2015.10.007

Phillips, N. J., Adin, D. M., Stabb, E. V., McFall-Ngai, M. J., Apicella, M. A., & Gibson, B. W. (2011). The Lipid A from Vibrio fischeri Lipopolysaccharide. *Journal of Biological Chemistry*, *286*(24), 21203–21219. https://doi.org/10.1074/jbc.M111.239475

Pierre, G., Delattre, C., Dubessay, P., Jubeau, S., Vialleix, C., Cadoret, J.-P., Probert, I., & Michaud, P. (2019). What Is in Store for EPS Microalgae in the Next Decade? *Molecules*, *24*(23), 4296. https://doi.org/10.3390/molecules24234296

Pinhassi, J., Farnelid, H., García, S. M., Teira, E., Galand, P. E., Obernosterer, I., Quince, C., Vila-Costa, M., Gasol, J. M., Lundin, D., Andersson, A. F., Labrenz, M., & Riemann, L. (2022). Functional responses of key marine bacteria to environmental change – toward genetic counselling for coastal waters. *Frontiers in Microbiology*, *13*, 869093. https://doi.org/10.3389/fmicb.2022.869093

Pointcheval, M., Massé, A., Floc'hlay, D., Chanonat, F., Estival, J., & Durand, M.-J. (2025). Antimicrobial properties of selected microalgae exopolysaccharide-enriched extracts: Influence of antimicrobial assays and targeted microorganisms. *Frontiers in Microbiology*, *16*, 1536185. https://doi.org/10.3389/fmicb.2025.1536185

Poli, A., Anzelmo, G., & Nicolaus, B. (2010). Bacterial Exopolysaccharides from Extreme Marine Habitats: Production, Characterization and Biological Activities. *Marine Drugs*, *8*(6), 1779–1802. https://doi.org/10.3390/md8061779

Pomin, V. H., & Mourao, P. A. S. (2008). Structure, biology, evolution, and medical importance of sulfated fucans and galactans. *Glycobiology*, *18*(12), 1016–1027. https://doi.org/10.1093/glycob/cwn085

Popa, M., & Atanase, L. I. (2021). *Drug Delivery Systems Based on Polysaccharides*. MDPI. https://doi.org/10.3390/books978-3-0365-1675-2

Popper, Z. A., Michel, G., Hervé, C., Domozych, D. S., Willats, W. G. T., Tuohy, M. G., Kloareg, B., & Stengel, D. B. (2011). Evolution and Diversity of Plant Cell Walls: From Algae to Flowering Plants. *Annual Review of Plant Biology*, *62*(1), 567–590. https://doi.org/10.1146/annurev-arplant-042110-103809

Poveda-Castillo, G. D. C., Rodrigo, D., Martínez, A., & Pina-Pérez, M. C. (2018). Bioactivity of Fucoidan as an Antimicrobial Agent in a New Functional Beverage. *Beverages*, *4*(3), 64. https://doi.org/10.3390/beverages4030064

Puchkova, T., Khapchaeva, S., Zotov, V., Lukyanov, A., & Solovchenko, A. (2020). *Microalgae as a Sustainable Source of Cosmeceuticals*. MEDICINE & PHARMACOLOGY. https://doi.org/10.20944/preprints202012.0696.v1

Qian, L., Wu, L., Yang, L., & Zhang, Z. (2021). Inoculation concentration modulating the secretion and accumulation pattern of exopolysaccharides in desert cyanobacterium *Microcoleus vaginatus*. *Biotechnology and Applied Biochemistry*, *68*(2), 330–337. https://doi.org/10.1002/bab.1930

Radchenkova, N., & Yaşar Yıldız, S. (2025). Advanced Optimization of Bioprocess Parameters for Exopolysaccharides Synthesis in Extremophiles. *Processes*, *13*(3), 822. https://doi.org/10.3390/pr13030822

Ragazzola, F., Raiteri, G., Fabbri, P., Scafè, M., Florio, M., Nannini, M., & Lombardi, C. (2017). Structural integrity of *Ellisolandia elongata* reefs: A mechanical approach to compare tensile strengths in natural and controlled environments. *Marine Ecology*, *38*(5), e12455. https://doi.org/10.1111/maec.12455

Raguenes, G., Christen, R., Guezennec, J., Pignet, P., & Barbier, G. (1997). Vibrio diabolicus sp. Nov., a New Polysaccharide-Secreting Organism Isolated from a Deep-Sea Hydrothermal Vent Polychaete Annelid, Alvinella pompejana. *International Journal of Systematic Bacteriology*, *47*(4), 989–995. https://doi.org/10.1099/00207713-47-4-989

Raguénès, G. H. C., Peres, A., Ruimy, R., Pignet, P., Christen, R., Loaec, M., Rougeaux, H., Barbier, G., & Guezennec, J. G. (1997). ***Alteromonas infernus*** sp. Nov., a new polysaccharide-producing bacterium isolated from a deep-sea hydrothermal vent. *Journal of Applied Microbiology*, *82*(4), 422–430. https://doi.org/10.1046/j.1365-2672.1997.00125.x

Rahman, M. A., & Halfar, J. (2014). First evidence of chitin in calcified coralline algae: New insights into the calcification process of Clathromorphum compactum. *Scientific Reports*, *4*(1), 6162. https://doi.org/10.1038/srep06162

Ramamoorthy, S., Gnanakan, A., S. Lakshmana, S., Meivelu, M., & Jeganathan, A. (2018). Structural characterization and anticancer activity of extracellular polysaccharides from ascidian

symbiotic bacterium Bacillus thuringiensis. *Carbohydrate Polymers*, *190*, 113–120. https://doi.org/10.1016/j.carbpol.2018.02.047

Raue, S., Fan, S.-H., Rosenstein, R., Zabel, S., Luqman, A., Nieselt, K., & Götz, F. (2020). The Genome of Staphylococcus epidermidis O47. *Frontiers in Microbiology*, *11*, 2061. https://doi.org/10.3389/fmicb.2020.02061

Raven, J. A., & Girard-Bascou, J. (2001). ALGAL MODEL SYSTEMS AND THE ELUCIDATION OF PHOTOSYNTHETIC METABOLISM. *Journal of Phycology*, *37*(6), 943–950. https://doi.org/10.1046/j.1529-8817.2001.01079.x

Restaino, O. F., Finamore, R., Diana, P., Marseglia, M., Vitiello, M., Casillo, A., Bedini, E., Parrilli, M., Corsaro, M. M., Trifuoggi, M., De Rosa, M., & Schiraldi, C. (2017). A multi-analytical approach to better assess the keratan sulfate contamination in animal origin chondroitin sulfate. *Analytica Chimica Acta*, *958*, 59–70. https://doi.org/10.1016/j.aca.2016.12.005

Rioux, L.-E., Beaulieu, L., & Turgeon, S. L. (2017). Seaweeds: A traditional ingredients for new gastronomic sensation. *Food Hydrocolloids*, *68*, 255–265. https://doi.org/10.1016/j.foodhyd.2017.02.005

Robertson, J. M., Garza, E. A., Stubbusch, A. K. M., Dupont, C. L., Hwa, T., & Held, N. A. (2024). Marine bacteria *Alteromonas* spp. Require UDP-glucose-4-epimerase for aggregation and production of sticky exopolymer. *mBio*, *15*(8), e00038-24. https://doi.org/10.1128/mbio.00038-24

Roier, S., Zingl, F. G., Cakar, F., Durakovic, S., Kohl, P., Eichmann, T. O., Klug, L., Gadermaier, B., Weinzerl, K., Prassl, R., Lass, A., Daum, G., Reidl, J., Feldman, M. F., & Schild, S. (2016). A novel mechanism for the biogenesis of outer membrane vesicles in Gram-negative bacteria. *Nature Communications*, *7*(1), 10515. https://doi.org/10.1038/ncomms10515

Romalde, J. L., Dieguez, A. L., Lasa, A., & Balboa, S. (2014). New Vibrio species associated to molluscan microbiota: A review. *Frontiers in Microbiology*, *4*. https://doi.org/10.3389/fmicb.2013.00413

Rupérez, P., Ahrazem, O., & Leal, J. A. (2002). Potential Antioxidant Capacity of Sulfated Polysaccharides from the Edible Marine Brown Seaweed *Fucus vesiculosus*. *Journal of Agricultural and Food Chemistry*, *50*(4), 840–845. https://doi.org/10.1021/jf010908o

Sacramento, M. M. A., Borges, J., Correia, F. J. S., Calado, R., Rodrigues, J. M. M., Patrício, S. G., & Mano, J. F. (2022). Green approaches for extraction, chemical modification and processing of marine polysaccharides for biomedical applications. *Frontiers in Bioengineering and Biotechnology*, *10*, 1041102. https://doi.org/10.3389/fbioe.2022.1041102

Saggese, A., Di Gregorio Barletta, G., Vittoria, M., Donadio, G., Isticato, R., Baccigalupi, L., & Ricca, E. (2022). CotG Mediates Spore Surface Permeability in Bacillus subtilis. *mBio*, *13*(6), e02760-22. https://doi.org/10.1128/mbio.02760-22

Sandeep, K. P., Avunje, S., Dayal, J. S., Balasubramanian, C. P., Sawant, P. B., Chadha, N. K., Ambasankar, K., & Vijayan, K. K. (2021). Efficiency of different microalgae as monospecific and bispecific diets in larval rearing of *Penaeus indicus* with special reference to growth, nutrient composition and antimicrobial activity of microalgae. *Aquaculture Research*, *52*(11), 5146–5154. https://doi.org/10.1111/are.15382

Sankaran, K., & Wu, H. C. (1994). Lipid modification of bacterial prolipoprotein. Transfer of diacylglyceryl moiety from phosphatidylglycerol. *Journal of Biological Chemistry*, *269*(31), 19701–19706. https://doi.org/10.1016/S0021-9258(17)32077-X

Saranya, N., Sri Abarajitha, R., Anandhasayanan, T., Jaivignesh, D., Mugunthan, B., Dinakarkumar, Y., & Shanmugam, K. (2023). Screening of Antiviral Efficacy of Few Seaweeds of Tamil Nadu Coast. *Proceedings of Anticancer Research*, *7*(5), 17–29. https://doi.org/10.26689/par.v7i5.5161

Schwechheimer, C., & Kuehn, M. J. (2015). Outer-membrane vesicles from Gram-negative bacteria: Biogenesis and functions. *Nature Reviews Microbiology*, *13*(10), 605–619. https://doi.org/10.1038/nrmicro3525

Shao, Z., & Duan, D. (2022). The Cell Wall Polysaccharides Biosynthesis in Seaweeds: A Molecular Perspective. *Frontiers in Plant Science*, *13*, 902823. https://doi.org/10.3389/fpls.2022.902823

Sieburth, J. McN., Smetacek, V., & Lenz, J. (1978). Pelagic ecosystem structure: Heterotrophic compartments of the plankton and their relationship to plankton size fractions 1. *Limnology and Oceanography*, *23*(6), 1256–1263. https://doi.org/10.4319/lo.1978.23.6.1256

Soto-Vásquez, M. R., Alvarado-García, P. A. A., Youssef, F. S., Ashour, M. L., Bogari, H. A., & Elhady, S. S. (2022). FTIR Characterization of Sulfated Polysaccharides Obtained from Macrocystis integrifolia Algae and Verification of Their Antiangiogenic and Immunomodulatory Potency In Vitro and In Vivo. *Marine Drugs*, *21*(1), 36. https://doi.org/10.3390/md21010036

Squillaci, G., Finamore, R., Diana, P., Restaino, O. F., Schiraldi, C., Arbucci, S., Ionata, E., La Cara, F., & Morana, A. (2016). Production and properties of an exopolysaccharide synthesized by the extreme halophilic archaeon Haloterrigena turkmenica. *Applied Microbiology and Biotechnology*, *100*(2), 613–623. https://doi.org/10.1007/s00253-015-6991-5

Stevenson, G., Andrianopoulos, K., Hobbs, M., & Reeves, P. R. (1996). Organization of the Escherichia coli K-12 gene cluster responsible for production of the extracellular polysaccharide colanic acid. *Journal of Bacteriology*, *178*(16), 4885–4893. https://doi.org/10.1128/jb.178.16.4885-4893.1996

Sun, L., Fang, L., Zhang, Z., Chang, X., Penny, D., & Zhong, B. (2016). Chloroplast Phylogenomic Inference of Green Algae Relationships. *Scientific Reports*, *6*(1), 20528. https://doi.org/10.1038/srep20528

Sun, L., Wang, C., Shi, Q., & Ma, C. (2009). Preparation of different molecular weight polysaccharides from Porphyridium cruentum and their antioxidant activities. *International Journal of Biological Macromolecules*, *45*(1), 42–47. https://doi.org/10.1016/j.ijbiomac.2009.03.013

Sun, M.-L., Liu, S.-B., Qiao, L.-P., Chen, X.-L., Pang, X., Shi, M., Zhang, X.-Y., Qin, Q.-L., Zhou, B.-C., Zhang, Y.-Z., & Xie, B.-B. (2014). A novel exopolysaccharide from deep-sea bacterium Zunongwangia profunda SM-A87: Low-cost fermentation, moisture retention, and

antioxidant activities. *Applied Microbiology and Biotechnology*, *98*(17), 7437–7445. https://doi.org/10.1007/s00253-014-5839-8

Sun, Y., Ma, X., & Hu, H. (2021). Marine Polysaccharides as a Versatile Biomass for the Construction of Nano Drug Delivery Systems. *Marine Drugs*, *19*(6), 345. https://doi.org/10.3390/md19060345

Sun, Z.-Z., Ji, B.-W., Zheng, N., Wang, M., Cao, Y., Wan, L., Li, Y.-S., Rong, J.-C., He, H.-L., Chen, X.-L., Zhang, Y.-Z., & Xie, B.-B. (2021). Phylogenetic Distribution of Polysaccharide-Degrading Enzymes in Marine Bacteria. *Frontiers in Microbiology*, *12*, 658620. https://doi.org/10.3389/fmicb.2021.658620

Tsai, C.-M., & Frasch, C. E. (1982). A sensitive silver stain for detecting lipopolysaccharides in polyacrylamide gels. *Analytical Biochemistry*, *119*(1), 115–119. https://doi.org/10.1016/0003-2697(82)90673-X

Turmel, M., De Cambiaire, J.-C., Otis, C., & Lemieux, C. (2016). Distinctive Architecture of the Chloroplast Genome in the Chlorodendrophycean Green Algae Scherffelia dubia and Tetraselmis sp. CCMP 881. *PLOS ONE*, *11*(2), e0148934. https://doi.org/10.1371/journal.pone.0148934

Turnbull, L., Toyofuku, M., Hynen, A. L., Kurosawa, M., Pessi, G., Petty, N. K., Osvath, S. R., Cárcamo-Oyarce, G., Gloag, E. S., Shimoni, R., Omasits, U., Ito, S., Yap, X., Monahan, L. G., Cavaliere, R., Ahrens, C. H., Charles, I. G., Nomura, N., Eberl, L., & Whitchurch, C. B. (2016). Explosive cell lysis as a mechanism for the biogenesis of bacterial membrane vesicles and biofilms. *Nature Communications*, *7*(1), 11220. https://doi.org/10.1038/ncomms11220

Urvoy, M., Labry, C., L'Helguen, S., & Lami, R. (2022). Quorum Sensing Regulates Bacterial Processes That Play a Major Role in Marine Biogeochemical Cycles. *Frontiers in Marine Science*, *9*, 834337. https://doi.org/10.3389/fmars.2022.834337

Usov, A. I. (2011). Polysaccharides of the red algae. In *Advances in Carbohydrate Chemistry and Biochemistry* (Vol. 65, pp. 115–217). Elsevier. https://doi.org/10.1016/B978-0-12-385520-6.00004-2

Van Selm, S., Van Cann, L. M., Kolkman, M. A. B., Van Der Zeijst, B. A. M., & Van Putten, J. P. M. (2003). Genetic Basis for the Structural Difference between *Streptococcus pneumoniae* Serotype 15B and 15C Capsular Polysaccharides. *Infection and Immunity*, *71*(11), 6192–6198. https://doi.org/10.1128/IAI.71.11.6192-6198.2003

Varasteh, T., Ahmadi, R. A., Mendonça, B., De Oliveira Santos, E., Shokri, M. R., Tschoeke, D., Thompson, C., & Thompson, F. (2025). Genome diversity of Alteromonas macleodii isolated from the Persian Gulf and the Atlantic Ocean. *Regional Studies in Marine Science*, *85*, 104140. https://doi.org/10.1016/j.rsma.2025.104140

Vásquez - Piñeros, M. A., Rondón - Barragan, I. S., & Eslava- Mocha, P. R. (2012). Inmunoestimulantes en teleosteos: Probióticos, β-glucanos y LPS. *Orinoquia*, *16*(1), 46–62. https://doi.org/10.22579/20112629.264

Venuleo, M., & Giordano, M. (2019). Different Nutritional Histories Affect the Susceptibility of Algae to Grazing. *Journal of Phycology*, *55*(5), 997–1010. https://doi.org/10.1111/jpy.12901

Vergnes, J. B., Gernigon, V., Guiraud, P., & Formosa-Dague, C. (2019). Bicarbonate Concentration Induces Production of Exopolysaccharides by *Arthrospira platensis* That Mediate Bioflocculation and Enhance Flotation Harvesting Efficiency. *ACS Sustainable Chemistry & Engineering*, *7*(16), 13796–13804. https://doi.org/10.1021/acssuschemeng.9b01591

Vidhyalakshmi, R. (2013). Apoptosis of Human Breast Cancer Cells (MCF-7) Induced by Polysacccharides Produced by Bacteria. *Journal of Cancer Science & Therapy*, *05*(02). https://doi.org/10.4172/1948-5956.1000181

Vinogradov, E., Nossova, L., Korenevsky, A., & Beveridge, T. J. (2005). The structure of the capsular polysaccharide of Shewanella oneidensis strain MR-4. *Carbohydrate Research*, *340*(10), 1750–1753. https://doi.org/10.1016/j.carres.2005.04.009

Vishwakarma, J., & Vavilala, S. L. (2019). Evaluating the antibacterial and antibiofilm potential of sulphated polysaccharides extracted from green algae *Chlamydomonas reinhardtii*. *Journal of Applied Microbiology*, *127*(4), 1004–1017. https://doi.org/10.1111/jam.14364

Vittoria, M., Saggese, A., Isticato, R., Baccigalupi, L., & Ricca, E. (2023). Probiotics as an Alternative to Antibiotics: Genomic and Physiological Characterization of Aerobic Spore Formers from the Human Intestine. *Microorganisms*, *11*(8), 1978. https://doi.org/10.3390/microorganisms11081978

Wan, A. H. L., Davies, S. J., Soler-Vila, A., Fitzgerald, R., & Johnson, M. P. (2019). Macroalgae as a sustainable aquafeed ingredient. *Reviews in Aquaculture*, *11*(3), 458–492. https://doi.org/10.1111/raq.12241

Wang, C., Fan, Q., Zhang, X., Lu, X., Xu, Y., Zhu, W., Zhang, J., Hao, W., & Hao, L. (2018). Isolation, Characterization, and Pharmaceutical Applications of an Exopolysaccharide from Aerococcus Uriaeequi. *Marine Drugs*, *16*(9), 337. https://doi.org/10.3390/md16090337

Wang, J., Zhang, Q., Zhang, Z., & Li, Z. (2008). Antioxidant activity of sulfated polysaccharide fractions extracted from Laminaria japonica. *International Journal of Biological Macromolecules*, *42*(2), 127–132. https://doi.org/10.1016/j.ijbiomac.2007.10.003

Wang, W., Ju, Y., Liu, N., Shi, S., & Hao, L. (2023). Structural characteristics of microbial exopolysaccharides in association with their biological activities: A review. *Chemical and Biological Technologies in Agriculture*, *10*(1), 137. https://doi.org/10.1186/s40538-023-00515-3

Wei, S., Wang, L., Yang, J., Xu, R., Jia, R., & He, P. (2024). Protective Effect of Polysaccharides Isolated from Sargassum horneri against H2O2-Induced Oxidative Stress Both In Vitro, in Vero Cells, and In Vivo in Zebrafish. *Biology*, *13*(9), 651. https://doi.org/10.3390/biology13090651

Whitfield, C. (1988). Bacterial extracellular polysaccharides. *Canadian Journal of Microbiology*, *34*(4), 415–420. https://doi.org/10.1139/m88-073

Whitfield, C. (2006). Biosynthesis and Assembly of Capsular Polysaccharides in *Escherichia coli*. *Annual Review of Biochemistry*, *75*(1), 39–68. https://doi.org/10.1146/annurev.biochem.75.103004.142545

Wijesekara, I., Pangestuti, R., & Kim, S.-K. (2011). Biological activities and potential health benefits of sulfated polysaccharides derived from marine algae. *Carbohydrate Polymers*, *84*(1), 14–21. https://doi.org/10.1016/j.carbpol.2010.10.062

Wu, S., Liu, G., Jin, W., Xiu, P., & Sun, C. (2016). Antibiofilm and Anti-Infection of a Marine Bacterial Exopolysaccharide Against Pseudomonas aeruginosa. *Frontiers in Microbiology*, *7*. https://doi.org/10.3389/fmicb.2016.00102

Xiao, R., Yang, X., Li, M., Li, X., Wei, Y., Cao, M., Ragauskas, A., Thies, M., Ding, J., & Zheng, Y. (2018). Investigation of composition, structure and bioactivity of extracellular polymeric substances from original and stress-induced strains of Thraustochytrium striatum. *Carbohydrate Polymers*, *195*, 515–524. https://doi.org/10.1016/j.carbpol.2018.04.126

Xie, C., Lee, Z. J., Ye, S., Barrow, C. J., Dunshea, F. R., & Suleria, H. A. R. (2024). A Review on Seaweeds and Seaweed-Derived Polysaccharides: Nutrition, Chemistry, Bioactivities, and Applications. *Food Reviews International*, *40*(5), 1312–1347. https://doi.org/10.1080/87559129.2023.2212055

Xue, M., Ge, Y., Zhang, J., Wang, Q., Hou, L., Liu, Y., Sun, L., & Li, Q. (2012). Anticancer Properties and Mechanisms of Fucoidan on Mouse Breast Cancer In Vitro and In Vivo. *PLoS ONE*, *7*(8), e43483. https://doi.org/10.1371/journal.pone.0043483

Yang, J.-I., Yeh, C.-C., Lee, J.-C., Yi, S.-C., Huang, H.-W., Tseng, C.-N., & Chang, H.-W. (2012). Aqueous Extracts of the Edible Gracilaria tenuistipitata are Protective Against H2O2-Induced DNA Damage, Growth Inhibition, and Cell Cycle Arrest. *Molecules*, *17*(6), 7241–7254. https://doi.org/10.3390/molecules17067241

Yang, X., Liu, Z., Zhang, Y., Shi, X., & Wu, Z. (2024). Dinoflagellate–Bacteria Interactions: Physiology, Ecology, and Evolution. *Biology*, *13*(8), 579. https://doi.org/10.3390/biology13080579

Yangthong, M., Hutadilok-Towatana, N., & Phromkunthong, W. (2009). Antioxidant Activities of Four Edible Seaweeds from the Southern Coast of Thailand. *Plant Foods for Human Nutrition*, *64*(3), 218–223. https://doi.org/10.1007/s11130-009-0127-y

Ye, J., Zhu, Z., Song, Z., Xu, H., Xu, T., & Liu, H. (2024). Application of microbubble air flotation to harvest *Microcystis* sp. from agriculture wastewater: The regulation and mechanisms. *Biotechnology and Bioengineering*, *121*(12), 3742–3753. https://doi.org/10.1002/bit.28836

Yermak, I. M., Davydova, V. N., & Volod'ko, A. V. (2022). Mucoadhesive Marine Polysaccharides. *Marine Drugs*, *20*(8), 522. https://doi.org/10.3390/md20080522

Yim, J. H., Son, E., Pyo, S., & Lee, H. K. (2005). Novel sulfated polysaccharide derived from red-tide microalga Gyrodinium impudicum strain KG03 with immunostimulating activity in vivo. *Marine Biotechnology*, *7*(4), 331–338. https://doi.org/10.1007/s10126-004-0404-6

Zhang, G., Meredith, T. C., & Kahne, D. (2013). On the essentiality of lipopolysaccharide to Gram-negative bacteria. *Current Opinion in Microbiology*, *16*(6), 779–785. https://doi.org/10.1016/j.mib.2013.09.007

Zhang, Z., Cai, R., Zhang, W., Fu, Y., & Jiao, N. (2017). A Novel Exopolysaccharide with Metal Adsorption Capacity Produced by a Marine Bacterium Alteromonas sp. JL2810. *Marine Drugs*, *15*(6), 175. https://doi.org/10.3390/md15060175

Zhang, Z., Chen, Y., Wang, R., Cai, R., Fu, Y., & Jiao, N. (2015). The Fate of Marine Bacterial Exopolysaccharide in Natural Marine Microbial Communities. *PLOS ONE*, *10*(11), e0142690. https://doi.org/10.1371/journal.pone.0142690

Zhong, H., Gao, X., Cheng, C., Liu, C., Wang, Q., & Han, X. (2020). The Structural Characteristics of Seaweed Polysaccharides and Their Application in Gel Drug Delivery Systems. *Marine Drugs*, *18*(12), 658. https://doi.org/10.3390/md18120658

Zhou, L., Li, K., Duan, X., Hill, D., Barrow, C., Dunshea, F., Martin, G., & Suleria, H. (2022). Bioactive compounds in microalgae and their potential health benefits. *Food Bioscience*, *49*, 101932. https://doi.org/10.1016/j.fbio.2022.101932

Zhu, F., Tan, X., Wang, X., & Zhang, Q. (2024). Does periphyton turn less palatable under grazing pressure? *ISME Communications*, *4*(1), ycae146. https://doi.org/10.1093/ismeco/ycae146